Facies (2023) 69:11
https://doi.org/10.1007/s10347-023-00662-x

ORIGINAL ARTICLE

Facies character and evolution of a mixed carbonate–siliciclastic shelf: Upper Triassic–Lower Jurassic succession in the eastern Northern Calcareous Alps (Stumpfmauer, Austria)

Giovanna Della Porta[1] · **Alessandro Mancini**[1] · **Fabrizio Berra**[1]

Received: 17 May 2022 / Accepted: 14 March 2023

Abstract
Western Tethys sedimentary successions constitute fundamental archives of Late Triassic–Early Jurassic environmental, carbonate production and tectonic changes. During the Late Triassic, the Northern Calcareous Alps (Austria) belonged to the Western Tethys passive margin, characterised by the deposition of the early-dolomitized peritidal Hauptdolomit (Norian) adjacent basinward to the Dachstein carbonate shelf and passing upward to the mixed carbonate–siliciclastic Kössen Formation (Upper Norian–Rhaetian). The Kössen Fm. was subdivided into the lower shallow-water Hochalm Member and the upper Eiberg Member, accumulated in an intraplatform basin coeval to shallow-water carbonates (Upper Rhaetian Limestone). The Eiberg Mb. and overlying Jurassic strata were extensively studied as a continuous marine record across the Triassic/Jurassic boundary. In contrast, shallow-water successions, time-equivalent to the Eiberg Mb. and Upper Rhaetian Limestone, located North of the Eiberg Basin, are poorly investigated. This study focusses on the approximately 350 m thick Norian to Lower Jurassic succession cropping out in the eastern Northern Calcareous Alps (Stumpfmauer). The 32 distinguished lithofacies compose seven, vertically superimposed, sedimentary units (A–G), belonging to the Hochalm Mb. of the Kössen Fm. (Unit A peritidal cyclothems, Unit B claystone/marlstone with fossiliferous beds, Unit C coral boundstone to floatstone), Upper Rhaetian Limestone (Unit D subtidal cyclothems with claystone), shallow-water carbonate strata transitional to Lower Jurassic (Unit E ooidal coated grain peloidal grainstone with basal transgressive lag, Unit F bivalve-rich, microbialite and oncoidal lithofacies, previously attributed to the Upper Rhaetian Limestone) and Hettangian–Sinemurian Kalksburg Fm. (Unit G cross-laminated coated grain peloidal grainstone with quartz and chert). The detailed lithofacies characterisation presented in this study contributes to the knowledge on the Northern Calcareous Alps stratigraphy and depositional environments across the Triassic/Jurassic boundary. The identified sedimentary units can be framed in the evolution of Western Tethys and share similarities with depositional systems from the Western Carpathians, Transdanubian Range, Southern Alps and Dinarides suggesting coherent sedimentary response and environmental, climate and tectonic controls in different palaeogeographic domains.

Keywords Carbonate facies · Rhaetian · Jurassic · Kössen Formation · Northern Calcareous Alps · Austria

Introduction

Carbonate successions are unparalleled archives of global and local environmental, climate and accommodation changes responding through variations in depositional environments, vertical and lateral facies patterns and biota associations (Schlager 2003; Flügel 2004; Wright and Burgess 2005; Pomar and Hallock 2008). In Western Tethys, the Norian (Upper Triassic)–Jurassic sedimentary successions (Fig. 1) recorded changes in depositional regime and facies associations governed by sea-level oscillations, climate, biotic crisis and extensional

✉ Giovanna Della Porta
giovanna.dellaporta@unimi.it

Alessandro Mancini
alessandro.mancini@unimi.it

[1] Dipartimento di Scienze Della Terra "A. Desio", Università degli Studi di Milano, Via Mangiagalli 34, 20133 Milan, Italy

Published online: 01 June 2023

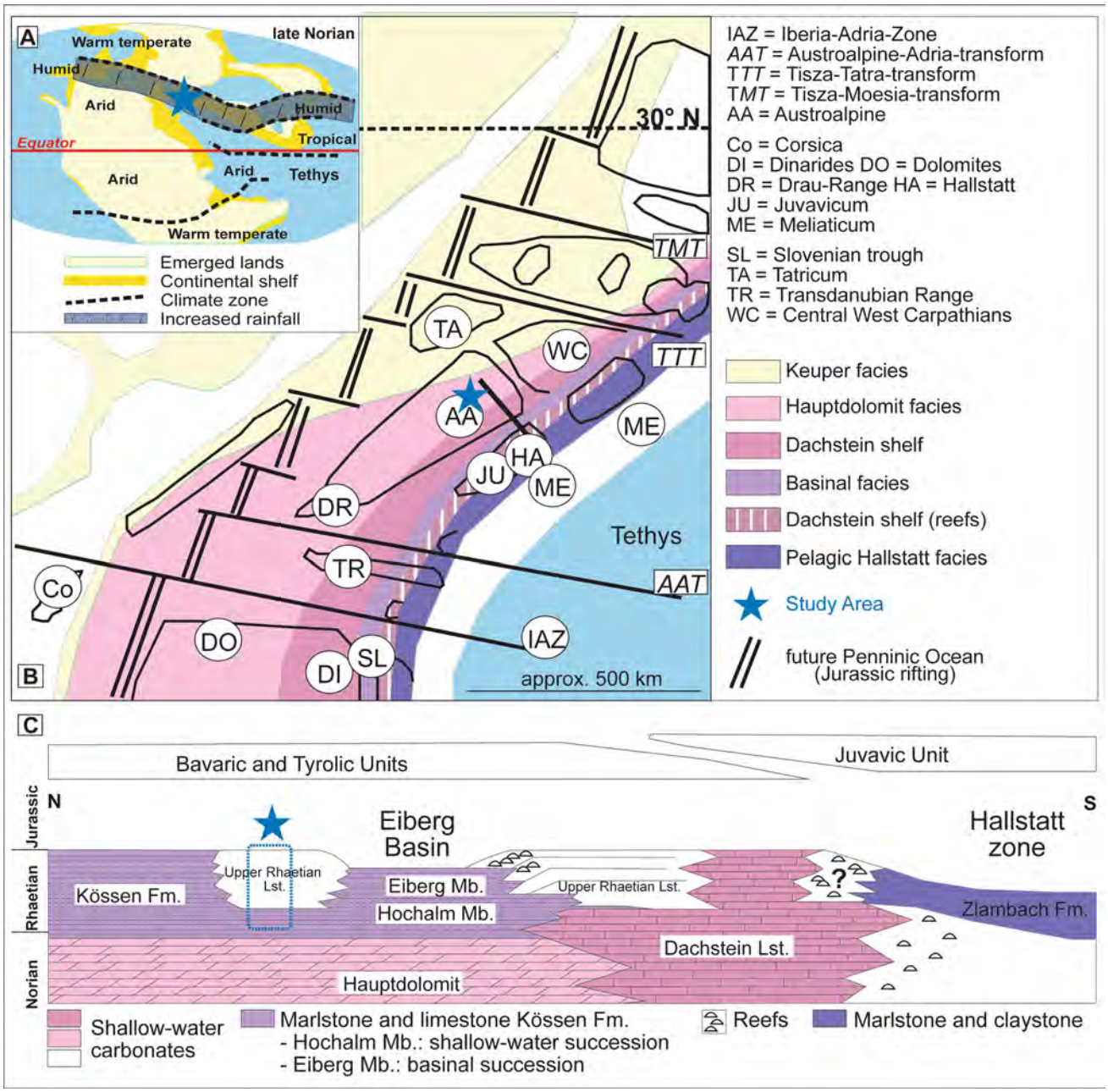

Fig. 1 **A** Palaeogeographic map during the fine siliciclastic input in the late Norian showing the climatic belts, with the arrows indicating the possible extent of the humid belt, characterised by an increase in rainfall precipitation (redrafted after Berra et al. 2010). **B** Reconstruction of the Western Tethys passive margin during the late Norian (redrafted after Haas et al. 1995 as modified in Mandl 2000). **C** N–S Norian to Rhaetian lithofacies cross section of the Northern Calcareous Alps (NCA) from the Hauptdolomit to the development of the Eiberg Basin (modified after Mandl 2000; Krystyn et al. 2005). The blue star and blue dashed line rectangle represent the approximate location of the studied stratigraphic succession

tectonics (Flügel 2002; Krystyn et al. 2005; Gawlick et al. 2009; Kaufmann 2009; Berra et al. 2010). The end-Triassic mass extinction, one of the big five biotic crises, affected diverse marine and terrestrial groups and coincided with major changes in palynological assemblages (Sepkoski 1996; Hallam 2002; Hesselbo et al. 2002; Hillebrandt and Urlichs 2008; Ruhl et al. 2009; Clémence et al. 2010; McRoberts et al. 2012; Pálfy and Zajzon 2012; Richoz et al. 2012; Wignall and Atkinson 2020). This extinction was driven by environmental perturbations related to volcanic CO_2 emissions of the CAMP basalts (Central Atlantic Magmatic Province; Marzoli et al. 2004). The study of Western Tethys Norian–Lower Jurassic successions in the Northern Calcareous Alps

(NCA, Austroalpine, Austria; Figs. 1, 2) contributes to unravel the interplay of factors influencing carbonate sedimentary environments at a regional scale. In fact, from late Norian to early Jurassic, these depositional settings witnessed: (a) the demise of a long-lasting, hundreds of kilometres wide and over 1000 m thick, Norian early-dolomitized inner platform (Hauptdolomit) adjacent to hundreds of kilometres wide carbonate shelf (Dachstein Limestone and Reef); (b) a major late Norian–Rhaetian change in sediment supply with the input of fine siliciclastics, previously absent, alternating with carbonate strata (Hochalm and Eiberg members of the Kössen Formation), attributed to a change towards more humid climatic conditions (Berra et al. 2010); (c) the late Rhaetian development of intraplatform basins (Eiberg Basin; Golebiowski 1990; Kaufmann 2009; Mette et al. 2012; Krystyn et al. 2005; Restental Basin; Gawlick et al. 2009; Richoz et al. 2012; Hillebrandt et al. 2013), passing laterally to shallow-water carbonates (*Oberrhätkalk*/Upper Rhaetian Limestone; Schäfer 1979; Golebiowski 1990; Krystyn et al. 2005) with margins with coral patch reefs (Bernecker et al. 1999; Bernecker 2005; Kaufmann 2009) or distally steepened ramp with skeletal packstone/grainstone and mounds (Piller 1981; Stanton and Flügel 1989, 1995; Flügel 1981, 2002); (d) a sea-level fall followed by rapid rise and biotic turnover across the end-Triassic extinction event (McRoberts et al. 2012); (e) the late early Jurassic rifting leading to the opening of the Penninic Ocean (Bernoulli 1964; Eberli 1988; Gawlick et al. 2009).

The continuity of the Norian–Lower Jurassic succession cropping out in the NCA provides optimal conditions for the investigation of the sedimentary responses of shallow-water settings to some of the most significant environmental, climatic and tectonic changes affecting the Upper Triassic–Lower Jurassic stratigraphic record. Despite several studies performed on the Eiberg Basin in the western NCA (Hillebrandt et al. 2013), and on the Eiberg Basin southern margins (Upper Rhaetian Limestone; Stanton and Flügel 1989, 1995; Satterley et al. 1994; Bernecker et al. 1999; Tomašových 2006; Rizzi et al. 2020), shallow-water carbonate facies of the Kössen Fm. and Upper Rhaetian Limestone (time-equivalent to the Eiberg Basin), were not investigated in detail in the eastern NCA. To improve the knowledge on NCA stratigraphy and sedimentary evolution, the succession in the Stumpfmauer area (central eastern Austria; Fig. 2) was investigated for detailed facies characterisation and compared with other palaeogeographic domains of Western Tethys.

Geological setting of the NCA

The NCA (Fig. 2A) are a ~ 500 km long WSW–ENE-striking fold and thrust belt belonging to the Austroalpine domain (Tollmann 1976; Ratschbacher et al. 1989, 1991; Gawlick et al. 1999; Mandl 1999, 2000; Frisch et al. 2000; Frisch and Gawlick 2003; Schmid et al. 2004). The Triassic Austroalpine passive margin faced the Neo-Tethys to the E–SE (with ophiolite obduction in the Middle Jurassic; Gawlick et al. 2008). From the early–middle Jurassic, the Austroalpine became separated from Europe by the opening of the Penninic Ocean to the N–W (Gawlick and Missoni 2019). In the NCA, an Upper Permian to Eocene sedimentary succession is exposed, with the Triassic shallow-water carbonates representing the thickest deposits (Tollmann 1965, 1976, 1985; Mandl 2000; Krystyn et al. 2005). In this study, following Gawlick et al. (1999), the classical tectonic subdivision of the complex internal structure of the NCA in a lower Bavaric, intermediate Tyrolic and an upper Juvavic nappe group is used descriptively, without any structural significance of these units.

Upper Triassic–Lower Jurassic stratigraphy of the NCA

The Norian succession consists of thousands of square kilometres wide and more than 1000 m thick inner platform facies (Figs. 1B, C, 2B), pervasively early dolomitized, known as Hauptdolomit (Tollmann 1965, 1976, 1985; Fruth and Scherreicks 1982, 1984). This unit, with different lithostratigraphic names and some differences in the stratigraphic range, extends to the Western Carpathians, Transdanubian Range, Southern Alps, Dinarides and Southern Apennines (Iannace and Frisia 1994; Buckovic et al. 2001; Vlahović et al. 2005; Berra et al. 2010; Caggiati et al. 2018; Héja et al. 2018; Haas et al. 2022). Landward, the NCA Hauptdolomit interfingered with the Keuper shallow-marine hypersaline environments, with carbonate, siliciclastic and evaporite deposits. Basinward, the Hauptdolomit was adjacent to lagoonal subtidal–peritidal cyclic strata (Lofer cyclothems of the Dachstein Limestone; Fischer 1964; Enos and Samankassou 1998; Missoni et al. 2005), passing to the Dachstein Reef shelf margin (Fig. 1C). The Dachstein Reef (Flügel 2002; Bernecker 2005) faced the Hallstatt outer shelf of the Neo-Tethys Ocean (Matzner 1986; Kozur 1991; Gawlick et al. 1999; Gawlick and Böhm 2000; Köppen and Carter 2000). The Hauptdolomit is overlain by a well-bedded, 10–400 m thick, only partly

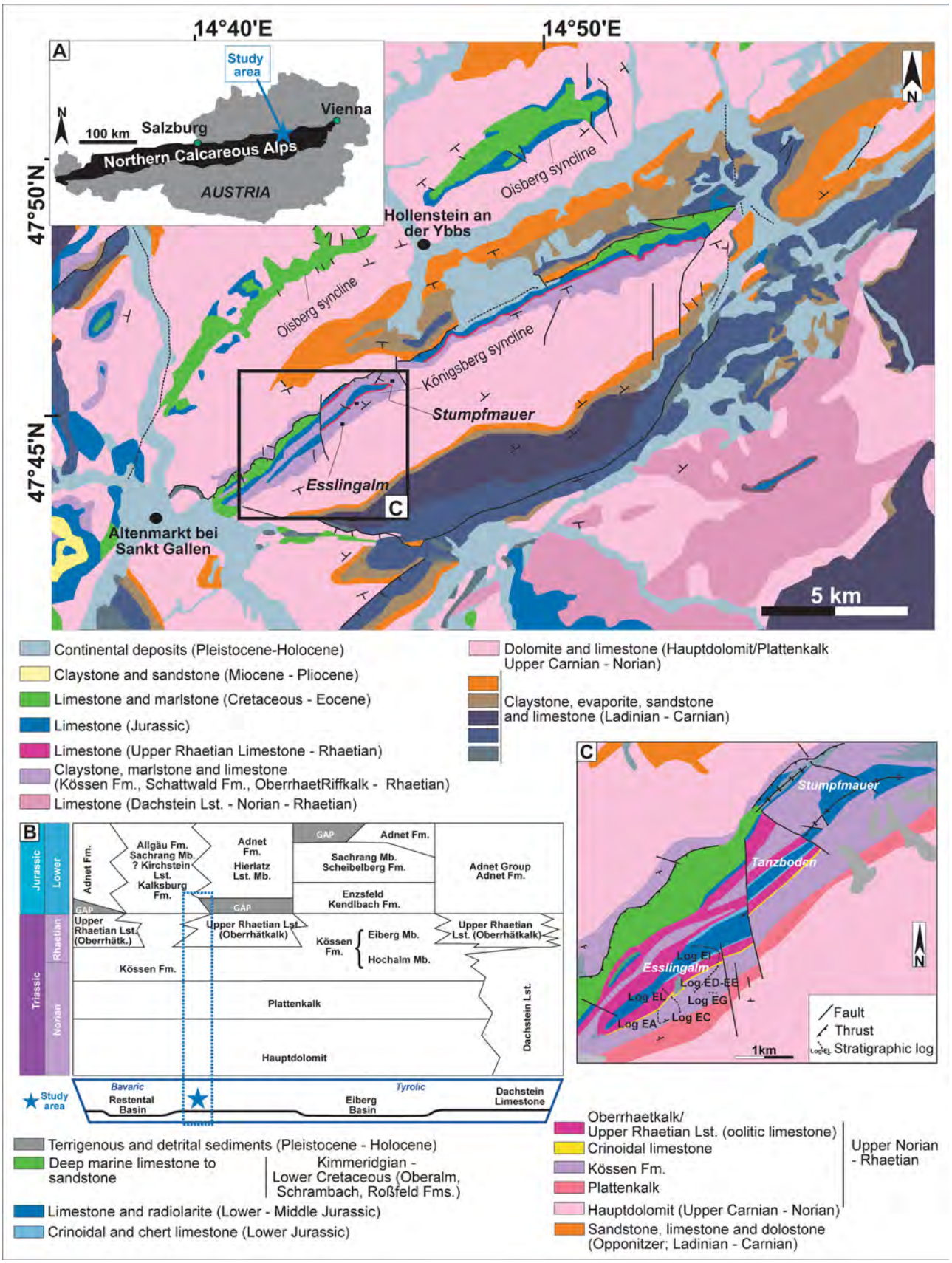
14°40'E
14°50'E
47°50'N
47°45'N
A
Study area
Vienna
Salzburg
100 km
Northern Calcareous Alps
AUSTRIA
N
Hollenstein an der Ybbs
Oisberg syncline
Königsberg syncline
Stumpfmauer
Esslingalm
C
Altenmarkt bei Sankt Gallen
5 km
Continental deposits (Pleistocene-Holocene)
Claystone and sandstone (Miocene - Pliocene)
Limestone and marlstone (Cretaceous - Eocene)
Limestone (Jurassic)
Limestone (Upper Rhaetian Limestone - Rhaetian)
Claystone, marlstone and limestone (Kössen Fm., Schattwald Fm., OberrhaetRiffkalk - Rhaetian)
Limestone (Dachstein Lst. - Norian - Rhaetian)
Dolomite and limestone (Hauptdolomit/Plattenkalk Upper Carnian - Norian)
Claystone, evaporite, sandstone and limestone (Ladinian - Carnian)
B
Jurassic
Lower
Triassic
Rhaetian
Norian
Adnet Fm.
Allgäu Fm.
Sachrang Mb.
? Kirchstein Lst.
Kalksburg Fm.
Hierlatz Lst. Mb.
GAP
Sachrang Mb.
Scheibelberg Fm.
Enzsfeld
Kendlbach Fm.
Adnet Group
Upper Rhaetian Lst. (Oberrhätk.)
Upper Rhaetian Lst. (Oberrhätkalk)
Kössen Fm.
Eiberg Mb.
Hochalm Mb.
Plattenkalk
Hauptdolomit
Dachstein Lst.
Study area
Bavaric
Restental Basin
Tyrolic
Eiberg Basin
Dachstein Limestone
C
Stumpfmauer
Tanzboden
Esslingalm
Log EI
Log ED-EE
Log EL
Log EG
Log EA
Log EC
1km
Fault
Thrust
Stratigraphic log
Terrigenous and detrital sediments (Pleistocene - Holocene)
Deep marine limestone to sandstone
Kimmeridgian - Lower Cretaceous (Oberalm, Schrambach, Roßfeld Fms.)
Limestone and radiolarite (Lower - Middle Jurassic)
Crinoidal and chert limestone (Lower Jurassic)
Oberrhaetkalk/ Upper Rhaetian Lst. (oolitic limestone)
Crinoidal limestone
Kössen Fm.
Plattenkalk
Hauptdolomit (Upper Carnian - Norian)
Sandstone, limestone and dolostone (Opponitzer; Ladinian - Carnian)
Upper Norian - Rhaetian

◂**Fig. 2** **A** Geological map of the study area (redrafted after Schnabel et al. 2002). Insert in the upper left corner shows the map of Austria with the location of the study area in the eastern NCA. **B** Chronostratigraphic scheme of the NCA proposed by Gawlick et al. (2009) reporting the nomenclature of the lithostratigraphic units in the study area. The blue dashed line rectangle marks the stratigraphic succession in the study area comprised between the Eiberg and Restental Basins. In grey stratigraphic gaps in the sedimentary succession (redrafted after Gawlick et al. 2009). **C** Geological map redrafted after Kreuss (2014) showing the investigated area between Esslingalm and Stumpfmauer peak in the Königsberg syncline with the location of the measured stratigraphic logs (redrafted after the GEOFAST *Geologische Bundesanstalt* 1:50,000, 100 – Hieflau compiled by Kreuss 2014)

dolomitized, carbonate unit, labelled as Plattenkalk (Steiner 1965a, b; Czurda and Nicklas 1970; Golebiowski 1989). Fruth and Scherreiks (1982, 1984) considered the Plattenkalk as part of the Hauptdolomit, representing its uppermost transitional calcareous portion.

Terrigenous input affected the carbonate shelf during the latest Norian–Rhaetian time with the deposition of the Kössen Fm., consisting of the Hochalm and the Eiberg members (Kuss 1983; Golebiowski 1989, 1990; Rizzi et al. 2020). The Hochalm Mb. represents an upper Norian–lower Rhaetian shallow-water succession, which was divided in four units by Golebiowski (1989). Units 1 and 2 (*Lumachellen realm*) consist of shallowing-upward cyclothems similar to those in the Hauptdolomit and Dachstein Limestone, at times capped by marlstone, indicative of an intertidal to open subtidal shelf. Unit 2 facies are similar to Unit 1 but indicative of more open marine conditions. The overlying Unit 3 is dominantly siliciclastic with marlstone and claystone alternating with metre-thick calcareous beds. Unit 3 documents a transgressive event at regional scale, corresponding to the maximum transgression of the Kössen Fm. onto the margin of the Dachstein Limestone shelf in the south, close to the Norian–Rhaetian boundary (Golebiowski 1989; Satterley 1996a, b). Unit 4 of the Hochalm Mb. is a massive, 10–20 m thick, laterally continuous unit rich in corals, labelled as *Hauptlithodendronkalk* (Suess and Mojsisovics 1868), *Lithodendronkalk* (Schlager and Schöllnberger 1974; Golebiowski 1989), or *Korallenkalke* (Kuss 1983) traceable for about 300 km across an E–W transect in the NCA (Golebiowski 1990). The overlying upper Rhaetian Eiberg Mb. represents deposition in an intraplatform basin of estimated water depth up to 150–300 m (Golebiowski 1990; Kaufmann 2009; Mette et al. 2012; Krystyn et al. 2005; Hillebrandt et al. 2013). The Eiberg Mb. is subdivided into 4 units, consisting of well-bedded bioclastic limestone rich in echinoderm debris passing upward to alternating calcareous mudstone and marlstone with *Zoophycus* burrows, documenting a deepening trend (Golebiowski 1989; Mette et al. 2012, 2016). The Eiberg Basin was lateral to shallow-marine carbonates (*Oberrhätkalk*/Upper Rhaetian Limestone; Figs. 1C, 2B) overlying the coral-rich Unit 4 of the Hochalm Mb. (Golebiowski 1990; Wegerer and Gawlick 1999; Bernecker 2005; Rizzi et al. 2020). The southern margin of the Eiberg Basin at the Steinplatte was interpreted as a distally steepened carbonate ramp formed by the deposition of autochthonous biogenic sediment (massive mound facies with bioclastic sand and shell coquinas) on an antecedent homoclinal ramp (Stanton and Flügel 1995; Flügel 2002), laterally adjacent to the Dachstein Limestone shelf (Kaufmann 2009).

The Triassic–Jurassic transition was affected by a sea-level fall followed by a long-term sea-level rise during the Hettangian (Kaufmann 2009; McRoberts et al. 2012), with the drowning of the Dachstein shelf (Gawlick et al. 2009; Gawlick and Missoni 2019). The early Jurassic extensional tectonics, leading to the opening of the Penninic Ocean, produced half-graben basins and structural highs (Bernoulli and Jenkyns 1974; Eberli 1988; Manatschal and Bernoulli 1999) with condensed successions accumulated on footwall highs (i.e. Kalksburg Fm., Adnet Fm., Hierlatz Limestone Mb., Allgäu Fm.) between the Hettangian and early Toarcian, followed by Middle–Upper Jurassic pelagic deposits (Ruhpolding Radiolarite Group; upper Bajocian–lower Tithonian; Eberli 1988; Böhm et al. 1995; Ebli 1997; Gawlick et al. 2009).

Stratigraphy of the study area

The study area between the Stumpfmauer and Esslingalm is part of the Königsberg syncline (Fig. 2; Mandl 2000; Schnabel et al. 2002; Strauss et al. 2020). Steiner (1965a, b, 1967) identified the following units above the Hauptdolomit, from base to top: (1) 100 m of partly dolomitized limestone beds, attributed to the Plattenkalk (uppermost Norian); (2) 30 m of marlstone alternating with highly fossiliferous limestone, labelled as *Mergel- und fossilreiche Kössener Schichten* (Kössen Beds, Rhaetian); (3) 60 m of well-bedded limestone with corals and marlstone (*Kössener Schichten, Hauptlithodendronkalk, Mergellagen*); (4) 2 m of crinoid-rich limestone (*Krinoidenkalk* marker bed, upper Rhaetian); (5) 30 m of oolitic limestone labelled by Steiner (1967) as *Oberrhätkalk* (*heller, dickbankiger Oberrhät Oolithkalk*, also reported as *Pseudoolithkalk*). According to Steiner (1967), in the study area, the *Oberrhätkalk*/Upper Rhaetian Limestone consists of micrite coated grains,

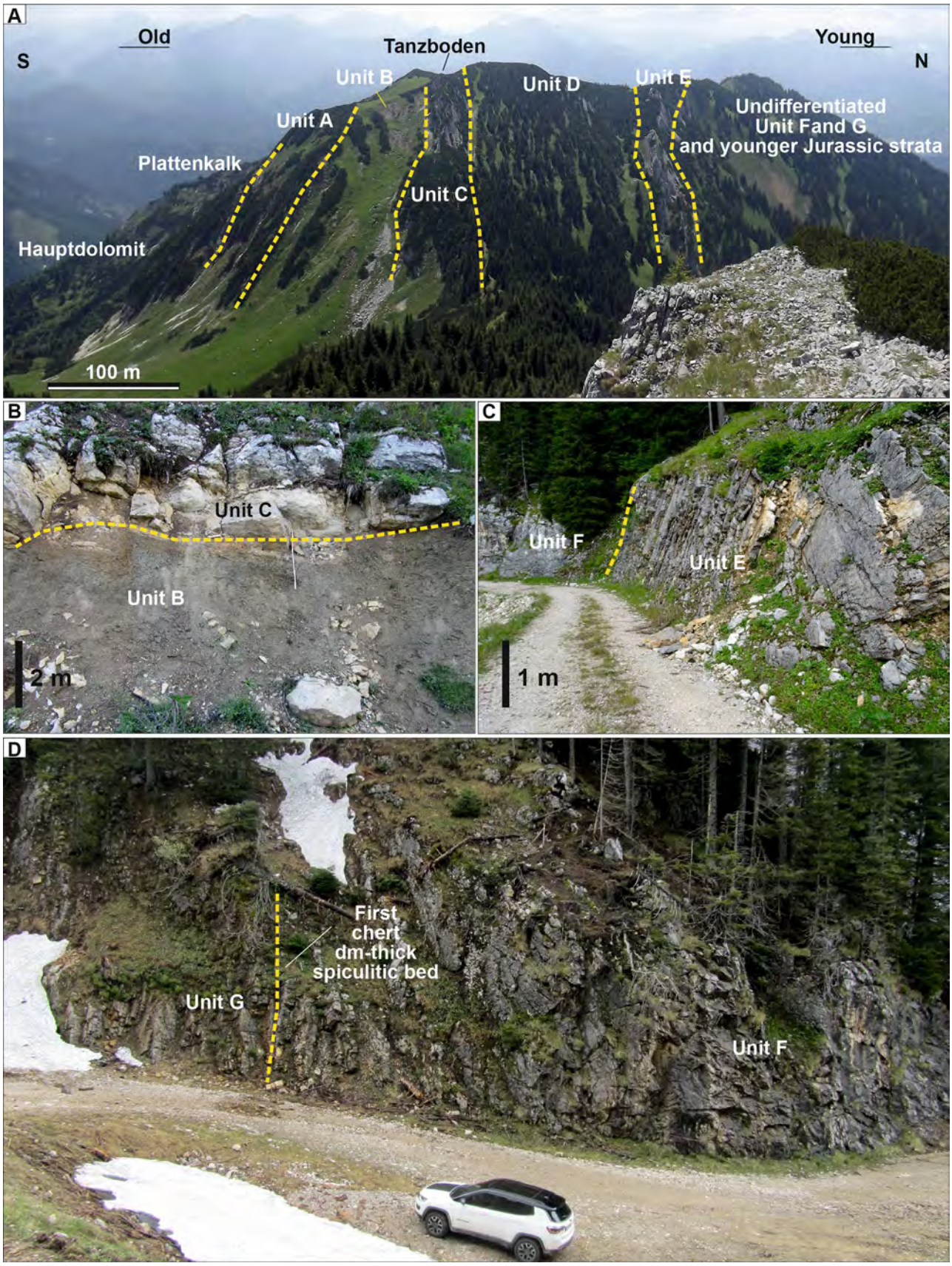
A
Old
S
Tanzboden
Young
N
Unit B
Unit D
Unit E
Unit A
Undifferentiated
Unit F and G
and younger Jurassic strata
Plattenkalk
Unit C
Hauptdolomit
100 m
B
Unit C
Unit B
2 m
C
Unit F
Unit E
1 m
D
First
chert
dm-thick
spiculitic bed
Unit G
Unit F

◂**Fig. 3** **A** Panoramic view of the studied succession at Tanzboden, SW of the Stumpfmauer peak (see Fig. 2C for location), with yellow dashed lines marking the boundaries between the distinguished sedimentary units. **B** Outcrop photo showing the boundary between Unit B marlstone/claystone and the overlying coral boundstone of Unit C in Log EC at 3.55 m. **C** Outcrop photo showing the boundary between Unit E and the overlying Unit F in Log EI at 57 m with different bedding attitude suggesting an angular unconformity. **D** Outcrop photo of the upper part of Log EI showing the boundary between Units F and G at 95.10 m in Log EI. Legend and key of the stratigraphic logs reported in Figs. 4 and 5

aggregate grains, peloidal and ooidal grainstone facies. Nevertheless, the Upper Rhaetian Limestone in the southern margin of the Eiberg Basin includes coral and calcareous sponge reefs, reef mounds and bioclastic facies (Bernecker 2005; Krystyn et al. 2005; Kaufmann 2009). The Kreuss (2014) GEOFAST geological map (Fig. 2C) confirms the mapping proposed by Steiner (1967) and does not provide a nomenclature of the Lower Jurassic lithostratigraphic units.

Methods

The Norian–Lower Jurassic succession was investigated from the Esslingalm area to the Stumpfmauer peak in the Königsberg syncline (Figs. 2C, 3). Six stratigraphic logs (Figs. 4, 5) were measured: Log EA (103 m thick), Log EC (31 m thick), Log EG (54.7 m thick), Log EL (34.5 m thick), Log ED–EE (117.9 m thick) and Log EI (129.4 m thick). More than 330 thin sections were analysed through standard petrographic analysis. Staining with alizarin red and potassium ferricyanide (Dickson 1966) was performed to identify the presence of dolomite and ferroan calcite. Detailed information about sample location is reported in the Online Supplementary Information.

Results

The logged succession (Figs. 3, 4, 5) consists of 32 lithofacies types, labelled from F1 to F32 (Table 1). Associations of these lithofacies compose seven vertically superimposed sedimentary units, labelled from base to top as Units A–G (Table 2), spanning the upper Norian to lower Jurassic. The investigated sedimentary succession overlies hundreds of metres of massive to decimetre-thick beds of replacive fabric-retentive to destructive dolomite (Hauptdolomit) and partially dolomitized (Plattenkalk) peritidal inner shelf carbonates (Fig. 2C).

Unit A

Unit A includes lithofacies from F1 to F10 and F20. Bioturbated calci-mudstone with rare peloids and skeletal fragments (F1; Fig. 6A) can occur replaced by dolomicrite to anhedral non-planar dolomicrosparite (F1D), at the base of log EA (Fig. 4). Skeletal wackestone to packstone (F2), sometimes dolomitized (F2D), contains bivalves, gastropods, brachiopods, aulotortid foraminifera and reworked lithoclasts (Fig. 6B). Wackestone to packstone beds with ostracods (F3) are associated with centimetre-thick claystone intervals (Fig. 6C). Peloidal calci-mudstone/wackestone to packstone with fenestrae (F4) and laminated stromatolite boundstone (F5) alternate and occur capped by erosional surfaces (Fig. 6D–F). Lithofacies F6 represents skeletal wackestone/packstone to floatstone/rudstone with brachiopods and bivalves (including decimetre-size megalodontids), gastropods and aulotortid foraminifera (Fig. 6G). The label F7 is used to address all the fine-grained siliciclastic deposits (claystone, marlstone, argillaceous mudstone) forming millimetre, decimetre to metre-scale beds (Fig. 3B). Skeletal peloidal packstone (F8) includes bivalves, gastropods, foraminifera (aulotortids, duostominids, textulariids, *Triasina hantkeni)*, and dasyclad algae (Fig. 6H). Bioturbated packstone with moulds of ooids with peloids as nuclei characterises lithofacies F9 (Fig. 7A). Grainstone beds with isopachous rims of fibrous marine cement (F10) contain micrite coated grains, radial ooids, aggregate grains, intraclasts, foraminifera (*Aulotortus* sp., *Triasina hantkeni*) and peloids (Fig. 7B). Unit A includes also beds of packstone/rudstone with reworked bioclasts, lithoclasts and intraclasts of lithofacies F1, F2, F4 and F5, overlying erosional surfaces (F20; Fig. 6D).

Unit A (38–55 m thick) is organised in vertically stacked, metre-scale (2–10 m thick) lithofacies packages (Fig. 4) with basal F1, F2, F3, F6, F8 and top F4, F5, F9, F10 separated by erosional surfaces, few millimetres to centimetres thick claystone (F7) and lithoclastic beds (F20; Fig. 6D). The lower boundary of Unit A with the Plattenkalk is transitional and placed at the first

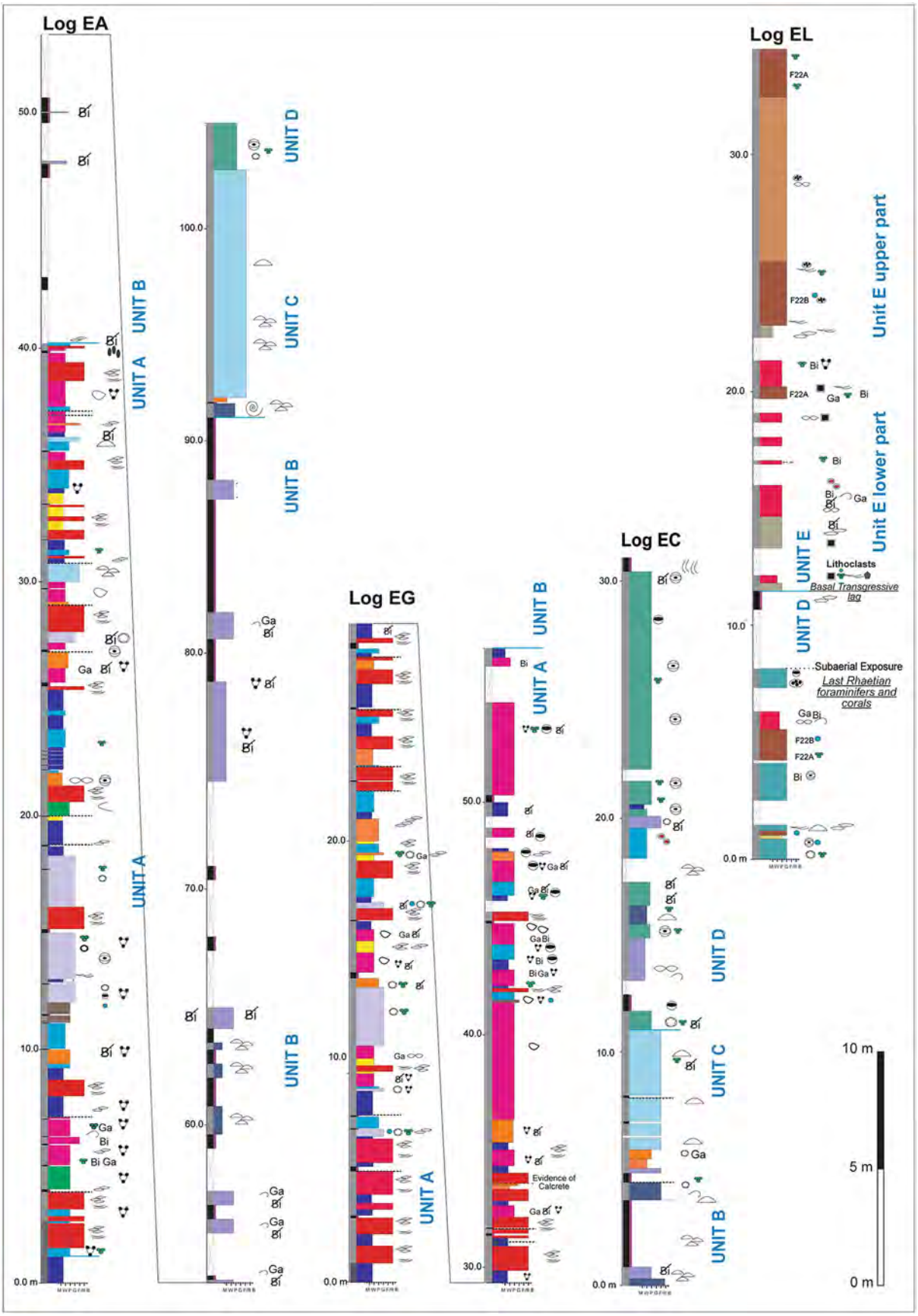
Log EA
Log EG
Log EC
Log EL
UNIT A
UNIT B
UNIT C
UNIT D
UNIT E
Unit E upper part
Unit E lower part
Lithoclasts
Basal Transgressive lag
Subaerial Exposure
Last Rhaetian foraminifers and corals
Evidence of Calcrete
10 m
5 m
0 m

◀ **Fig. 4** Stratigraphic logs EA, EG, EC and EL measured in the Esslingalm area (see Fig. 2C for location) showing the superimposed lithofacies types grouped in the sedimentary units A, B, C, D and E. Legend for Figs. 4 and 5 is reported in a separate page

metre-scale intercalation of claystone, associated with the gradual disappearance of dolomitized beds, whereas the upper boundary with Unit B is sharp and marked by the onset of the ~ 50 m thick claystone/marlstone succession (F7).

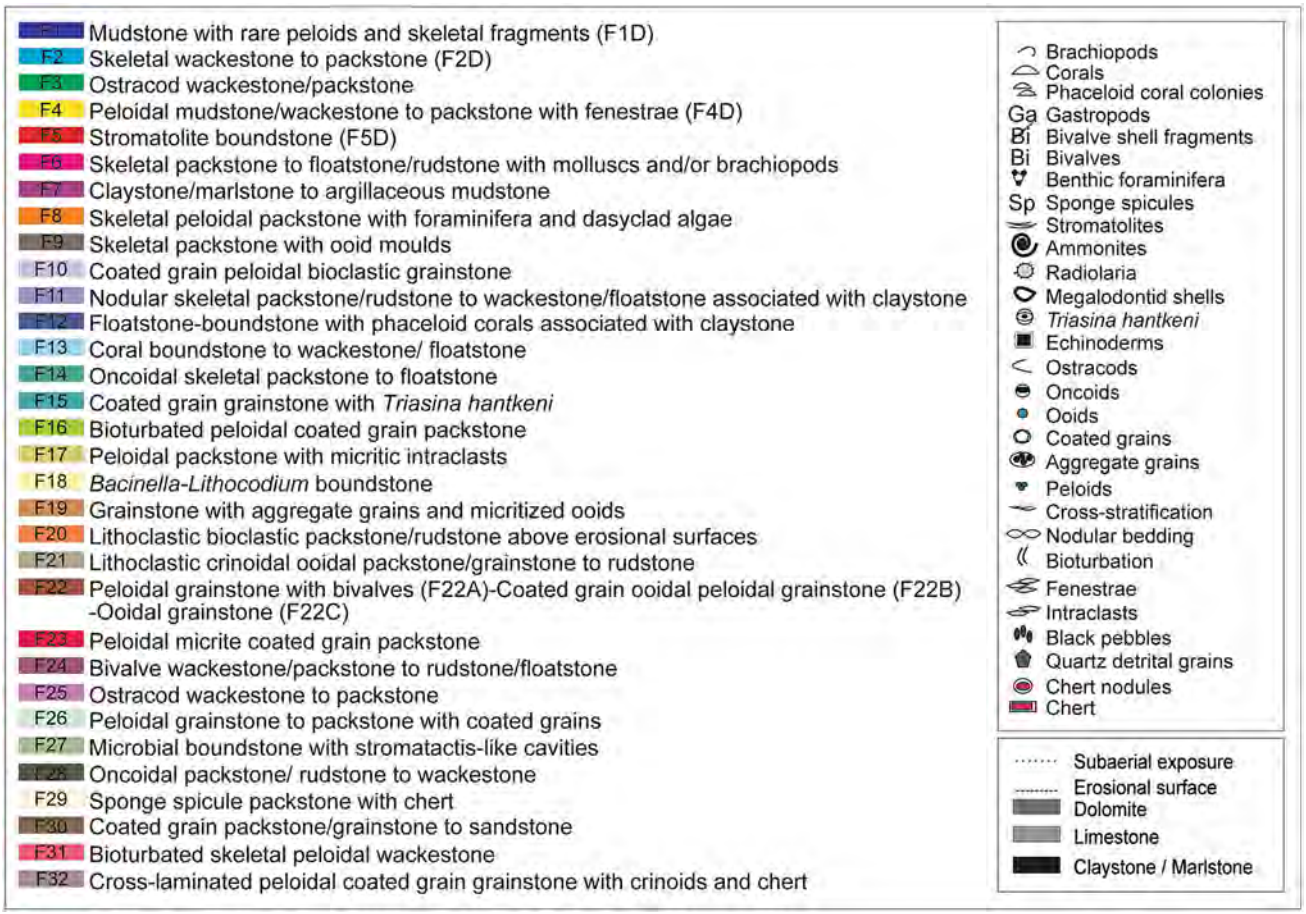

Fig. 4 (continued)

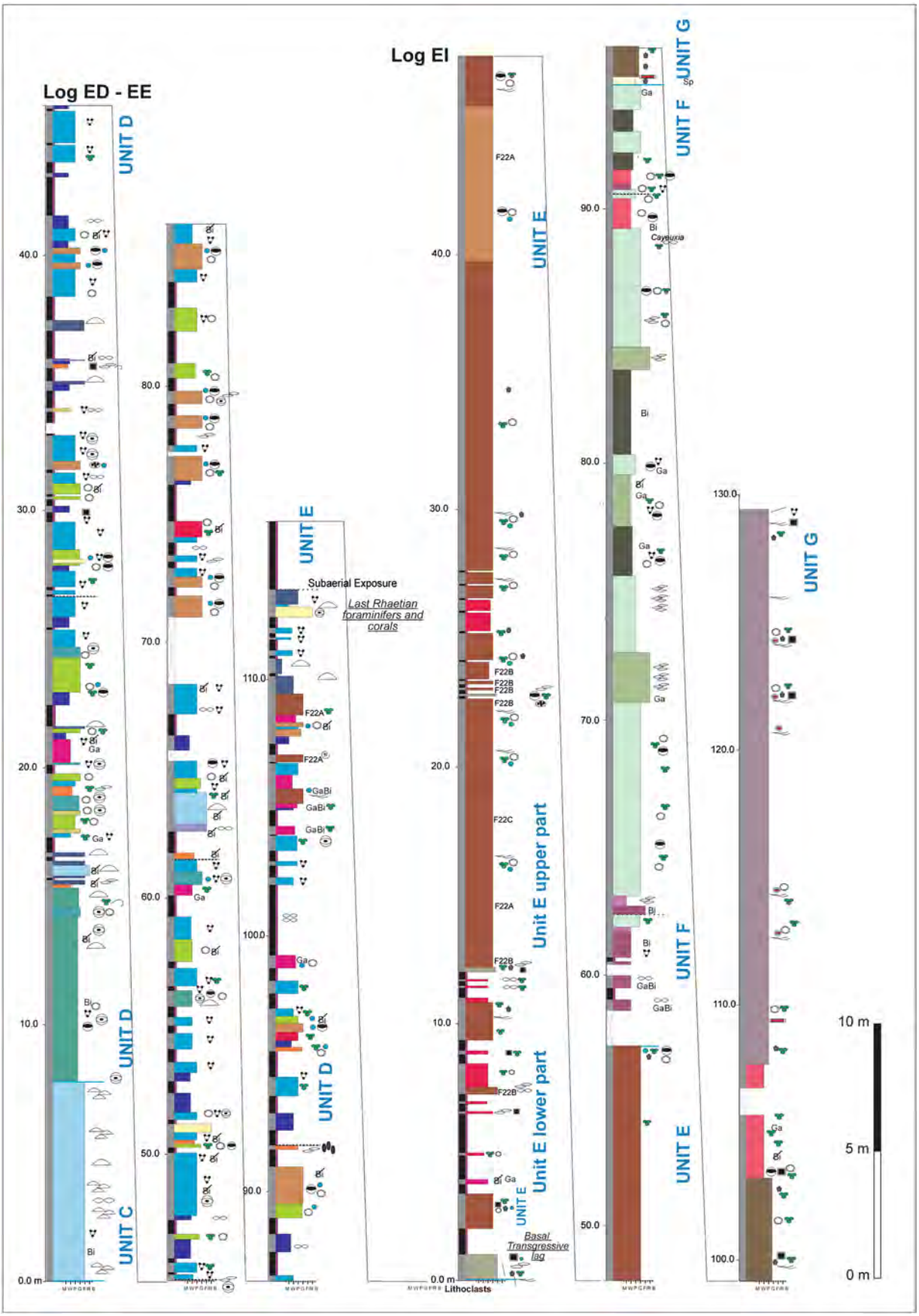
Log ED - EE
Log EI
UNIT D
UNIT C
UNIT E
UNIT F
UNIT G
Subaerial Exposure
Last Rhaetian foraminifers and corals
Unit E upper part
Unit E lower part
Basal Transgressive lag
Lithoclasts
10 m
5 m
0 m

◂**Fig. 5** Stratigraphic logs ED–EE and EI measured in the Esslingalm area (see Fig. 2C for location) showing the superimposed lithofacies types grouped in sedimentary units C, D, E, F and G. Legend for Figs. 4 and 5 is reported in a separate page

Unit B

Unit B (Figs. 3A, B, 4) consists of brown to black claystone and marlstone (F7) alternating with 0.5–1 m thick calcareous beds (F11, F12). Lithofacies F11 consists of nodular beds of bioturbated skeletal wackestone/floatstone to packstone/rudstone with common bivalves, brachiopods, gastropods and echinoderms (Fig. 7C). Phaceloid coral boundstone to floatstone (F12) forms decimetre to metre-thick beds. *Retiophyllia* and *Thecosmilia*-type corals are sometimes encrusted by *Bacinella-Lithocodium* or serpulids and occur in marly skeletal wackestone/packstone with crinoids, brachiopods, rare calcareous and siliceous sponges and ammonoids (Figs. 7D, H, 8A).

Unit B is approximately 50 m thick but tectonic displacement prevents a reliable estimate of the thickness. The lower and upper boundaries are sharp (Fig. 3B).

Unit C

Unit C consists of metre-scale massive boundstone and floatstone with corals (F12, F13) associated with lithofacies F8, F11 and F20. Phaceloid corals form decimetre- to metre-scale colonies (Fig. 8B). Corallites are often encrusted by *Bacinella-Lithocodium* and surrounded by wackestone/packstone with bivalves, gastropods, brachiopods, calcareous and siliceous sponges (Fig. 8B, C); rare chert nodules are present.

Unit C (8–11 m thick) basal and top boundaries are sharp (Fig. 3B). Siliciclastic input is rare and occurs only at the base.

Unit D

Unit D consists of lithofacies F1, F2, from F6 to F20, and F22 organised in 2–5 m thick stacked lithofacies packages separated by metre-thick intervals of claystone/marlstone (F7; Fig. 5). Unit D distinctive lithofacies are: (a) packstone–wackestone to floatstone with oncoids and abundant aulotortid and *Triasina hantkeni* foraminifera (F14; Fig. 8D); (b) coated grain grainstone with cross-lamination, micrite coated *Triasina hantkeni*, molluscs and rare calcareous and siliceous sponges and corals with isopachous fibrous marine and meniscus and pendant cement (F15; Fig. 8E, F)*;* and (c) bioturbated packstone with micrite coated grains, aggregate grains and peloids (F16; Fig. 8G). Rare packstone with peloids and micritic intraclasts (F17; Fig. 8H) forms decimetre-thick irregular beds. *Bacinella-Lithocodium* boundstone (F18) is characterised by clotted peloidal micrite, rare corals, siliceous and calcareous sponges and millimetre-wide, irregular-shaped voids filled by blocky sparite cement (Fig. 9A, B). Grainstone to rarely packstone with abundant aggregate grains contains micritized ooids and coated grains with micrite envelopes, bivalves, gastropods, *Triasina hantkeni* and *Parafavreina* (F19; Fig. 9C, D). Beds of packstone/rudstone with reworked intraclasts and lithoclasts overlie erosional surfaces (F20; Fig. 9E). Decimetre-thick beds of cross-laminated coated grain ooidal grainstone (F22) also occur.

Unit D is 80–110 m thick with the lower boundary with Unit C marked by a sharp transition from massive coral boundstone (F13) to several metres-thick oncoidal skeletal packstone/floatstone (F14). The upper boundary with Unit E is characterised by an erosional surface at the top of Unit D, overlying both coated grain grainstone with *Triasina hantkeni* (F15, Log EL; Fig. 4) and boundstone to floatstone with phaceloid corals associated with claystone (F12, Log ED; Fig. 5) with irregular dissolution vugs, vadose pendant and meniscus cement and red iron oxide stained micritic crusts (Fig. 8F).

Unit E

Unit E constitutes a prominent ridge, forming the crest of the Stumpfmauer (Fig. 3A). This unit (57 m thick) is subdivided into a lower and upper part. The lower part (13 m thick) is characterised by packstone/grainstone to rudstone beds (up to 1 m thick) with centimetre-size rounded lithoclasts, partially silicified, radial ooids, micrite coated grains, peloids, abundant crinoids and bivalves (F21; Figs. 9F–H, 10A). Lithoclasts are mostly ooidal grainstone (F22) with isopachous fibrous marine cement followed by meniscus and pendant cement. The F21 basal bed is overlain by claystone (F7) and fine-grained bioturbated peloidal packstone with siliceous sponge spicules (F23; Fig. 10B, C). The upper part of Unit E (45 m thick) consists of grainstone with aggregate grains (F19)

Table 1 Descriptions of the lithofacies from F1 to F32 identified in the studied succession

Lithofacies	Texture	Grain size	Non skeletal grains	Skeletal grains	Bedding and sedimentary structures	Diagenetic features
D1 Replacive fabric-destructive dolomite	Dolostone (dolomicrosparite and dolosparite)	–	–	–	10–20 cm thick to m-scale massive beds	Non-planar anhedral to planar euhedral mosaics. Dolomite crystal size 20–100 µm Saddle dolomite cement in voids
F1 (F1D) Calci-mudstone with rare peloids and skeletal fragments	Calci-mudstone with terrigenous clay input, sometimes associated with mimetic dolomicrite replacement (F1D)	Well sorted, 30–250 µm	Peloids	Bivalve and brachiopod fragments. Rare ostracods and benthic foraminifera (mostly hyaline taxa, e.g. nodosariids, *Frondicularia*), calcispheres, echinoid spines and crinoid fragments	10 cm to 1 m thick beds Bioturbation Bedding parallel lamination	Mechanical compaction and pressure solution. Micrite recrystallized into microsparite. Dolomicrite replacement
F2 (F2D) Skeletal wackestone to packstone	Wackestone to fine-grained packstone F2 may be completely dolomitized by mimetic dolomicrite and dolomicrosparite with anhedral non-planar mosaics (F2D)	Poorly sorted, 30–400 µm	Peloids; carbonate lithoclasts reworked during transgression from underlying F1 calci-mudstone or F5 stromatolite boundstone	Bivalves, gastropods, brachiopods, ostracods, echinoid spines. Common biomoulds of benthic foraminifera (hyaline nodosariids, textulariids, and *Aulotortus* sp., *Valvulina azzouzi*, *Frondicularia*, *Mililiopora*, *Gandinella appenninica*, *Reophax* sp., *Triasina hantkeni*)	10–50 cm thick beds. sub-horizontal lamination Bioturbation	Mechanical compaction and pressure solution, commonly deformed skeletal components Locally dissolution vugs indicative of subaerial exposure are filled by burial blocky calcite cement; vadose meteoric meniscus and pendant cement may occur
F3 Ostracod wackestone/packstone	Wackestone to packstone alternating with mm thick layers of claystone	Moderately sorted, 30–100 µm	Lithoclasts of F1, F4, F5; oncoids	Ostracods, bivalves and benthic foraminifera	10–50 cm thick beds	Mechanical compaction and pressure solution
F4 (F4D) Peloidal calci-mudstone/wackestone to packstone with fenestrae	Peloidal calci-mudstone to wackestone or packstone with mm-size fenestrae and locally bed-parallel stromatolite lamination, sometimes dolomitized by replacive mimetic dololomicrite and dolomicrosparite. (F4D)	Well sorted, 10–20 µm	Peloids, intraclasts	Ostracods, rare bivalves and gastropods. Sparite-filled biomoulds of calcispheres	10–40 cm thick beds Parallel lamination of clotted peloidal micrite	Meniscus micrite, vadose meteoric cement. Fenestral porosity filled by burial blocky sparite or poikilotopic calcite. Evidences of mechanical compaction and pressure solution
F5 (F5D) Stromatolite boundstone	Laminated stromatolite microbial boundstone with mm-size fenestrae, sometimes dolomitized (F5D). Stromatolite laminae consist of leiolitic (structureless) or clotted peloidal micrite	Well sorted, 10–20 µm	Peloids	Ostracods, gastropods, biomoulds of benthic foraminifera	15–50 cm thick to m-scale beds	Fenestral porosity filled by blocky sparite or poikilotopic calcite. In some cases, burial cement preceded by pendant micritic cement indicative of meteoric vadose diagenesis. Replacive mimetic dololomicrite and dolomicrosparite
F6 Skeletal packstone to floatstone/rudstone with molluscs and/or brachiopods	Skeletal wackestone/packstone to floatstone/rudstone with bivalves, gastropods and/or brachiopods and benthic foraminifera	Poorly sorted, 30–500 µm	Peloids, lithoclasts of lithofacies F1, F5 and black pebbles	Bivalves (including dm-size megalodontids), gastropods, brachiopods (terebratulids, e.g. *Rhaetina gregaria*). Sparse foraminifera (*Aulotortus gaschei*, *Parvalamella friedli Aulotortus* sp., *Auloconus*, *Austrocolomia*, *Gandinella apenninica, Miliolipora, Glomospira, Glomospirella)*	Parallel planar to planar cross-bedding beds 20–80 cm thick	2–5 mm wide, convex-up bivalve shells produce shelter porosity, filled by drusy or blocky sparite

Table 1 (continued)

Lithofacies	Texture	Grain size	Non skeletal grains	Skeletal grains	Bedding and sedimentary structures	Diagenetic features
F7 Claystone/marlstone to argillaceous mudstone	Claystone/marlstone to argillaceous mudstone	Well sorted	Detrital quartz silt. Peloids	Faecal pellets, bivalves (*Rhaetavicula contorta*) and echinoderms	From mm- to dm- and m-scale beds poorly exposed, up to 50 m thick. Bioturbation	Mechanical compaction and pressure solution
F8 Skeletal peloidal packstone with foraminifera and dasyclad algae	Skeletal peloidal packstone with bivalves, common foraminifera and gastropods and sparse dasyclad algae	Poorly sorted, 30–500 µm to 1 mm	Peloids	Common mm-size bivalve and gastropods, benthic foraminifera (*Aulotortus* sp., *Aulotortus sinuosus*, *Gandinella*, *Glomospirella, Frondicularia*, duostominids, textulariids, *Triasina hantkeni*) and dasyclad algae (e.g. *Griphoporella curvata, Acicularia*); sparse crinoids, echinoid spines and ostracods	3–60 cm thick beds	Some beds are affected by meteoric diagenesis with vadose meniscus cement occurring below erosional surfaces
F9 Skeletal packstone with ooid moulds	Packstone to wackestone with superficial ooid moulds, rare benthic foraminifera and lithoclasts	Moderately sorted (100–500 µm)	Superficial ooid moulds, likely originally aragonitic, 100–200 µm in size with dissolved cortex replaced by sparite and preserved peloidal nuclei. Lithoclasts of F4. Peloids	Fragments of bivalves and gastropods. Foraminifera (*Aulotortus tumidus)*	dm-scale beds alternating with claystone. Sometimes nodular beds with stylolitized contacts. Bioturbation	Mouldic coated grains associated with coarse (mm-size, up to 1 cm), totally recrystallized bivalve shells and gastropods. Both bio- and oo-mouldic porosity filled by blocky sparite
F10 Coated grain peloidal bioclastic grainstone	Grainstone with cortoid, micrite coated grains, ooids (also with radial fibrous arrangement) and skeletal fragments	Moderate to well sorted (10–500 µm to 1 mm)	Micrite coated grains/cortoids with micrite envelopes, radial ooids, peloids. Intraclasts and lithoclasts	Up to 1 cm-wide bivalve shell fragments or gastropods sometimes isoriented Foraminifera (*Aulotortus, Triasina hantkeni*)	10–50 cm thick beds. Cross-lamination	Compaction (i.e. pressure solution seams, stylolites), well cemented by marine isopachous rims of fibrous cement followed by burial blocky sparite
F11 Nodular skeletal packstone/rudstone to wackestone/floatstone associated with claystone	Nodular, highly fossiliferous, wackestone/floatstone to packstone/rudstone embedded within claystones or marlstone	Poorly sorted (1–500 µm to several cms)	Peloids, faecal pellets, oncoids and cortoids with micrite envelopes	Bivalves (e.g. *Rhaetavicula contorta*), gastropods, ammonoids, brachiopods and echinoderms. In some cases, phaceloid corals crinoids and echinoid debris (echinoid spines and whole tests), benthic foraminifera (*Gandinella, Frondicularia, Gandinella, Glomospirella, Austrocolomia*), siliceous sponges	Nodular irregular 0.5–1 m thick beds within siliciclastic argillaceous/marly successions. Burrows due to bioturbation	Compaction (i.e. pressure solution seams, stylolites) and blocky calcite cements
F12 Boundstone to floatstone with phaceloid corals associated with claystone	Boundstone to floatstone with phaceloid *Retiophyllia* and *Thecosmilia*-type corals or as recumbent fragments. Corals surrounded by marly skeletal wackestone/packstone with crinoids, brachiopods, benthic foraminifera and ammonoids. Corals encrusted by *Bacinella* and *Lithocodium*	Poorly sorted (200–500 µm to 2 mm)	Peloids	10–50 cm-wide colonies of phaceloid corals (e.g. *Parathecosmilia sellae*/*Retiophyllia paraclathrata*), in some cases in life position, bivalves, gastropods, brachiopods, crinoids, echinoid spines, serpulids, rare calcareous and siliceous sponges, ostracods, benthic foraminifera (*Frondicularia, Trocholina Tetrataxis)*, ammonoids	Dm to m-scale beds, sometimes intercalated with claystone and marlstone. Bioturbation	Corallites poorly preserved/recrystallized replaced by blocky sparite; some corallites exhibit brown colour marine isopachous cement within the septa. Compaction produced pressure solution seams/stylolites (e.g. the edges of the corals are sutured in some cases)

Table 1 (continued)

Lithofacies	Texture	Grain size	Non skeletal grains	Skeletal grains	Bedding and sedimentary structures	Diagenetic features
F13 Coral boundstone to wackestone/floatstone	Metre-scale to massive wackestone/floatstone to boundstone with recrystallized phaceloid corals. Coral colonies surrounded by skeletal wackestone/packstone. Corals encrusted by *Bacinella* and *Lithocodium*	Poorly sorted (200–500 µm to 2 mm)	Peloids, oncoids and rare chert nodules	*Retiophyllia* and *Thecosmilia*-type phaceloid corals. Corals are sometimes encrusted by *Bacinella-Lithocodium* and serpulids. bivalves, gastropods, brachiopods, ostracods, benthic foraminifera (*Frondicularia*, *Trocholina* sp., *Auloconus*, *Aulotortus sinuosus, A. tumidus*, *Triasina hantkeni, Tetrataxis, Glomospirella),* rare calcareous and siliceous sponges, solenoporaceans, rare dasyclad algae (*Griphoporella, Acicularia)*, rare *Thaumatoporella parvovesiculifera*, crinoids, echinoid spines, sponge spicules, faecal pellets	Massive 1–1.5 m thick limestone beds	Phaceloid corals affected by pervasive recrystallization because of their original aragonitic mineralogy. Both sparse fragments and the dm-size colonies have been replaced by blocky or drusy sparite
F14 Oncoidal skeletal packstone to floatstone	Packstone–wackestone to floatstone, with oncoids, cortoids/micrite coated grains, foraminifera (*Triasina hantkeni)* and rare coral fragments encrusted by *Bacinella-Lithocodium*	Poorly sorted (30–500 µm to 1 mm)	Oncoids (mm-size), micrite coated grains, peloids, sub-mm wide micritic intraclasts Shell fragments may be strongly micritized, producing cortoids or with thick micritic possibly biogenic envelopes producing oncoids	Benthic foraminifera (*Triasina hantkeni*, *Aulotortus* sp., *Frondicularia, Trocholina,* duostominids*).* commonly partly micritized and coated exhibiting micritic envelopes. Brachiopods, bivalve shells, gastropods, crinoids, echinoid spines, coral fragments coated by *Bacinella-Lithocodium*, sub-mm wide, fragmented dasyclad algae (*Acicularia, Griphoporella*), *Thaumatoporella parvovesiculifera*	10–50 cm thick beds. Nodular	Skeletal fragments may be completely replaced by blocky sparite, likely corresponding to shells or phaceloid corals that have been seriously affected by pervasive recrystallization because of a potentially former aragonitic mineralogy
F15 Coated grain grainstone with *Triasina hantkeni*	Foraminiferal grainstone, with common micrite coated grains and coated *Triasina hantkeni*	Moderately sorted (500 µm to 1 mm)	Peloids are common; in some cases, radial partly micritized ooids can occur (Log EC, EL) and reworked carbonate lithoclasts	*Triasina hantkeni, Aulotortus* spp. (including *A. sinuosus, A. tumidus*), *Auloconus*, *Glomospirella* sp., *Gandinella* sp., *Trocholina*. Tests of foraminifera are at times totally dissolved and partly micritized, displaying micritic envelopes. Echinoid spines, crinoid fragments, fragmented dasyclad algae thalli, and sub-mm wide bivalves, gastropods and coral fragments may occur	10–40 cm thick beds, sometimes nodular and irregular. Cross-bedding, cross-lamination, fining-upward trend	Concavo-convex grain contacts due to compaction. Interparticle space filled by marine isopachous fibrous and burial blocky sparite cement. Meteoric diagenesis with dissolution and micritic meniscus vadose cement
F16 Bioturbated peloidal coated grain packstone	Bioturbated packstone to locally grainstone (in burrows) with peloids, micrite coated grains, aggregate grains and skeletal grains	Poorly sorted (30–500 µm)	Peloids, faecal pellets, aggregate grains and micrite coated grains	Fragments of bivalves, gastropods, dasyclad alga *Acicularia*, benthic foraminifera (nodosariids, *Aulotortus* sp., *Triasina hantkeni*, *Ammobaculites rhaeticus)*	5–50 cm thick irregular and nodular beds. Bioturbation	Blocky to microsparite calcite cement

Table 1 (continued)

Lithofacies	Texture	Grain size	Non skeletal grains	Skeletal grains	Bedding and sedimentary structures	Diagenetic features
F17 Peloidal packstone with micritic intraclasts	Bioturbated compacted packstone with peloids and micritic intraclasts with quartz silt	Well sorted (50–500 µm)	Silt-sized quartz crystals in intraclasts. Micritic intraclasts have irregular shapes, angular, deformed due to mechanical compaction. They are commonly coated, exhibiting micritic envelopes. Peloids	Rare sub-mm size mollusc fragments and rare benthic foraminifers (*Glomospirella)*	10–20 cm thick irregular beds. Surfaces are generally undulated. Bioturbation	Compaction (e.g. pressure solution seams, concavo-convex grain contacts); interparticle space partly filled by micrite or microsparite or blocky sparite post-dating compaction
F18 *Bacinella–Lithocodium* boundstone	*Bacinella–Lithocodium* microbial boundstone with *Entobia* borings made of clotted peloidal and leiolitic micrite		Peloids	*Bacinella irregularis. Lithocodium aggregatum*, *Thaumatoporella parvovesiculifera*, rare corals, rare siliceous and calcareous sponges Some cavities, exhibiting a globular shape, likely resulted from borings by sponges (ichnogenus *Entobia*) encrusting microbialite crusts	40 cm thick massive beds	Elongated, irregularly shaped, 5–10 mm wide voids filled by blocky sparite. In some cases, cavities correspond to geopetal structures, having clotted peloidal micrite at the bottom
F19 Grainstone with aggregate grains	Grainstone to locally packstone with aggregate grains, coated grains with micrite envelops, micritized ooids and rare radial ooids	Well- to moderately sorted (500 µm to 1 mm)	Aggregate grains, micritized ooids, micrite coated grains, rare radial ooids, peloids. Micritic intraclasts Detrital quartz grains and silicified lithoclasts (only in Unit E)	Fragments of bivalves, gastropods, brachiopods, crinoids, benthic foraminifera only in Unit D (*Triasina hantkeni, Trocholina* sp., *Aulotortus* sp., *Aulotortus sinuosus*, *Auloconus)*	20–40 cm thick beds	Isopachous rims of fibrous marine cement; the remaining interparticle space filled by burial blocky sparite. In packstone, microsparitic/micritic matrix in interparticle porosity
F20 Lithoclastic intraclastic packstone/rudstone above erosional surfaces	Packstone/rudstone with lithoclasts, and intraclasts F20 overlies erosional subaerial exposure surfaces	Poorly sorted (1–10 mm)	Angular to sub-rounded lithoclasts (black pebbles, stained by Fe–Mn oxides), siliciclastic extraclasts and intraclasts of various sizes (F1, F2, F4, F5). Peloids, sub-mm wide micritic grains. Detrital monocrystalline quartz grains only in Unit E siltstone, and terrigenous clay input	Fragments of bivalves, echinoderm debris (crinoids and echinoid spines), abraded foraminifera (*Triasina hantkeni*, biomoulds of aulotorids, e.g. *Auloconus, Aulotortus*)	1–10 cm. F20 grades into lithofacies F2, F6, F11, F17	Mechanical compaction with lithoclasts with sutured grain contacts

Table 1 (continued)

Lithofacies	Texture	Grain size	Non skeletal grains	Skeletal grains	Bedding and sedimentary structures	Diagenetic features
F21 Lithoclastic crinoidal ooidal packstone/grainstone to rudstone	Packstone/grainstone to rudstone with mm- to cm-size rounded lithoclasts	Poorly sorted (30–500 µm to 10 cm)	Rounded lithoclasts (from a few mm to several cm in size, ooidal grainstone/packstone with meteoric meniscus cement; black pebbles, calci-mudstone) with reworked radial ooids, micrite coated grains, peloids, pisoids, recrystallized or silicified ooids as reworked grains as well. Detrital quartz grains	Bivalve, gastropods, ostracods, brachiopods, siliceous sponge spicules,. Abundant crinoid ossicles (up to 1–5 cm) may be abraded or micritized with microborings or with micrite envelopes	Beds may be nodular to planar, 10–20 cm thick forming nearly 1 m thick intervals. Cross-lamination and cross-bedding	Lithoclasts, skeletal fragments and ooids can show silicification with chalcedony and microquartz. Ooids may be fringed by isopachous rims of marine fibrous cement and/or by meniscus vadose meteoric cement In between grains micrite or cement can occur (early marine fibrous cement, syntaxial calcite on crinoids, burial blocky sparite)
F22 Peloidal (F22A), mixed coated grain (F22B) and ooidal (F22C) grainstone	Cross-laminated and cross-bedded grainstone with marine isopachous fibrous cement, peloids, micrite coated grains, and radial ooids Petrographic analysis distinguished three lithofacies (F22A, F22B, F22B), based on grain composition indistinguishable in the field	Well to moderately sorted (100 µm to 1 mm) Bivalves 1–2 mm	**F22A:** fine- and medium-grained peloidal grainstone with few mm wide lithoclasts, intraclasts (calci-mudstone), detrital quartz. **F22B:** grainstone with peloids, micrite coated grains, radial ooids, pisoids, lithoclasts (calci-mudstone/wackestone or peloidal ooidal packstone/grainstone like F21), quartz grains and silicification **F22C:** grainstone with radial ooids, marine fibrous cement and bivalves; quartz grains	Bivalve and gastropods shell fragments, brachiopods, echinoderm debris. Skeletal fragments are commonly abraded or micritized, recrystallized and partly silicified *Parafavreina* also at ooid nuclei	10–30 cm thick beds. Planar cross-bedding and cross-lamination	Isopachous rims of marine fibrous cement, followed by burial blocky sparite. Two to 5 mm wide, generally convex-up bivalve shells produce shelter porosity, filled by blocky sparite Dissolution vugs Silicification
F23 Peloidal packstone	Peloidal packstone, fine-grained, with micrite coated grains and siliceous sponge spicules (in Unit E)	Well to moderately sorted 10–50 µm	Peloids, faecal pellets, micrite coated grains, superficial ooids. Detrital quartz silt	Rare bivalves, gastropods and echinoderm debris; siliceous sponge spicules	10–30 cm thick beds. Bioturbation	Mechanical compaction and silicification
F24 Bivalve wackestone/packstone to rudstone/floatstone	Dark grey to black bivalve dominated wackestone/packstone to rudstone/floatstone	Poorly sorted (50 µm–5 mm)	Peloids	Bivalves are associated with gastropods, crinoids, and rare dasyclad algae; ostracods; *Parafavreina*	5–50 cm thick beds Bioturbation Some beds show undulated erosional base	Recrystallization of bivalve shells because of the former aragonitic mineralogy

Table 1 (continued)

Lithofacies	Texture	Grain size	Non skeletal grains	Skeletal grains	Bedding and sedimentary structures	Diagenetic features
F25 Ostracod wackestone to packstone	Dark grey to black ostracod dominated wackestone to packstone	Moderately sorted (20–100 µm)	Peloids	Ostracods and rare associated thin-shelled bivalves	10–30 cm thick beds. Bioturbation	Mechanical compaction, stylolites
F26 Peloidal grainstone to packstone with coated grains	Peloidal and micrite coated grain grainstone, or packstone	Poorly sorted (30–500 µm to 2 mm)	Micrite coated grains, peloids, oncoids, detrital quartz grains also as nuclei of coated grains	Bivalves, gastropods, *Thaumatoporella parvovesiculifera*, *Cayeuxia* calcified microbe, and benthic foraminifera (textulariids, possible *Siphovalvulina,* lituolids *Evertyciclammina praevirguliana*, *Ammobaculites).* Stromatolite laminae with vugs	Massive 10–20 cm beds. Parallel and cross-lamination	Keystone vugs (mm-size fenestrae), vadose meteoric micritic meniscus cement and marine isopachous rims of fibrous cement. Vugs are filled by burial blocky sparite; silicification can be present; mechanical compaction preceding cementation
F27 Microbial boundstone with cement-filled cavities	Microbial boundstone of leiolitic and clotted peloidal micrite with cement-filled cavities	Well sorted, (10–20 µm)	–	Boundstone framework made of clotted peloidal micrite and dense leiolitic micrite and rare laminated crusts with calcified microbes (*Cayeuxia*), *Thaumatoporella parvovesiculifera*	Massive to 1 m thick beds	The mm-size primary cavities are filled by fibrous cement and blocky sparite and peloidal micrite (geopetally restricted to the bottom part of cavities). Irregular dissolution vugs filled by vadose silt and blocky sparite as evidence of vadose dissolution and subaerial exposure
F28 Oncoidal packstone/rudstone to wackestone	Packstone/rudstone to wackestone with oncoids, peloids, micrite coated grains, gastropods and bivalves	Poorly sorted (30–500 µm to 1 cm)	Peloids. Oncoids (5 mm to 1 cm in diameter Lithoclasts	*Thaumatoporella parvovesiculifera*, *Cayeuxia*, benthic foraminifera (mostly textulariids, lituolids *Evertyciclammina praevirguliana Ammobaculites*), gastropods, bivalves, echinoderms, rare dasyclad algae	10–60 cm thick beds. Bioturbation	Some samples show evidence of meteoric dissolution with irregular vugs filled by geopetal sediment and blocky sparite
F29 Sponge spicule packstone with chert	Red to grey colour packstone with siliceous sponge spicules partially to completely silicified in chert	Well sorted, 10–20 µm to 1 mm	Detrital silt-size quartz grains Chert nodules	Siliceous sponge spicules (mostly monoaxone)	20 cm to massive beds, nodular and bioturbated beds	Evidences of mechanical compaction Partially or completely silicified by micro- to mega-quartz
F30 Coated grain packstone/grainstone to sandstone	Mixed carbonate-siliciclastic packstone/grainstone to sandstone with detrital quartz grains, echinoderm debris, micrite coated grains, angular lithoclasts and peloids	Fine- to medium-sand grained (grain size: 200–500 µm), moderately sorted	Angular lithoclasts and peloids are common, coated grains with micrite envelopes or micritic lithoclasts. Detrital quartz (300–400 µm in size angular to subangular grains). Some beds correspond to sandstone, since quartz detrital grains become dominant	Echinoid fragments (crinoids, echinoid spines), bivalves, gastropods and rare benthic foraminifera (probable *Siphovalvulina*)	10 cm–1 m thick beds of mixed carbonate–siliciclastic layers. Locally bioturbated	Peloids show micrite recrystallization. Evidences of mechanical compaction

Table 1 (continued)

Lithofacies	Texture	Grain size	Non skeletal grains	Skeletal grains	Bedding and sedimentary structures	Diagenetic features
F31 Bioturbated skeletal peloidal wackestone	Massive to metre-scale beds of skeletal calci-mudstone/wackestone with fragments of bivalves, gastropods, sponge spicules, ostracods, peloids, rare quartz grains and coated grain lithoclasts	Poorly sorted (10–500 µm to 1 mm)	Peloids, rare quartz grains, oncoids and coated grain lithoclasts	Fragments of bivalves, gastropods, possible monoaxone siliceous sponge spicules, ostracods In some samples: benthic foraminifera (*Siphovalvulina*, *Evertyciclammina praevirguliana*), *Aeolisaccus* and rare laminated crusts with calcified microbes (*Cayeuxia*, *Thaumatoporella parvovesiculifera*)	Massive to m-scale beds, sometimes bioturbated	Evidence of mechanical compaction
F32 Cross-laminated peloidal coated grain grainstone with crinoids and chert	Peloidal coated grain grainstone with abundant crinoids, cm-size chert nodules and glaucony	Well sorted, (10–20 µm to 1 mm)	Micrite coated grains, peloids, micritic lithoclasts Detrital quartz, chert nodules and glaucony	Abundant crinoid ossicles, echinoid spines and bivalves	10 cm to 40 cm- of cross-bedded and cross-laminated (bidirectional) thick beds	Grainstone texture is cemented by probably marine fibrous cement and blocky sparite

and cross-bedded peloidal coated grain ooidal grainstone with bivalves and sparse quartz grains (F22). F22 can be divided in F22A, F22B and F22C, based on the dominant grain types. F22A is a fine- and medium-grained grainstone dominated by peloids (Fig. 10D); F22B includes peloids, micrite coated grains and radial ooids (Fig. 10E, F). F22C is dominated by radial ooids with isopachous fibrous cement, quartz grains and bivalves (Fig. 10G). Lithofacies F19 and F22 occur both in Units D and E but in Unit E, they lack aulotortid foraminifera.

The boundary with the underlying Unit D shows an abrupt lithofacies change, coinciding with an erosional surface (F15 in Log EL in Fig. 4, F12 and F7 in log ED in Fig. 5). The upper boundary with Unit F is sharp and marked by a rapid lithofacies change between cross-bedded peloidal ooidal grainstone with millimetre-size fenestral voids below (F22A; Fig. 10H) and dark grey bivalve wackestone/packstone to rudstone/floatstone above (F24; Figs. 3C, 5).

Unit F

Unit F (39 m thick; Fig. 5) is subdivided into two parts based on lithofacies associations. The lower part (7 m thick) consists of dark grey bioturbated bivalve wackestone/packstone to rudstone/floatstone with rare dasyclad algae (F24; Fig. 11A, B) and ostracod wackestone/packstone (F25; Fig. 11C). The upper part (32 m thick) is characterised by peloidal grainstone to packstone (F26) with micrite coated grains, oncoids, bivalves, gastropods, *Thaumatoporella parvovesiculifera, Cayeuxia,* and benthic foraminifera (textularids, possible *Siphovalvulina*, lituolids, *Evertyciclammina praevirguliana*; Fig. 11D–G). F26 is alternating with metre-thick massive microbial boundstone (F27; Figs. 11H, 12A) or oncoidal packstone/rudstone (F28; Fig. 12B), with evidence of dissolution vugs, pendant and meniscus cement. F27 microbial boundstone consists of leiolitic and clotted peloidal micrite with *Cayeuxia*, *Thaumatoporella parvovesiculifera* and millimetre-size cavities filled by peloidal micrite, isopachous rims of marine fibrous cement and blocky sparite (Figs. 11H, 12A).

Unit F overlies Unit E cross-bedded grainstone with fenestrae (F22A) with a sharp contact, possibly associated with an angular unconformity (Fig. 3C). The upper boundary with Unit G is also sharp and marked by F26 and F28 with centimetre-size black lithoclasts sharply overlain by the chert and sponge spicule packstone (F29; Fig. 12C) belonging to Unit G (Fig. 3D).

Table 2 Sedimentary units from A to G and lithofacies associations identified in the study area from upper Norian to lower Jurassic with the interpreted depositional environments

Unit/thickness	Lithofacies associations and depositional setting	Interpretation
Unit A (38–55 m)	**F1 (F1D) Calci-mudstone with rare peloids and skeletal fragments:** low-energy subtidal restricted setting (below or immediately overlying subaerial exposure surfaces). **F2 (F2D) Skeletal wackestone to packstone:** low-energy subtidal setting; when lithoclasts are presents transgressive lag F20 **F3 Ostracod wackestone/packstone:** overlying erosional surfaces and transgressive lags (F20) with terrigenous input and ostracods suggesting brackish salinity **F4 (F4D) Peloidal calci-mudstone/wackestone to packstone with fenestrae. F5 (F5D) Stromatolite boundstone:** intertidal to supratidal low-energy setting (muddy tidal flat) **F6 Skeletal packstone to floatstone/rudstone with molluscs and/or brachiopods:** subtidal, open marine, intermittent high-energy setting affected by current or storm events **F7 Claystone/marlstone to argillaceous mudstone:** terrigenous input following in some cases events of subaerial exposure **F8 Skeletal peloidal packstone with foraminifera and dasyclad algae:** shallow (above photic zone), subtidal, protected low to moderate-energy setting **F9 Skeletal packstone with ooid moulds. F10 Coated grain peloidal bioclastic grainstone:** shallow subtidal high-energy shoal above effective fair-weather wave base **F20 Lithoclastic intraclastic packstone/rudstone above erosional surfaces:** transgressive lag, above disconformities at shallowing-upward cyclothem boundaries	**Unit A peritidal cyclothems:** low to high-energy, subtidal to intertidal and supratidal, restricted to open carbonate shelf influenced by currents and storm events and affected by metre-scale accommodation changes marked by erosional surfaces and subaerial exposures followed by terrigenous input and lithoclastic transgressive lags at high-frequency cycle boundaries Upper Norian Hochalm Mb. of the Kössen Fm. (Unit 1 and 2 by Golebiowski 1990)
Unit B (40–50 m)	**F7 Claystone/marlstone to argillaceous mudstone:** terrigenous input in deep shelf **F11 Nodular skeletal packstone/rudstone to wackestone/floatstone associated with claystone:** deep low-energy subtidal environment to high-energy storm beds with reworked bioclasts (from below to above storm wave base) **F12 Boundstone to floatstone with phaceloid corals associated with claystone:** low-energy subtidal environment within the photic zone	**Unit B claystone/marlstone with fossiliferous beds:** low-energy subtidal environment below the effective wave and above and below storm wave base, at intervals photic with corals and *Bacinella-Lithocodium*. Upper Norian to Lower Rhaetian Hochalm Mb. of the Kössen Fm. (Unit 3 by Golebiowski 1990)
Unit C (7–11 m)	**F8 Skeletal peloidal packstone with foraminifera and dasyclad algae:** shallow subtidal protected low- to moderate-energy setting **F11 Nodular skeletal packstone/rudstone to wackestone/floatstone associated with claystone. F12 Boundstone to floatstone with phaceloid corals associated with claystone:** low-energy subtidal environment deep but within the photic zone **F13 Coral boundstone to wackestone/floatstone:** shallow, low-energy setting within the photic zone with reduced terrigenous inputs with respect to F12 **F20 Lithoclastic intraclastic packstone/rudstone above erosional surfaces:** transgressive lag, above disconformities at shallowing-upward cyclothem tops	**Unit C coral boundstone to floatstone:** shallow to deep subtidal low-energy environment above the photic zone and between the effective fair-weather wave base and storm wave base. *Hauptlithodendronkalk* – Lower Rhaetian Hochalm Mb. of the Kössen Fm. (Unit 4 by Golebiowski 1990)

Table 2 (continued)

Unit/thickness	Lithofacies associations and depositional setting	Interpretation
Unit D (80–110 m)	**F1 Calci-udstone with rare peloids and skeletal fragments:** Low-energy subtidal setting (below or immediately overlying subaerial exposure surfaces) **F2 Skeletal wackestone to packstone:** Low-energy subtidal setting when lithoclasts are present (transgressive above erosional surface as F20) **F6 Skeletal packstone to floatstone/rudstone with molluscs and/or brachiopods:** Subtidal, open marine, intermittent high-energy setting **F7 Claystone/marlstone to argillaceous mudstone:** Terrigenous input following in some cases events of subaerial exposure **F11 Nodular skeletal packstone/rudstone to wackestone/floatstone associated with claystone – F12 Boundstone to floatstone with phaceloid corals associated with claystone:** low-energy subtidal environment deep but within the photic zone **F13 Coral boundstone to wackestone/floatstone:** shallow, low-energy setting with reduced terrigenous inputs with respect to F12 **F14 Oncoidal skeletal packstone to floatstone – F15 Coated grain grainstone with *Triasina hantkeni* – F16 Bioturbated peloidal coated grain packstone – F17 Peloidal packstone with micritic intraclasts – F18 *Bacinella–Lithocodium* boundstone:** Low to moderate-energy shallow open marine subtidal shelf **F19 Grainstone with aggregate grains:** shallow moderate to high-energy subtidal setting, adjacent to ooidal shoals (back shoal) **F20 Lithoclastic intraclastic packstone/rudstone above erosional surfaces:** transgressive lag, above disconformities at shallowing-upward cyclothem tops **F22A Peloidal grainstone – F22C Ooidal grainstone:** shallow subtidal high-energy setting (inner ramp ooidal grainstone barrier shoal belt)	**Unit D subtidal cyclothems with claystone:** low to high-energy subtidal, open marine to restricted carbonate shelf within the photic zone influenced by currents, above and below the effective wave base; sometimes affected by subaerial exposure on subtidal lithofacies and terrigenous input. There is no evidence of intertidal and supratidal deposition. The top of Unit D shows evidence of subaerial exposure with dissolution vugs, meniscus and pendant vadose meteoric cement, red Fe oxide crusts. Upper Rhaetian shallow-water succession time-equivalent to the Eiberg Mb. of the Kössen Fm. overlying the *Hauptlithodendronkalk*: Upper Rhaetian Limestone
Unit E (57 m; lower part: 11–13 m; upper part 44 m)	**F7 Claystone/marlstone to argillaceous mudstone:** terrigenous input following in some cases events of subaerial exposure **F19 Grainstone with aggregate grains:** shallow moderate to high-energy subtidal setting, adjacent to ooidal shoals (back shoal) **F21 Lithoclastic crinoidal ooidal packstone/grainstone to rudstone:** subtidal open marine high-energy setting reworking an eroded substrate of ooidal grainstone; transgressive lag at the base of Unit E **F22A Peloidal grainstone – F22B mixed coated grain grainstone—F22C Ooidal grainstone:** shallow subtidal high-energy setting above wave base (inner ramp ooidal grainstone shoal belt) **F23 Peloidal packstone:** shallow to deeper low-energy setting either adjacent to ooidal shoals (back shoal) or deep shelf with sponge spicules above the transgressive lag F21	**Unit E ooidal coated grain peloidal grainstone with basal transgressive lag:** deep subtidal environment (basal part) with basal transgressive lag overlying subaerial exposure at the top of Unit D, passing to shallow subtidal high-energy shoal environment (upper part) above the effective wave base, sometimes affected by coarse quartz input. Post end-Triassic extinction and sea-level fall, transitional to Lower Jurassic: Schattwald Beds and shallow-water strata to be correlated with Löruns oolite but mapped as Oberrhätkalk/Upper Rhaetian Limestone
Unit F (39 m; lower part 6–7 m; upper part 32 m)	**F24 Bivalve wackestone/packstone to rudstone/floatstone – F25 Ostracod wackestone to packstone:** low-energy subtidal setting, shallow and restricted **F26 Peloidal grainstone to packstone with coated grains:** low- to moderate-energy shallow from subtidal to intertidal/supratidal setting with evidence of subaerial exposures **F27 Microbial boundstone with cement-filled cavities:** low-energy shallow stressed marine settings linked to biotic crisis **F28 Oncoidal packstone/rudstone to wackestone:** low to moderate-energy subtidal setting	**Unit F bivalve-rich, microbialite and oncoidal lithofacies:** low-energy subtidal restricted (lower part) to moderate-energy shallow subtidal to intertidal environment (abundance of microbialites probably related to end-Triassic extinction) within the photic zone with evidence of subaerial exposure. Post-extinction Lower Jurassic shallow-water strata but mapped as Oberrhätkalk/Upper Rhaetian Limestone
Unit G (34 m)	**F29 Sponge spicule packstone with chert:** deep water low-energy setting **F30 Coated grain packstone/grainstone to sandstone:** subtidal shelf setting with siliciclastic sand input **F31 Bioturbated skeletal peloidal wackestone:** subtidal, restricted low-energy setting **F32 Cross-laminated peloidal coated grain grainstone with crinoids and chert:** open marine high-energy shelf setting with quartz sand and bidirectional (tidal) current	**Unit G cross-laminated coated grain peloidal grainstone with quartz and chert:** subtidal shelf environment with quartz input, affected by tidal currents passing to open marine conditions representing the onset of the flooding and drowning of subtidal shallow-water carbonates Lower Jurassic Hettangian–Sinemurian Kalksburg Fm

Unit G

Unit G is composed of lithofacies F29, F30, F31 and F32 with the dominance of F32 (Fig. 5). Red to dark grey, 20 cm thick siliceous sponge spicule packstone are sometimes completely silicified (F29; Fig. 12C) and overlain by packstone/grainstone with abundant detrital quartz grains to sandstone, echinoderm debris, micrite coated grains, angular lithoclasts and peloids (F30; Fig. 12D). Lithofacies F31 consists of massive to metre-scale beds of bioturbated skeletal wackestone with bivalves, gastropods, ostracods, peloids, benthic foraminifera (possible *Siphovalvulina*, *Evertyciclammina praevirguliana*), *Thaumatoporella parvovesiculifera* and *Aeolisaccus* (Fig. 12E). Lithofacies F32 is characterised by 10 to 40 cm thick cross-bedded and cross-laminated (bidirectional) peloidal, micrite coated grain grainstone with abundant crinoids, decimetre-size chert nodules, quartz grains and rare glaucony (Fig. 12F–H).

Unit G is 34 m thick; its lower boundary is represented by the first sponge spicule packstone with chert (F29; Fig. 3D). The upper boundary is marked by the sharp occurrence of red colour crinoidal rudstone to packstone (Fig. 2B, C).

Interpretation of sedimentary units and depositional models

The nearly 350 m thick sedimentary succession from Units A to G (Fig. 13) recorded the evolution of the depositional environments in a shallow carbonate shelf or low-angle ramp system (Figs. 14, 15), located north of the intraplatform Eiberg Basin, across the Triassic to Jurassic boundary. The stratigraphic succession from Unit A to G includes the Hochalm Mb. of the Kössen Fm., Upper Rhaetian Limestone, Schattwald Beds, shallow-water strata transitional to Lower Jurassic and the Hettangian–Sinemurian Kalksburg Fm. (Figs. 2, 13).

Unit A peritidal cyclothems

Unit A is organised in metre-scale shallowing-upward cyclothems, showing in the lower part subtidal restricted (F1, F2, F3) to open marine (F6, F8), low-energy environments passing upward to intertidal and supratidal lithofacies (F4, F5) or high-energy shoal grainstone deposits (F9, F10; Fig. 14). Cyclothems are bounded by erosional surfaces with fine siliciclastic input (F7), overlain by transgressive lags reworking the lithoclasts of the underlying lithofacies (F20). Fragmented skeletal biota (bivalves, brachiopods, corals) testify for marine currents and/or storm events in subtidal open marine environments (F6).

Unit A asymmetric peritidal cyclothems are similar in terms of internal facies organisation to the cycles in the Dachstein Limestone (Lofer facies), described by Fischer (1964) as deepening upward cycles. The Dachstein Limestone Lofer cycles have been investigated by several authors concluding that these cyclothems are the result of the interplay of autocyclicity, tectonic activity, sea-level oscillations and climatic variations (Satterly and Brandner 1995; Satterley 1996a, b; Enos and Samankassou 1998; Samankassou and Enos 2019). Unit A cyclothems differ from those of the Dachstein Limestone for the presence of millimetre to decimetre-thick F7 claystone/marlstone layers, overlying the erosional cycle boundary (Fig. 6D). The predominance of cyclothems with capping intertidal-supratidal or high-energy shoal lithofacies suggests a progradational trend at the scale of the high-frequency accommodation oscillations, as also suggested by Satterley (1996a, b) in the basal part of the Dachstein Limestone. Nevertheless, the whole Unit A records an upward trend towards more open marine conditions, with the upward decrease in occurrence and thickness of the intertidal–supratidal F4 and F5 lithofacies and the increase in thickness of the subtidal open marine F6. The transitional lower boundary between the Plattenkalk and Unit A with the gradual decrease of dolomitized beds might reflect a climate change from arid to more humid conditions. This is supported by the siliciclastic input and the reduced efficiency of the early dolomitization processes, similarly to what is documented in the Southern Alps at the top of the Norian Dolomia Principale (Berra et al. 2010).

The occurrence of *Triasina hantkeni* in Unit A confirms at least a late Norian age because of its stratigraphic distribution as late Norian–Rhaetian (Zaninetti et al. 1992; Maurer et al. 2008). On the basis of lithofacies character and stratigraphic position, Unit A corresponds to Units 1 and 2 of the Hochalm Mb. of the Kössen Fm. by Golebiowski (1990). Units 1 and 2 accumulated in a shallow-marine, restricted peritidal setting evolving upward to open-shelf conditions, affected by episodic terrigenous input and storm events (Kuss 1983; Golebiowski 1990), as observed in Unit A. In the

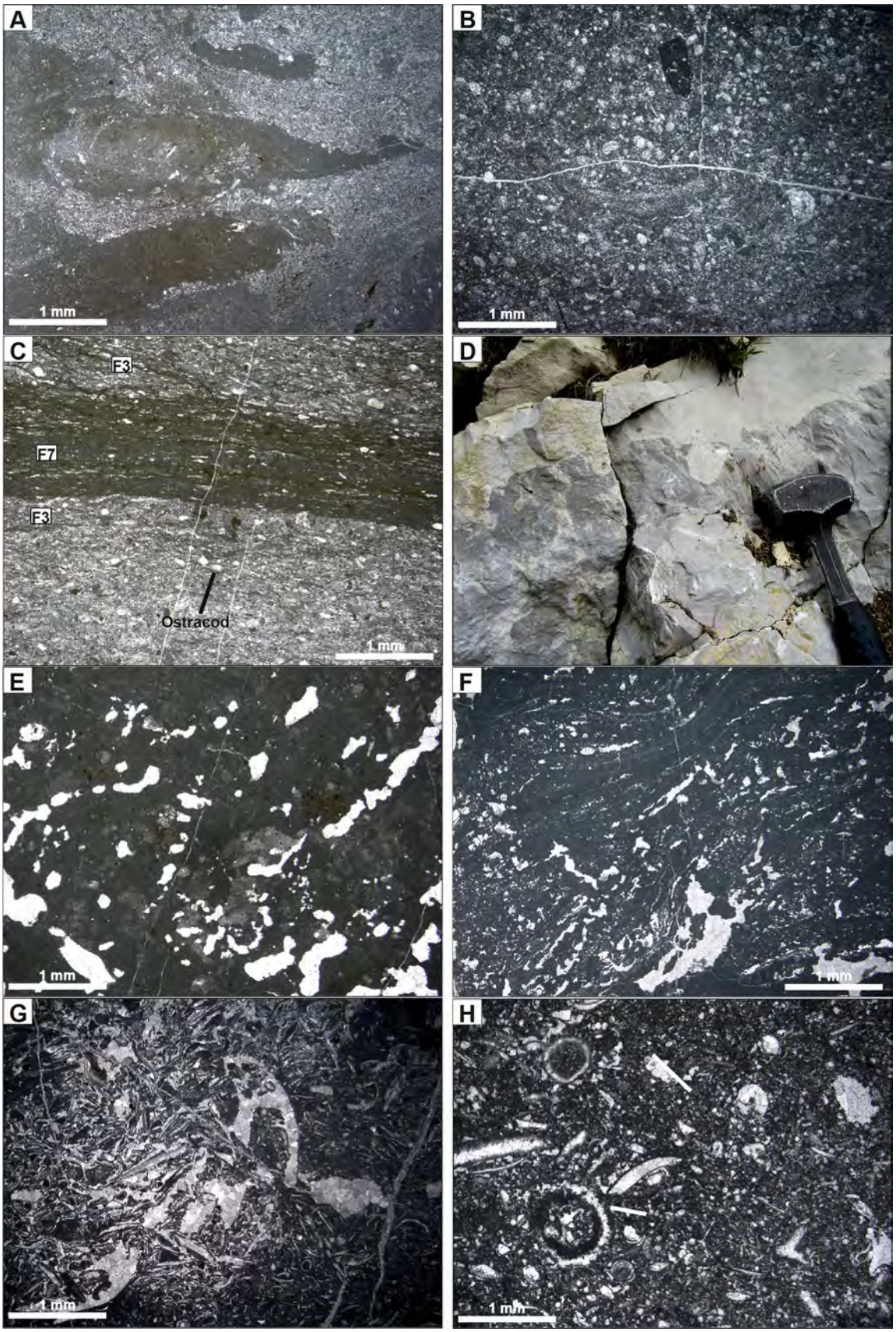
A
1 mm
B
1 mm
C
F3
F7
F3
Ostracod
1 mm
D
E
1 mm
F
1 mm
G
1 mm
H
1 mm

◂**Fig. 6** Photomicrographs and outcrop photos of lithofacies F1–F8 from Unit A. **A** Burrowed calci-mudstone with rare peloids and skeletal fragments showing claystone input and undetermined recrystallized bioclastic debris (F1; sample EA0.02 at 0.02 m in Log EA). **B** Skeletal wackestone to packstone with biomoulds of aulotortid benthic foraminifera, bivalves and carbonate lithoclasts (F2; sample EA1.2 at 1.2 m in Log EA). **C** Marlstone/claystone interbedded with ostracod wackestone/packstone (F3; sample EA4.3 at 4.3 m in Log EA). **D** Erosional karstic surface at the top of F4 overlain by F1 calci-mudstone in log EA at 18.62 m. **E** Peloidal mudstone/wackestone with fenestrae (F4; sample EA19.9 at 19.9 m in Log EA). **F** Laminated stromatolite boundstone (F5; sample EA2.25 at 2.25 m in Log EA). **G** Skeletal packstone to floatstone/rudstone with bivalves (F6; sample EA29.6 at 29.6 m in Log EA). **H** Skeletal peloidal packstone with foraminifera and dasyclad algae (white arrow) (F8; sample EA27.35 at 27.25 m in Log EA)

Hochalm section, Units 1 and 2 are approximately 100 m thick and late Norian in age (Golebiowski 1990).

Unit B claystone/marlstone with fossiliferous beds

Unit B represents the thickest claystone and marlstone (F7) succession alternating with metre-scale fossiliferous packstone/rudstone to boundstone (Figs. 13, 14). F7 records the siliciclastic input in a low-energy subtidal environment with high turbidity, below storm wave base. The fossiliferous beds F11, rich in bivalves and brachiopods, might represent low to moderate-energy conditions below the fair-weather wave base and oscillating around the storm wave base (cf. Tomašových 2004, 2006). The F12 beds with phaceloid corals, calcareous and siliceous sponges encrusted by *Bacinella-Lithocodium* must have accumulated in shallower photic conditions, above storm wave base.

Unit B records a significant fine-grained siliciclastic input on the carbonate shelf, which could be related to a global climate change (Kaufmann 2009) responsible for a shift of climate belts during a cooling interval (Berra et al. 2010). Unit B corresponds to Golebiowski (1990) Unit 3 of the Hochalm Mb. of the Kössen Fm. that was interpreted as accumulated within an open subtidal shelf with terrigenous input in water depth > 20 m. This unit reflects the maximum extension of the Kössen Fm. towards the Dachstein Limestone shelf (Golebiowski 1989; Satterley 1996b). In the reference section, Unit 3 is 30 m thick and latest Norian–early Rhaetian in age (Golebiowski 1990), whereas in Rizzi et al. (2020), it is reported as early Rhaetian.

Unit C coral boundstone to floatstone

Unit C records the rapid expansion of phaceloid coral boundstone across the shelf coinciding with a decrease in siliciclastic input with respect to Unit B (Figs. 13, 14). Unit C was deposited in a low-energy environment, as inferred from the abundance of micrite matrix surrounding the corals. The presence of corals, rare dasyclad algae and *Bacinella-Lithocodium* in F13 suggests photic depths.

Unit C corresponds to a marker bed that can be traced across the NCA (*Hauptlithodendronkalk* Steiner 1967; Schlager and Schöllnberger 1974; Kuss 1983; Satterley 1996b) and coincides with the lower Rhaetian Unit 4 of the Hochalm Mb. of the Kössen Fm. (Golebiowski 1990).

Unit D subtidal cyclothems with claystone

Unit D sharply overlies Unit C coral boundstone; it is the thickest unit characterised by regular occurrences of metre-scale F7 claystone/marlstone alternating with diverse carbonate lithofacies from F1 to F22 (Figs. 13, 14). Calci-mudstone and bioclastic wackestone (F1, F2) are indicative of restricted low-energy subtidal deposition. Bioturbated packstone with oncoids, micrite coated grains, peloids, benthic foraminifera and microbial boundstone (F14, F16, F17, F18) represent subtidal, low- to moderate-energy, open marine, photic depositional environments as suggested by the occurrence of dasyclad algae (F14) and *Bacinella-Lithocodium* (F18). High-energy shoals, above effective wave base, are represented by grainstone with micrite coated grains, aggregate grains, micritized and radial ooids (F15, F19, F22A, F22C). Unit D shallowing-upward cyclothems consist of basal metre-scale intervals of claystone/marlstone (F7) overlain by low to moderate-energy bioturbated subtidal, skeletal packstone to wackestone beds (F1, F2, F6, F11–F14, F16–F18) evolving to high-energy coated grain skeletal grainstone (F15, F19, F22A, F22C). Cyclothems are capped by sharp erosional surfaces on subtidal lithofacies with centimetre-scale irregular karstic dissolution vugs overlain by claystone/marlstone (F7) and transgressive deposits reworking eroded lithoclasts (F20) filling the karstic dissolution cavities (Fig. 9E). Unit D is indicative of subtidal settings, periodically affected by

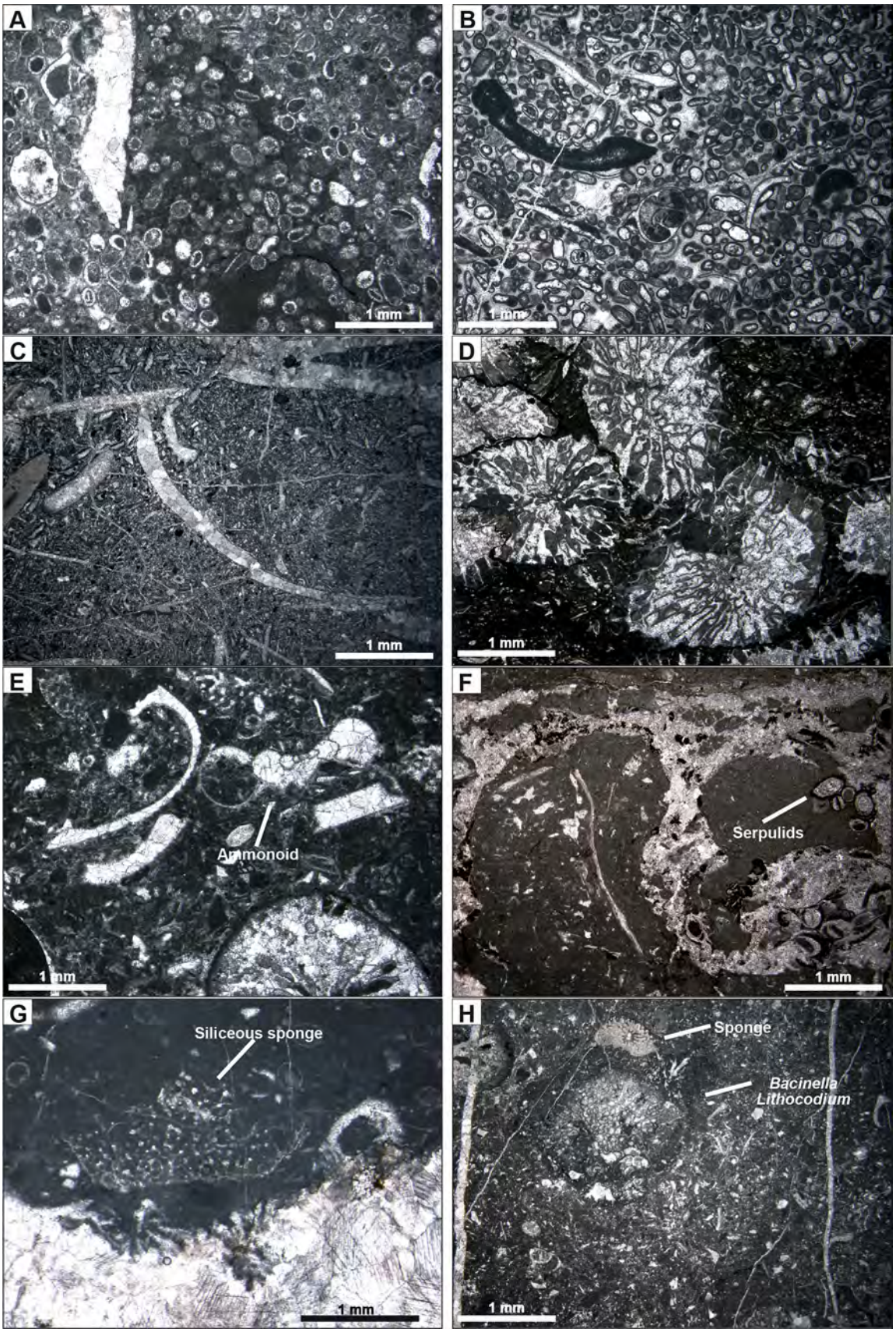
A
1 mm
B
1 mm
C
1 mm
D
1 mm
E
Ammonoid
1 mm
F
Serpulids
1 mm
G
Siliceous sponge
1 mm
H
Sponge
Bacinella
Lithocodium
1 mm

◂**Fig. 7** Photomicrographs of lithofacies F9–F10 from Unit A and F11–F12 from Unit B. **A** Packstone with moulds of superficial ooids with peloids as nuclei and burrows (F9; sample EA 11.2 at 11.2 m in Log EA). **B** Coated grain peloidal bioclastic grainstone with isopachous fibrous marine cement, bivalves, gastropods, radial ooids and intraclasts (F10; sample EA12.2 at 12.1 m in Log EA). **C** Nodular skeletal floatstone/rudstone with bivalves and echinoderms associated with claystone (F11; sample EA115.3 at 85.1 m in Log EA). **D** Boundstone to wackestone/floatstone with phaceloid corals associated with claystone forming solution seams due to compaction and pressure solution (F12; sample EA65.9 at 65.9 m in Log EA). **E** Corals are embedded in wackestone to packstone with bivalves, gastropods, brachiopods, rare ammonoids and siliceous sponges (F12; sample EA120.75 at 90.5 m in Log EA). **F** Phaceloid corals encrusted by serpulids surrounded by wackestone with brachiopod and bivalve fragments (F12; sample EC0.3 at 0.3 m in Log EC). **G** Coral colony in the lower part surrounded by wackestone with siliceous sponge (F12; sample K0.5 Tanzboden). **H** Skeletal wackestone to floatstone surrounding the corals with *Bacinella-Lithocodium* encrusting and infilling corals, calcareous sponge and bivalve bioclastic debris (F12; sample EC4.1 at 4.1 m in Log EC)

subaerial exposure and fine siliciclastic input, but lacking deposition in intertidal and supratidal environments as in Unit A. The absence of intertidal-supratidal lithofacies could be related to non-deposition or erosion. The occurrence of subaerial exposure surfaces at the top of subtidal lithofacies is indicative of sea-level falls, probably related to high-frequency eustatic oscillations controlled by climate or tectonics (Satterley 1996a, b).

In the Eiberg Basin, SW of the study area, the Kössen Fm. strata overlying the coral boundstone bed (Unit 4 of the Hochalm Mb. by Golebiowski 1990; Unit C in this study) correspond to deposition in an intraplatform basin (Eiberg Mb. of the Kössen Fm.; Golebiowski 1990). According to Golebiowski (1990, 1991), the shallow-marine successions resting upon Unit 4 coral boundstone, lateral to the Eiberg Basin, constitute the *Oberrhätkalk*/Upper Rhaetian Limestone. Hence, following Golebiowski (1990), Unit D in this study overlies Unit C coral boundstone and corresponds to the Upper Rhaetian Limestone, time-equivalent to the Eiberg Mb. and the Steinplatte complex facing the southern margin of the Eiberg Basin (Fig. 1C). Unit D lithofacies are similar to those described as Upper Rhaetian Limestone in the Bavarian Calcareous Alps, rich in *Triasina hantkeni* and with evidence of vadose meteoric cement (Schott 1983, 1984). In the geological maps by Schnabel et al. (2002) and Kreuss (2014), Unit D is mapped as Kössen Fm. and it is overlain by ooidal grainstone (Unit E in this study) mapped as *Oberrhätkalk*/Upper Rhaetian Limestone (Figs. 2, 13). Unit D upper boundary displays the evidence of vadose meteoric diagenesis due to subaerial exposure in different locations, at a present-day distance of 0.5 km (Figs. 4, 5, 13), that could be related to the regional sea-level fall associated with the onset of the end-Triassic extinction event (Satterley et al. 1994; Bernecker et al. 1999; Kaufmann 2009; McRoberts et al. 2012). This event was followed by the latest Rhaetian–Hettangian transgression passing to more open marine conditions (Delecat et al. 2011).

Unit E ooidal coated grain peloidal grainstone with basal transgressive lag

The basal part of Unit E with lithoclastic crinoidal ooidal packstone/grainstone to rudstone (F21) reworking clasts of ooidal grainstone affected by vadose meteoric diagenesis (e.g. meniscus, pendant cement, red matrix with iron oxide) represents a transgressive lag overlying an erosional surface at the top of Unit D, suggesting the reflooding of a subaerially exposed, shallow shelf and the presence of a stratigraphic gap between Unit D and E. The overlying claystone/marlstone (F7) and peloidal packstone with sponge spicules (F23) are indicative of low-energy, below storm wave base deposition. The upper part of Unit E consists of cross-bedded peloidal coated grain ooidal grainstone with bivalves, *Parafavreina* and quartz grains (F22) representing high-energy shoals, above wave base characterised by the first input of sand-grade quartz grains that will become abundant in the overlying Unit G.

The lower part of Unit E (F21, F7, F23) could be interpreted as the transgressive deposition, followed by the progradation of ooidal coated grain peloidal grainstone shoal (F22). The top of Unit E records a shallowing-upward trend to intertidal conditions, as documented by fenestrae in the uppermost peloidal grainstone (F22A; Fig. 10H), just below the contact with the bivalve packstone to rudstone (F24) of Unit F (Figs. 3C, 11A, B). In Unit E, benthic foraminifera as *Aulotortus* sp. and *Triasina hantkeni*, common in Unit D lithofacies F14 and F15 and indicative of Rhaetian age, were not identified.

In the Schnabel et al. (2002) and Kreuss (2014) geological maps (Fig. 2), Unit E is mapped as *Oberrhätkalk*/Upper Rhaetian Limestone, following the attribution by Steiner (1967). Strauss et al. (2020) instead mapped Unit E as Kössen Fm., not distinguishing the Kössen Fm. from the Upper Rhaetian Limestone. Unit E overlies an 80–110 m thick succession of subtidal cyclothems (Unit D) that, in this reconstruction, is attributed

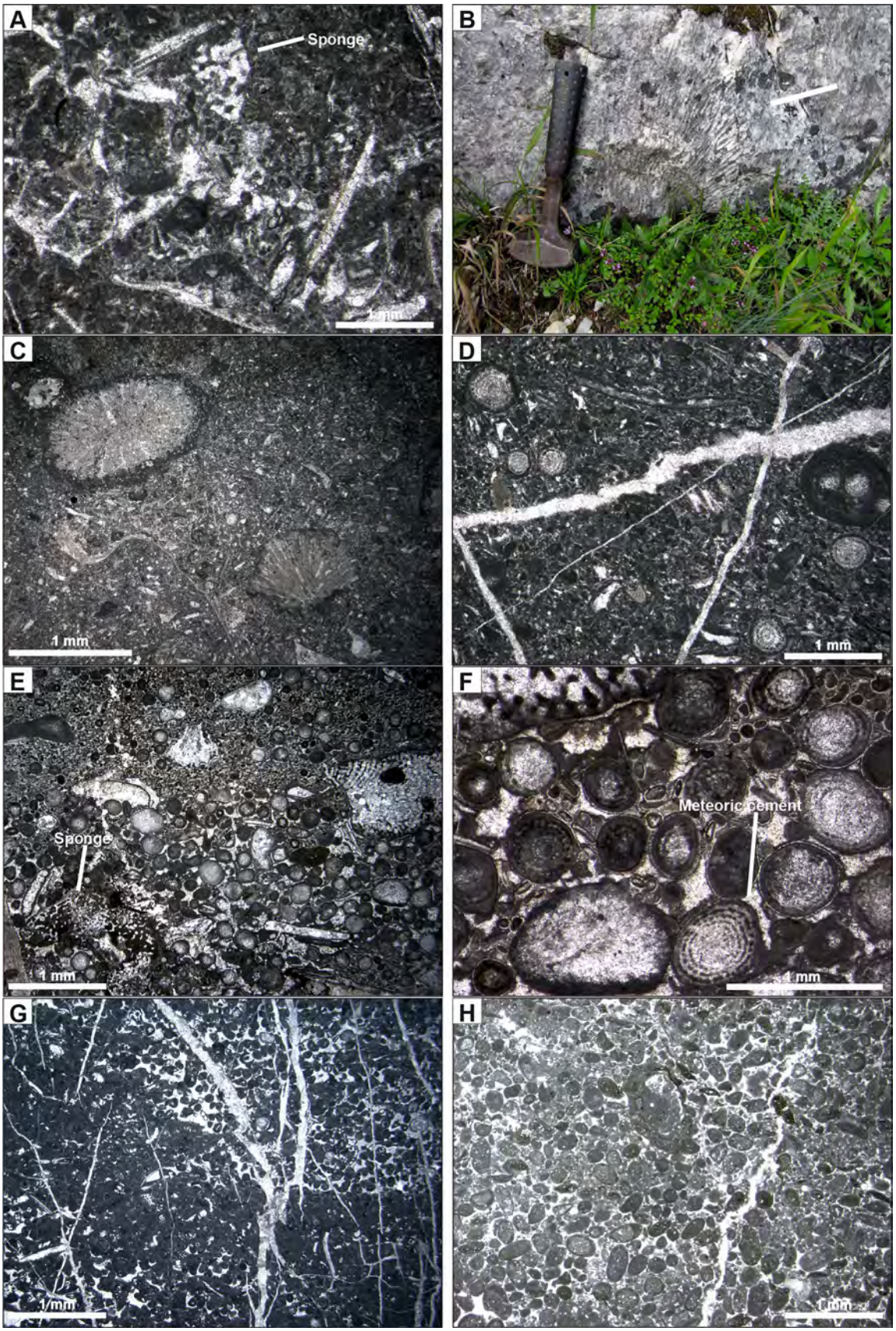
A
Sponge
1 mm
B
C
1 mm
D
1 mm
E
Sponge
1 mm
F
Meteoric cement
1 mm
G
1 mm
H
1 mm

◂**Fig. 8** Photomicrographs of lithofacies F12–F13 from Unit B and Unit C and F14–F17 from Unit D. **A** Skeletal peloidal wackestone to packstone with calcareous sponges, brachiopods, bivalves and *Lithocodium* surrounding phaceloid corals (F12; sample EC3.8 at 3.8 m in Log EC). **B** Outcrop photo of a phaceloid coral colony (F13; Log EA at 94.0 m). **C** Corals are embedded in skeletal peloidal wackestone/packstone with brachiopods and are encrusted by *Bacinella-Lithocodium* (F13; sample EC6.8 at 6.8 m in Log EC). **D** Skeletal packstone with oncoids, crinoids and micrite coated *Triasina hantkeni* (F14; sample EA133 at 102.8 m in Log EA). **E** Coated grain grainstone with *Triasina hantkeni*, siliceous and calcareous sponges and coral fragments (F15; sample EL4.1 at 4.1 m in Log EL). **F** Coated grain grainstone with *Triasina hantkeni,* calcareous sponges and meniscus and pendant vadose meteoric cement indicative of subaerial exposure and meteoric diagenesis (F15; sample EL4.1 at 4.1 m in Log EL). **G** Bioturbated peloidal coated grain packstone (F16; sample ED21.8 at 32.80 m in Log ED–EE). **H** Peloidal packstone with micritic intraclasts (F17; sample ED9.8 at 20.80 m in Log ED–EE)

to the Upper Rhaetian Limestone. Unit E postdates a laterally extensive, subaerial exposure at the top of Unit D that could correspond to the end-Triassic sea-level fall associated with the extinction event (McRoberts et al. 2012; Hillebrandt et al. 2013) and does not contain any biostratigraphic marker indicative of Rhaetian age (i.e. *Aulotortus sinuosus*, *Triasina hantkeni*). Hence, Unit E may represent the *Oberrhätkalk*/Upper Rhaetian Limestone time-equivalent to the Steinplatte and Adnet platform margin as originally mapped by Steiner (1967) and maintained in recent geological maps (Schnabel et al. 2002; Kreuss 2014; Strauss et al. 2020) but, as presented in this study, it could most likely correspond to a younger shallow-water succession transitional to the lower Jurassic, post-dating the end-Triassic extinction and sea-level fall. This revised stratigraphy would result similar to what described in the western NCA, where the top of the Kössen Fm. is marked by subaerial exposure, overlain by the uppermost Rhaetian Schattwald Beds, followed by the Hettangian Löruns oolite (McRoberts et al. 1997; Felber et al. 2015).

Unit F bivalve-rich, microbialite and oncoidal lithofacies

The low-diversity, low-energy bivalve- and ostracod-rich lithofacies (F24–F25), overlain by microbialite and oncoidal peloidal lithofacies (F26–F28), suggest a stressed environment, scarce in skeletal biota, possibly related to the aftermath of the end-Triassic extinction. Unit F lithofacies represents shallow, low-energy restricted (F24, F25, F27, F28) to moderate-energy (F26) depositional settings within the photic zone. The presence of meniscus cement and reworked lithoclasts in F26 and F28 suggests events of subaerial exposures followed by transgressions. As for Unit E, Unit F is mapped as Upper Rhaetian Limestone in the Schnabel et al. (2002) and Kreuss (2014) geological maps. However, the presence of *Aeolisaccus*, lituolid foraminifera as *Evertycyclammina praevirguliana*, *Thaumatoporella parvovesiculifera* and putative *Siphovalvulina* supports an early Jurassic age. The stratigraphic data from this study suggest that Unit F may correspond to a shallow-water inner shelf succession, possibly time-equivalent to the lower Jurassic part of the Kendlbach Fm. in other areas of the NCA. Microbialites with siliceous sponges are described in the Hettangian strata overlying the southern margin and slope into the Eiberg Basin in the outcrops in Adnet and Steinplatte (Schöll Fm.; Delecat and Reitner 2005; Delecat et al. 2011).

Unit G cross-laminated coated grain peloidal grainstone with quartz and chert

Unit G starts with sponge spicule packstone with chert (F29), suggesting a deepening with respect to the underlying oncoidal lithofacies F28 of Unit F (with evidence of subaerial exposure at the top) and records a significant input of detrital quartz (F30). The coated grain peloidal grainstone with crinoids, quartz grains and chert (F32) represents a mixed carbonate–siliciclastic open marine shelf affected by bidirectional tidal currents. Cross-laminated coated grainstone beds (F32) are attributed to the Kalksburg Fm. (Hettangian–Sinemurian; Fig. 2B).

The deepening trend documented by Unit G may reflect the onset of the extensional tectonics associated with the opening of the Penninic Ocean, recorded in different Lower Jurassic successions of the NCA (Gawlick et al. 2009). Drowning of the shelf is marked by the overlying red crinoidal rudstone with ammonites and belemnites belonging to the Hierlatz Limestone Member of the Adnet Fm. and the Allgäu Fm. (Figs. 1 C, 15).

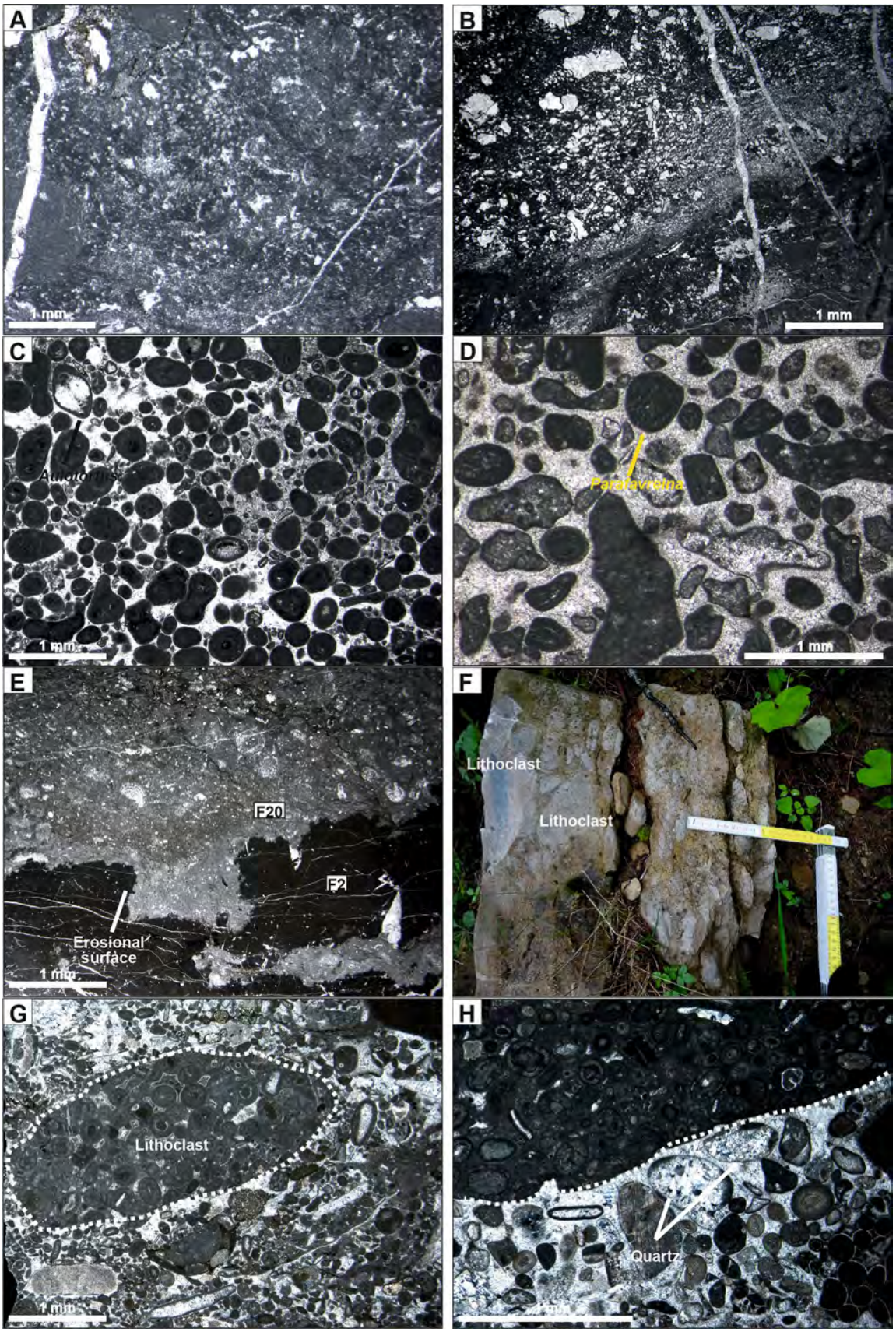
A
1 mm
B
1 mm
C
Ammonite
1 mm
D
Paraconcha
1 mm
E
F20
F2
Erosional surface
1 mm
F
Lithoclast
Lithoclast
G
Lithoclast
1 mm
H
Quartz

◂**Fig. 9** Photomicrographs of lithofacies F18, F19, F20 from Unit D and F19 and F21 from Unit E. **A** *Bacinella-Lithocodium* boundstone with clotted peloidal micrite microbialites (F18; sample ED21.5 at 32.50 m in Log ED–EE). **B** *Bacinella-Lithocodium* boundstone with clotted peloidal micrite and rare calcareous sponges (F18; sample ED52.2 at 43.20 m in Log ED–EE). **C** Grainstone with aggregate grains, micritized ooids and micrite coated *Aulotortus sinousus* with early marine fibrous cement (F19 in Unit D; sample ED86.5 at 77.50 m in Log ED–EE). **D** Grainstone with aggregate grains, micrite coated grains and *Parafavreina* faecal pellets with marine isopachous rims of fibrous cement (F19 in Unit E; sample EI40.2 at 40.20 m in Log EI). **E** Lithoclastic intraclastic packstone/rudstone (F20) above an erosional surface overlying lithofacies F1 and F2 reworking *Triasina hantkeni* (F20; sample ED45 at 38.5 m in Log ED–EE). **F** Outcrop photo of lithoclastic crinoidal ooidal rudstone with centimetre-size lithoclasts (F21; sample EI0.1. at 0.10 m at the base of Log EI). **G** Photomicrograph of lithoclastic rudstone with lithoclasts of F22 ooidal grainstone to packstone affected by meteoric diagenesis with vadose meniscus and pendant cement and crinoids (F21; sample EI0.1 at 0.10 m in Log EI). **H** Rudstone/grainstone with lithoclasts, peloids, crinoids, silicified bioclasts, ooids and quartz grains (F21; sample EI1 at 1.0 m in Log EI)

Discussion

The lithofacies characterisation and stratigraphic reconstruction of the Upper Triassic–Lower Jurassic succession in the Stumpfmauer study area provide detailed data for comparisons with coeval sedimentary successions in Western Tethys (Fig. 1) and for improving the understanding of the Tethyan depositional settings across the Triassic/Jurassic boundary.

Comparisons across Western Tethys

The investigated shallow-water Norian–Rhaetian to lower Jurassic lithofacies types and the superimposed sedimentary units display similarities with time-equivalent examples in the western NCA (McRoberts et al. 1997), Western Carpathians (Tomašovych 2004), Transdanubian Range (Vörös and Galácz 1998; Héja et al. 2018; Haas et al. 2022), Dinarides (Buckovic et al. 2001), Central Austroalpine (Furrer 1981; Berra and Cirilli 1997) and Southern Alps (Jadoul et al. 2004, 2005; Masetti et al. 2017).

Specifically, in the Western Carpathians, the Rhaetian Fatra Fm. consists of mixed carbonate–siliciclastic deposits with high lateral facies variability (Tomašovych 2004). Superimposed peritidal and shallow subtidal carbonate lithofacies and dark colour skeletal marlstone accumulated in inner-middle ramp to intraplatform basin settings under the influence of storm events (Tomašovych 2004). The Fatra Fm. lithofacies associations are similar to those recognised in the Hochalm Mb. of the Kössen Fm. and described in Units A, B, and C in this study. The abundance of calcareous sponges associated with corals in the Fatra Fm. suggests more stressed and ecologically unstable conditions with respect to the *Hauptlithodendronkalk* of the NCA (Unit C), likely due to the more landward and restricted palaeogeographic position with respect to the NCA (Tomašovych 2004). The absence of extensive coral patch reefs in the Western Carpathians may reflect water energy, salinity and turbidity unsuitable for corals (Tomašovych 2004).

A striking correspondence seems to exist between the study area and the Lombardy Basin in the Southern Alps (N Italy), where the peritidal early-dolomitized platform interior with fault-controlled intraplatform basins of the Dolomia Principale (Norian; Berra and Jadoul 1996; Berra et al. 2010) is followed by subtidal claystone (Riva di Solto Shales, upper Norian), shallowing-up into cyclic mixed carbonate–siliciclastic ramp (Zu Limestone, Rhaetian; Jadoul et al. 2004). The Riva di Solto Shales and Zu Limestone (together up to 1000 m thick) are time-equivalent to the NCA Kössen Fm. and Upper Rhaetian Limestone, with similar stratigraphic evolution and palaeoenvironmental affinities (Unit B, C, D), although the greater thickness reflects higher subsidence rate in the Lombardy Basin. The Zu Limestone was divided in three members, from base to top, Zu1, Zu2 and Zu3 (Masetti et al. 1989; Lakew 1990; Jadoul et al. 1994, 2004; Galli et al. 2005, 2007; Rigo et al. 2009). Zu1 Member is a cyclical succession of claystone, marlstone and micritic limestone with bivalves. Zu2 Member is a massive limestone unit, up to 25 m thick and laterally continuous for 160 km, consisting of coral patch reefs, bioturbated wackestone and ooidal packstone/grainstone, locally rich in megalodontid bivalves. Zu3 Member is composed of marlstone, marly and micritic limestone organised in asymmetric shallowing-upward cycles, with basal marlstone (10 m thick) passing to peloidal ooidal grainstone or packstone and bioturbated wackestone/packstone with *Triasina hantkeni*, corals, calcisponges, bryozoans, megalodontid bivalves and dasyclad algae (Lakew 1990; Jadoul et al. 1994; Galli et al. 2007). The top of Zu3 is affected by meteoric diagenesis due to subaerial exposure (Lakew 1990; Jadoul et al. 2005). The Rhaetian Zu2 and Zu3 members match with Unit C and D distinguished in this study, in terms of lithofacies types, benthic foraminifera association and cyclic patterns. The subaerial exposure identified at the top of Unit D can be correlated with the subaerial exposure

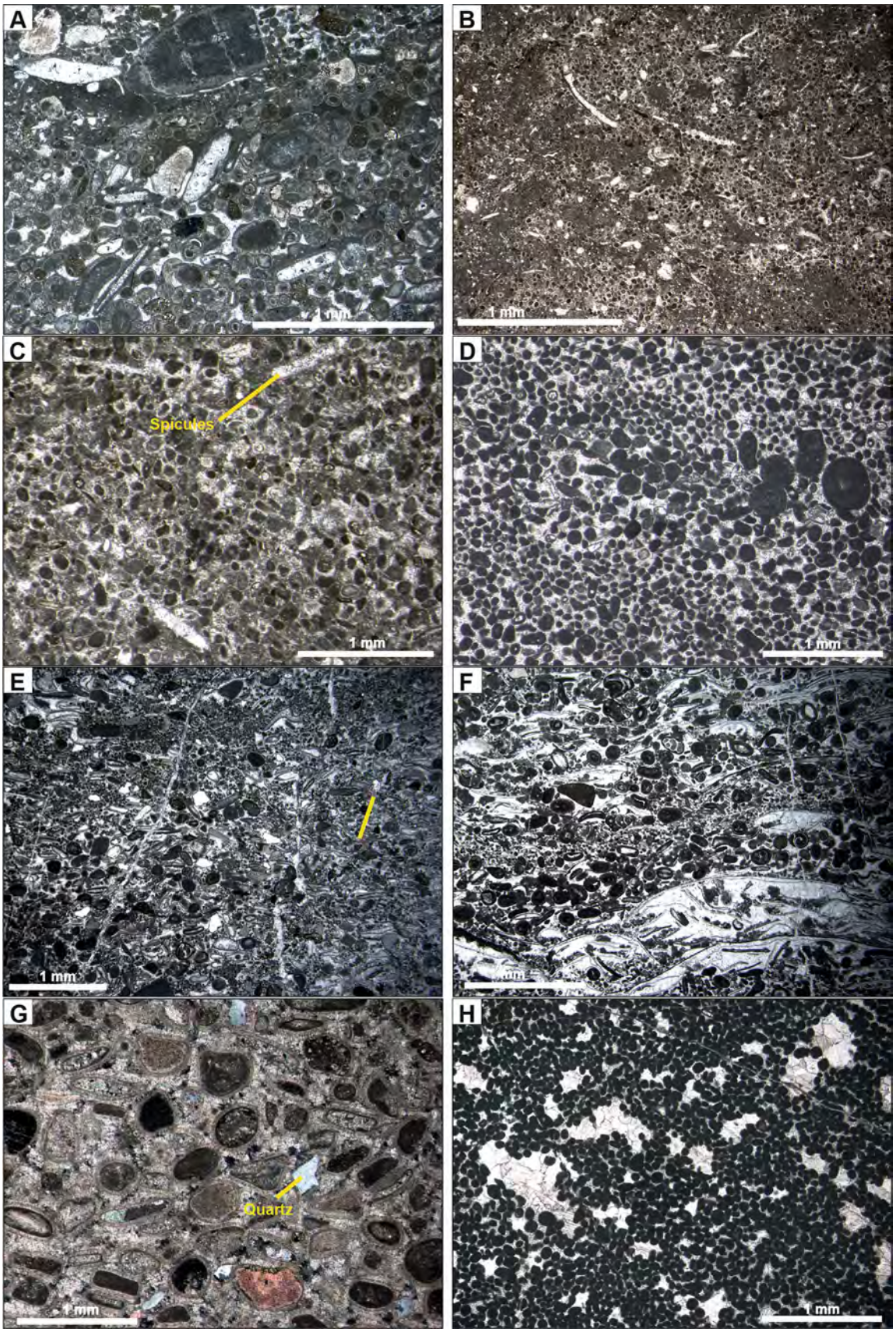
A
1 mm
B
1 mm
C
Spicules
1 mm
D
1 mm
E
1 mm
F
G
Quartz
1 mm
H
1 mm

◂**Fig. 10** Photomicrographs of lithofacies F21, F22 and F23 from Unit E. **A** Grainstone to packstone with radial ooids, peloids, crinoids and quartz grains with vadose meniscus cement followed by blocky sparite (F21; sample EI0.1 at 0.10 m in Log EI). **B** Bioturbated peloidal packstone with bivalves and siliceous sponge spicules (F23; sample EI5.4 at 5.40 m in Log EI). **C** Peloidal packstone with siliceous sponge spicules (F23; sample EL11 at 11.15 m in Log EL). **D** Peloidal grainstone with micritized ooids (F22A; sample EI57 at 56.5 m in Log EI). **E**, **F** Mixed coated grain ooidal peloidal grainstone with disarticulated and isoriented bivalve shells (F22B; sample EI52.9 at 52.9 m in Log EI). **G** Ooidal grainstone with radial ooids, quartz grains, bivalve shells and isopachous rims of marine fibrous cement in crossed polarizers showing the presence of detrital quartz grains (F22C; sample EI21.6 at 18.0 m in Log EI). **H** Peloidal grainstone with cement-filled voids (intertidal fenestrae/keystone vugs), at the top of Unit E made of bedded peloidal ooidal grainstone with planar cross-lamination (F22A; sample EI57B at 57.0 m in Log EI)

at the top of Zu3. The Zu3 Member is overlain by the Malanotte Formation (from latest Rhaetian to early Hettangian; Bottini et al. 2016) consisting of bedded marly limestone, with sparse claystone beds with quartz grains and bioturbated bioclastic limestone with thin-shelled bivalves and sponge spicules passing to grainstone–packstone with micritised ooids (Galli et al. 2005, 2007). The Malanotte Fm. resembles the strata in the lower Unit E dominated by peloidal packstone with siliceous sponge spicules (F23). Biostratigraphic and magnetostratigraphic studies located the Triassic/Jurassic boundary in the lower part of the Malanotte Fm. (Galli et al. 2007; Muttoni et al. 2010; Bottini et al. 2016; Zaffani et al. 2018). The overlying Hettangian Albenza Fm. consists of cross-bedded ooidal grainstone passing upward to peloidal packstone and bio-intraclastic grainstone (Galli et al. 2005, 2007; Jadoul and Galli 2008). The Albenza Fm. lithofacies are similar to the upper Unit E dominated by coated grain ooidal grainstone (F22). In western Lombardy, Jadoul et al. (2005) described a shallow-water subtidal to intertidal succession (35 m thick, Alpe Perino Limestone; Hettangian–lower Sinemurian) overlying the Albenza Fm. ooidal grainstone on structural highs before the Sinemurian deepening and pelagic limestone deposition (Moltrasio Fm.). Jadoul et al. (2005) reported lower Jurassic shallow-water carbonates developed on structural highs in the western (Varese High) and eastern (Botticino High) Lombardy Basin with lithofacies types (Alpe Perino Limestone, Corna Fm.) that are similar to lithofacies F26, F27 and F28 (Unit F) from this study.

The similarities between the Lombardy Basin and the NCA were already highlighted by Galli et al. (2007) who linked the Zu Limestone, Malanotte Fm. and Albenza Fm. succession to the Vorarlberg region of the western NCA, where the Kössen Fm. is overlain, above an erosional unconformity, by the marlstone and marly limestone of the Schattwald Beds and Lorüns oolite (McRoberts et al. 1997), as it is proposed for Unit E in this study.

The Triassic–Jurassic boundary in shallow-water carbonates from the eastern NCA

Integrating the results from this study with the regional reconstructions (Gawlick et al. 2009; Krystyn et al. 2005) and the comparison with other paleogeographic domains, a revised depositional reconstruction of the study area is proposed in Fig. 16. Unit D subtidal cyclothems with claystone, mapped as Kössen Fm. in the Kreuss (2014) geological map, is interpreted as time-equivalent to the Eiberg Mb. and the Upper Rhaetian Limestone at the southern margin of the Eiberg Basin. In fact, in the Steinplatte area the top of the Upper Rhaetian Limestone is affected by a subaerial exposure (Kaufmann 2009), similarly to the exposure at the top of Unit D. The overlying Unit E coated grain ooidal grainstone, mapped as Upper Rhaetian Limestone by Kreuss (2014), is interpreted as transitional to lower Jurassic, based on the lack of Rhaetian biostratigraphic markers as well as the lack of corals and diverse skeletal biota that characterise Units C and D before the end-Triassic extinction. This hypothesis is supported by the similarity of Unit E lithofacies (F19, F22) with aggregate grain and ooidal grainstone deposits dated to the Hettangian–Sinemurian described in the Lombardy Basin (Albenza Fm., Southern Alps, N Italy; Galli et al. 2005, 2007; Bottini et al. 2016), Trento Platform (Calcari Grigi Group, Southern Alps, NE Italy; Borsato et al. 1994; Preto et al. 2017; Masetti et al. 2017; Vulpius and Kiessling 2018; Julian Alps, Slovenia; Ciarapica and Passeri 1990), western Dinarides (Croatia; Buckovic et al. 2001), Transdanubian Range (Kardosrét Limestone, Hungary; Vörös and Galácz 1998), Western Carpathians (Tatra Mts., Hronicum domain, Poland; Rychliński et al. 2018) and Apennines (Central and Southern Italy, Calcare Massiccio; Ciarapica 2007), as well as in the western NCA (Löruns, Austria; McRoberts et al. 1997; Felber et al. 2015). The abundance of ooids in Unit E and of microbialites in Unit F might reflect the effect of the biotic crisis related to the end-Triassic extinction as observed elsewhere in the aftermath of extinction events (e.g. Permian–Triassic; Li et al. 2015; end-Triassic, United Arab Emirates; Ge et al. 2019). Unit G chert layers, the abundance of detrital quartz and the sedimentological features of lithofacies

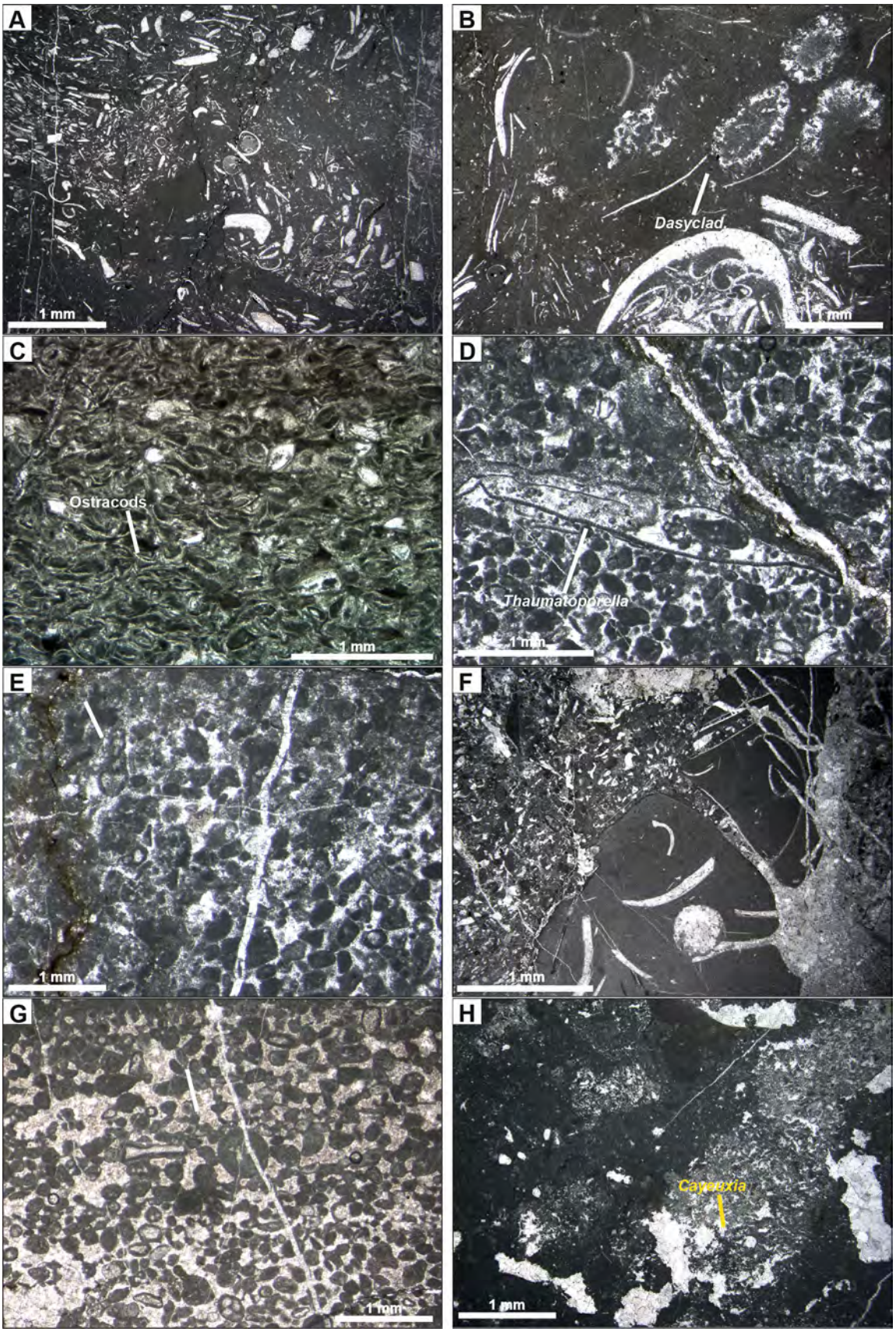
A
1 mm
B
Dasyclad
1 mm
C
Ostracods
1 mm
D
Thaumatoporella
1 mm
E
1 mm
F
1 mm
G
1 mm
H
Cayeuxia
1 mm

◂**Fig. 11** Photomicrographs of lithofacies F24, F25, F26 and F27 from Unit F. **A**, **B** Bioturbated skeletal packstone to floatstone dominated by bivalves with rare dasyclad algae (F24; sample EI58.5 at 58.5 m in Log EI). **C** Bioturbated packstone to wackestone with ostracods (F25; sample EI63.1 at 63.1 m in Log EI). **D** Peloidal grainstone to packstone with *Thaumatoporella parvovesiculifera*, micrite coated grains and lituolid benthic foraminifera (F26; sample EI68.7 at 71.3 m in Log EI). **E** Peloidal grainstone to packstone with possible lituolid foraminifer *Evertyciclammina praevirguliana* and vadose meteoric meniscus cement (F26; sample EI68.7 at 71.3 m in Log EI). **F** Lithofacies F26 at the top of Unit F showing lithoclasts of F24 bivalve wackestone/floatstone with borings, erosional features and meniscus cement related to reworking of a subaerially exposed substrate (F26; sample EI88.2 at 90.8 m in Log EI). **G** Peloidal grainstone to packstone with coated grains with vadose meniscus cement related to subaerial exposure followed by early marine isopachous fibrous cement (F26; sample EI86.7 at 89.3 m in Log EI). **H** Microbial boundstone with clotted peloidal and leiolitic micrite with *Cayeuxia* (F27; sample EI71 at 73.6 m in Log EI)

F32 correspond to the Kalksburg Fm. (Hettangian–Sinemurian; cf. Gawlick et al. 2009).

Controlling factors on the stratigraphy of Western Tethys

The similarities, in terms of lithofacies associations and stacking pattern, among coeval successions deposited in different palaeogeographic domains (i.e. eastern and western NCA, Central Austroalpine, Western Carpathians, Transdanubian Range, Dinarides, Southern Alps) reveal that the Norian to Jurassic stratigraphic evolution of Western Tethys was controlled by the interplay of environmental, climatic and tectonic regimes producing similar sedimentological responses at regional scales. These factors can be identified influencing the Western Tethys depositional settings: (a) climate change controlling the intensity of weathering triggering a major input of clay and the demise of the widespread early dolomitization, suggesting a transition towards humid conditions in the latest Norian–Rhaetian (Berra et al. 2010), (b) Rhaetian favourable conditions for the expansion of coral boundstone; (c) biocalcification crisis of the end-Triassic extinction event (McRoberts et al. 2012), (d) an end-Triassic sea-level fall followed by rapid rise (Hallam and Wignall 1999; Pálfy and Zajzon 2012), (e) early Jurassic recovery of carbonate production with ooidal grainstone and microbialites; (f) early Jurassic extensional tectonics with development of structural highs where shallow-water carbonates accumulated before the drowning represented by red crinoidal-rich and hemipelagic limestone (Bernoulli 1964; Eberli 1988; Jadoul et al. 2005; Gawlick et al. 2009; Gawlick and Missoni 2019).

This study performed in the eastern NCA on the upper Norian–Rhaetian to Jurassic mixed carbonate–siliciclastic sedimentary units and the comparison with coeval successions demonstrate that regional and global processes drove the stratigraphic evolution of Western Tethys, from the Austroalpine to the Southern Alps to Western Carpathians, as recorded by the strikingly similar lithofacies character and stratigraphic evolution.

Conclusions

The sedimentological investigation of the nearly 350 m thick, shallow-water Rhaetian–Lower Jurassic mixed carbonate–siliciclastic succession of the Stumpfmauer area in the eastern NCA allowed identifying 32 lithofacies, grouped in seven sedimentary units (from A to G), recording the stratigraphic evolution of shelf depositional environments, located north of the upper Rhaetian Eiberg Basin.

This shallow-water succession comprises: the Hochalm Mb. of the Kössen Fm. (Unit A peritidal cyclothems, Unit B claystone/marlstone with fossiliferous beds) and the regional coral limestone marker bed *Hauptlithodendronkalk* (Unit C coral boundstone to floatstone), the Upper Rhaetian Limestone time-equivalent to the Eiberg Mb. of the Kössen Fm. (Unit D subtidal cyclothems with claystone), shallow-water carbonate strata transitional to the Lower Jurassic up to the Kalksburg Fm. (Unit E ooidal coated grain peloidal grainstone with basal transgressive lag, Unit F bivalve-rich, microbialite and oncoidal lithofacies, Unit G cross-laminated coated grain peloidal grainstone with quartz and chert).

Differently from the published geological maps, in this study Units E and F are attributed to a lower Jurassic shallow-water depositional system post-dating a laterally extensive subaerial exposure surface at the top of Unit D, based on: (a) the sharp change in skeletal biota with the

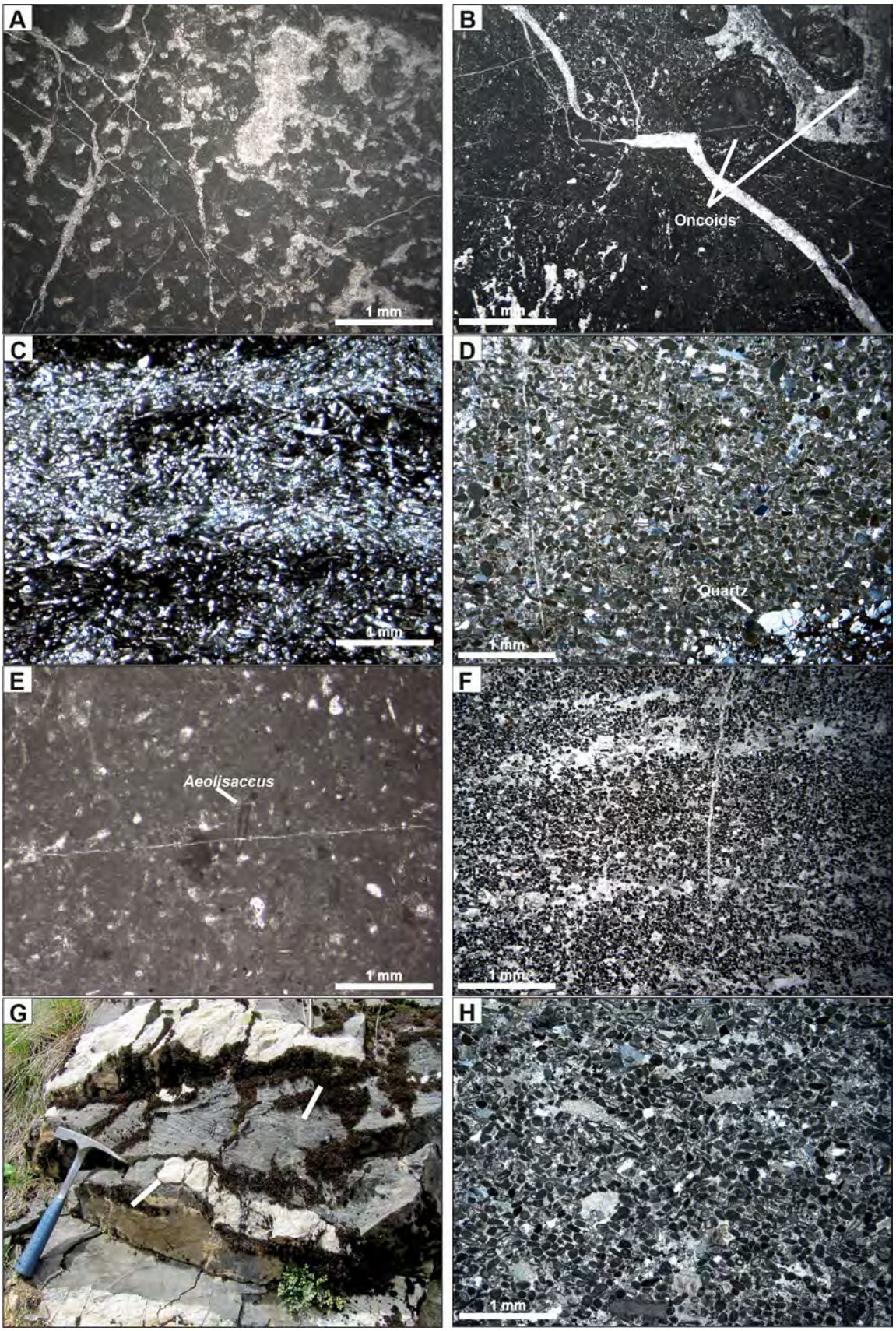
A
1 mm
B
Oncoids
1 mm
C
1 mm
D
Quartz
1 mm
E
Aeoljsaccus
1 mm
F
1 mm
G
H
1 mm

◂**Fig. 12** Photomicrographs of lithofacies F27 and F28 from Unit F and outcrop photo and photomicrographs of lithofacies F29, F30, F31 and F32 from Unit G. **A** Microbial boundstone with primary micrite-sustained cavities filled by marine fibrous isopachous and burial blocky sparite cement (F27; sample EI83.2 at 85.8 m in Log EI). **B** Packstone to floatstone/rudstone with oncoids at the top pf Unit F (F28; sample EI91.7 at 94.2 m in Log EI). **C** Siliceous sponge spicule packstone with chert (F29; sample EI92.8 at 95.4 m in Log EI). **D** Coated grain peloidal grainstone to sandstone with detrital monocrystalline and polycrystalline quartz grains (F30; sample EI93 at 96.2 m in Log EI). **E** Bioturbated skeletal peloidal wackestone with bivalves, gastropods and *Aeolisaccus* (F31; sample EI101.2 at 103.8 m in Log EI). **F** Cross-laminated peloidal coated grain grainstone with bidirectional lamination, crinoids and chert nodules (F32; sample EI117 at 117.0 m in Log EI). **G** Outcrop photo of lithofacies F32 cross-laminated peloidal coated grain grainstone with crinoids and chert showing bidirectional cross-lamination. **H** Peloidal coated grain grainstone with crinoids and detrital quartz (F32; sample EI117 at 117.0 m in Log EI)

disappearance of corals and Rhaetian foraminifera (e.g. *Triasina hantkeni*) common in the underlying Unit D; (b) the onset of abundant detrital quartz, siliceous sponge spicules and chert, and (c) the similarities with Lower Jurassic ooidal grainstone lithofacies and stratigraphic evolution in the western NCA, Southern Alps, Western Carpathians, Transdanubian Range and Dinarides. Unit E ooidal grainstone and Unit F microbial boundstone are interpreted to reflect the biotic crisis in the aftermath of the end-Triassic extinction.

The evolution of the studied succession demonstrates the influence of climate, environmental changes and extensional tectonics (linked to the opening of the Penninic Ocean) on the western Tethys carbonate shelf, driving similar responses in different palaeogeographic domains: a shift towards humid conditions required to explain the latest Norian–early Rhaetian clay input (Units A and B), the Rhaetian expansion of phaceloid coral boundstone (Unit C), a major sea-level fall (top of Unit D) followed by transgression and change in skeletal biota marking the end-Triassic extinction and transition to early Jurassic (Unit E), the aftermath of the biotic crisis manifested by abundance of ooidal grainstone and microbialites (Units E and F), lower Jurassic shallow-water carbonate strata on structural highs (Units E, F and G) and gradual deepening upward due to extensional tectonics.

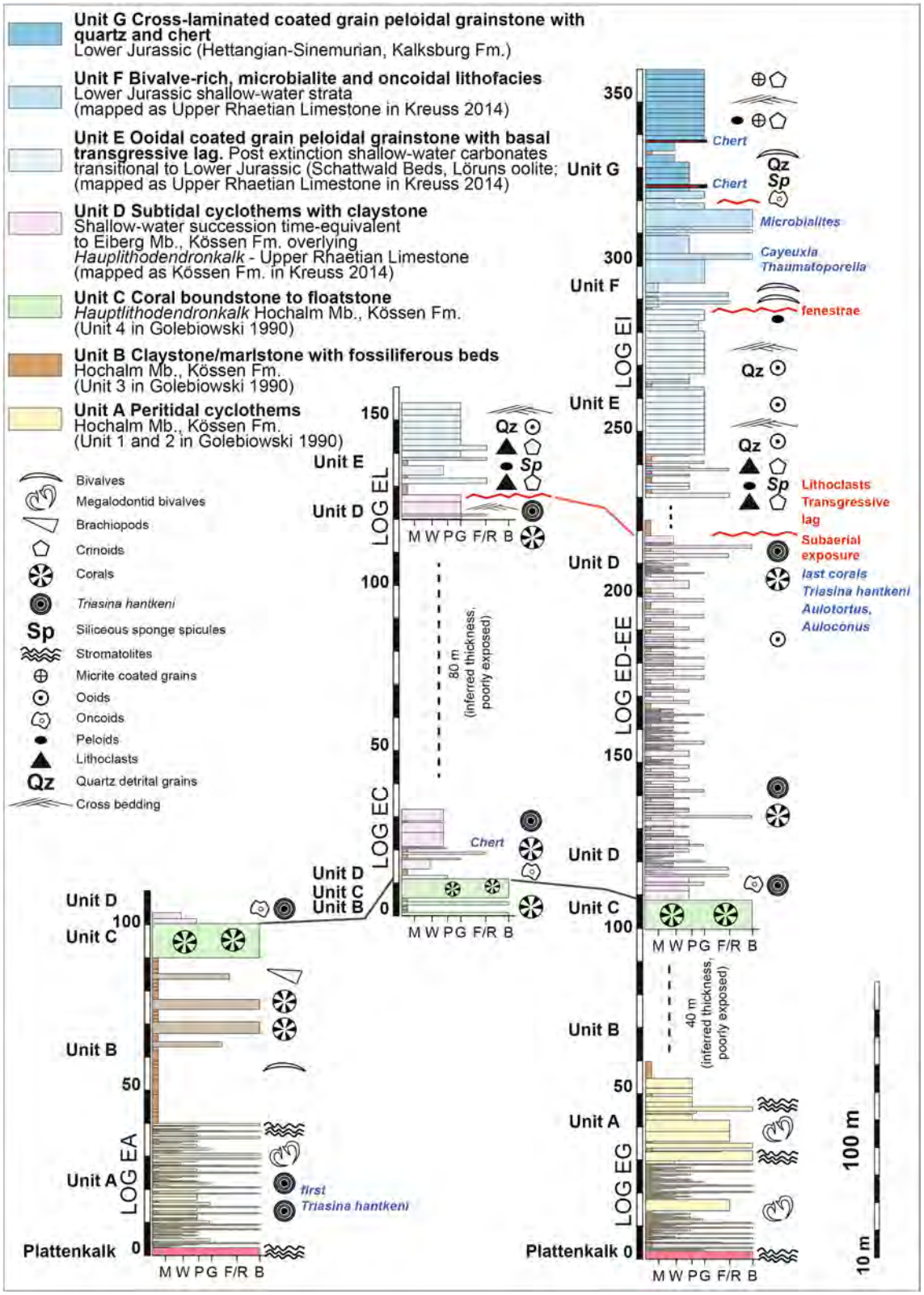

Fig. 13 Correlation panel showing the relationships between the different stratigraphic units identified in the study area. The transition from Triassic to Jurassic is tentatively located in the lower part of Unit E above the subaerial exposure at the top of Unit D and the transgressive lag with carbonate lithoclasts, detrital quartz and crinoids followed by F23 peloidal packstone with sponge spicules. For the log details refer to Figs. 4 and 5; for the location of the logs refer to Fig. 2

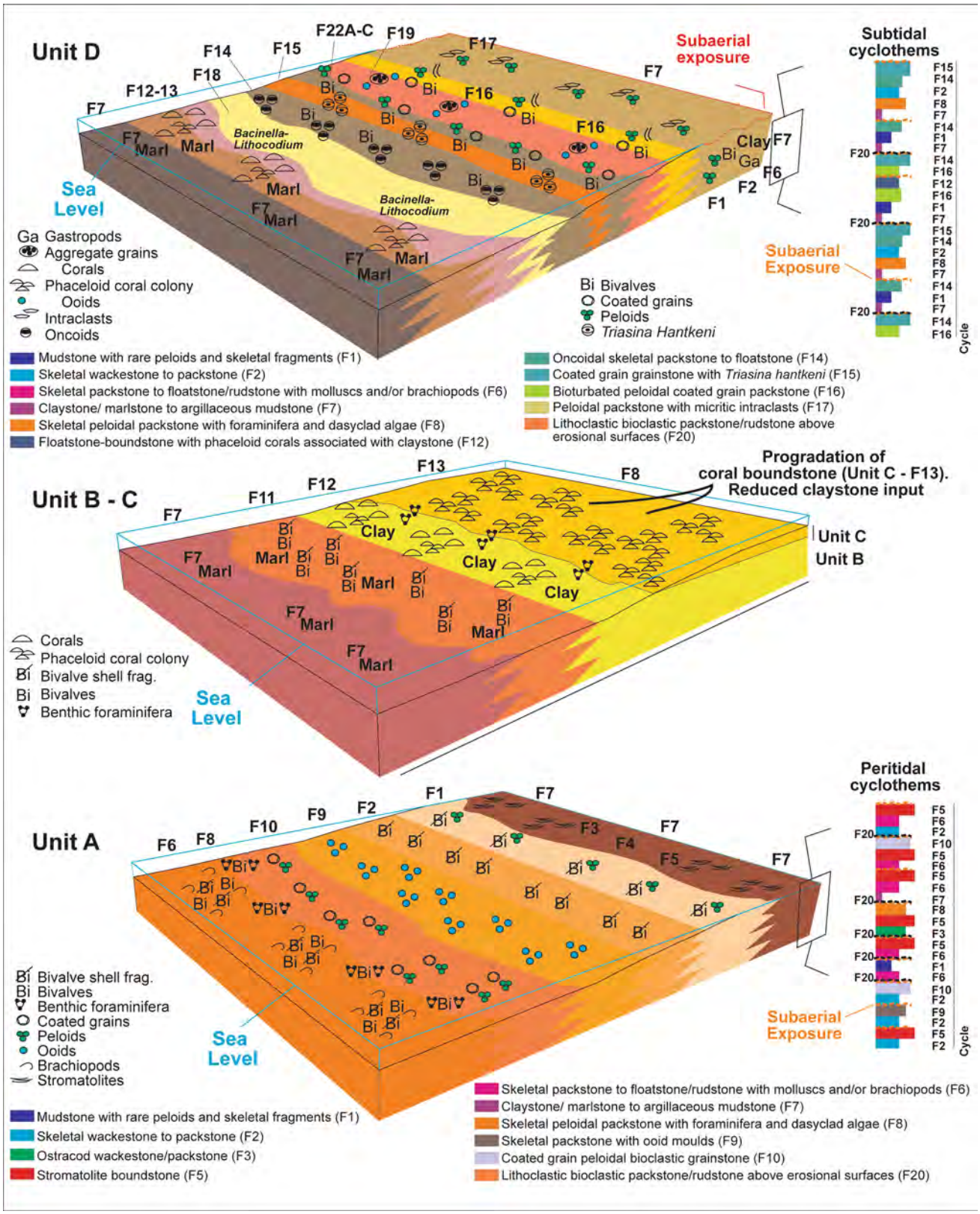

Fig. 14 Simplified diagram showing the depositional environments and lithofacies distribution during the vertical evolution of the succession from Unit A to D based on the stratigraphic logs measured and reported in Figs. 4 and 5

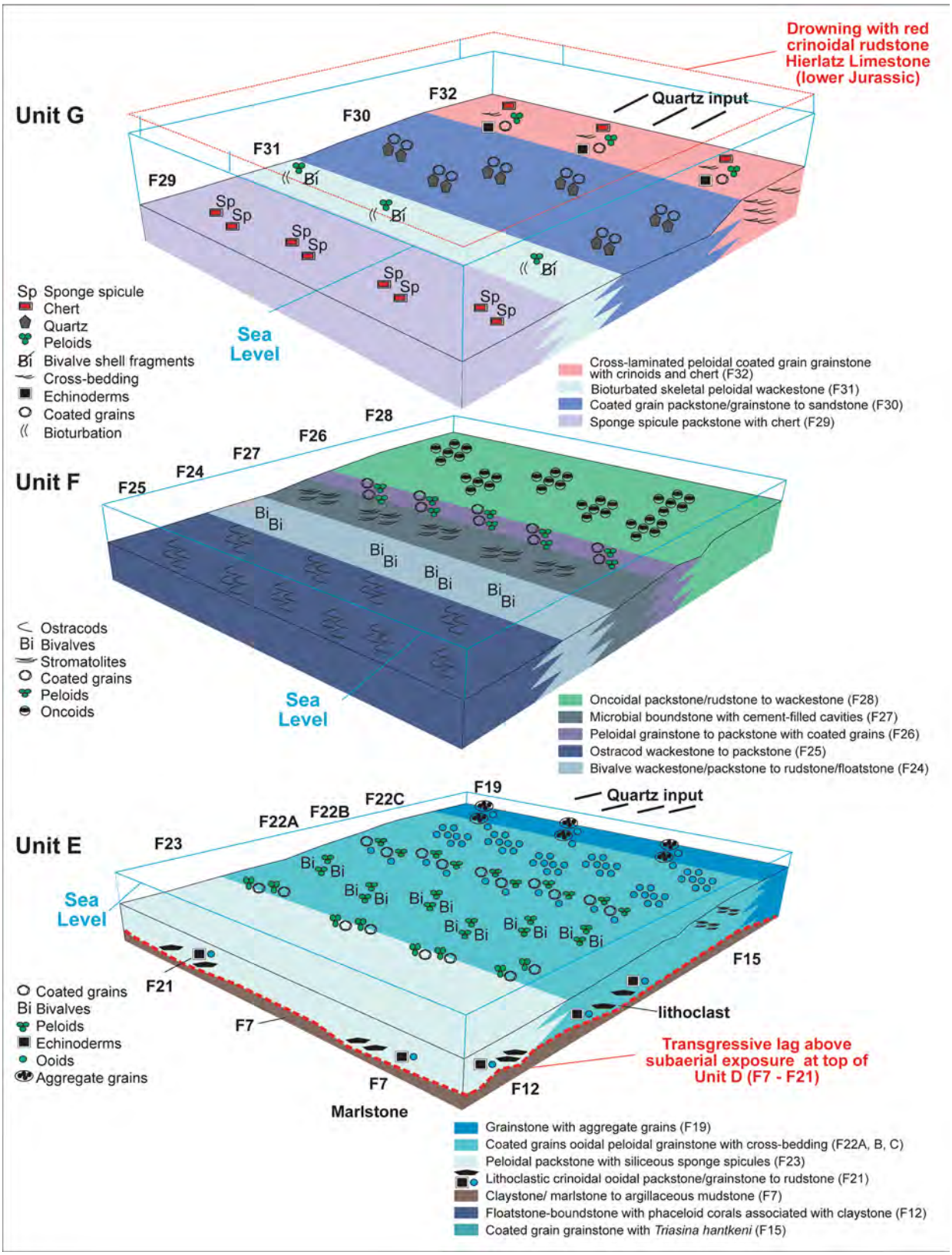

Fig. 15 Simplified diagram showing the depositional environments and lithofacies distribution during the vertical evolution of the succession from Unit E to G based on the stratigraphic logs measured and reported in Figs. 4 and 5

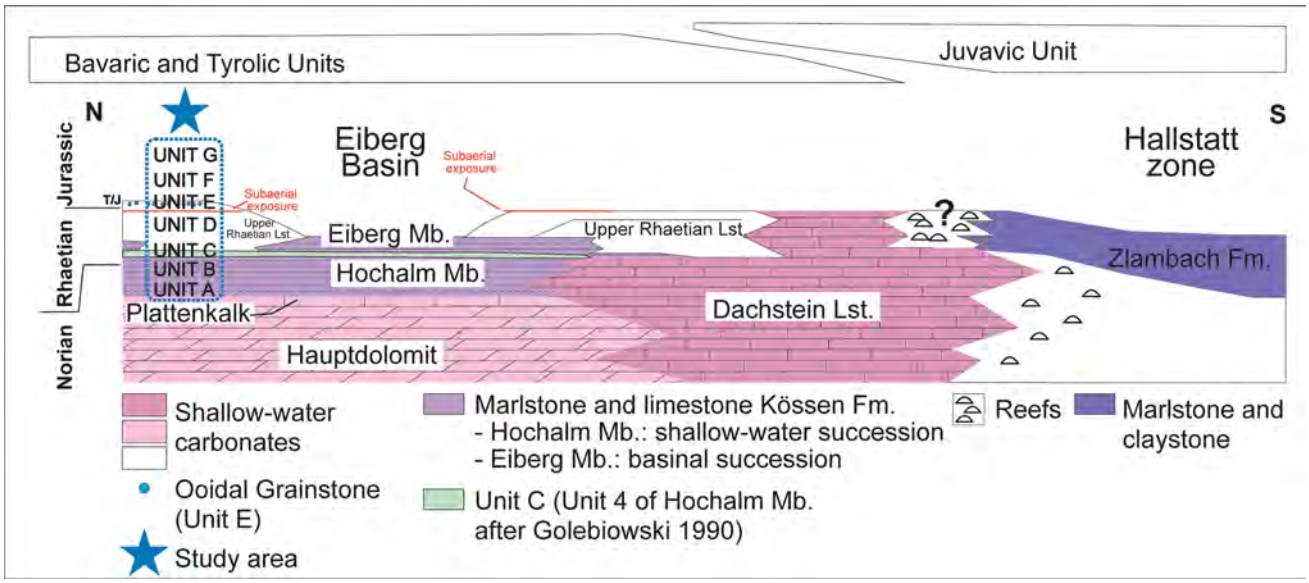

Fig. 16 Modified depositional model cross section partially redrafted after Krystyn et al. (2005) as reported in Fig. 1C including stratigraphic and palaeogeographic information reported in Gawlick et al. (2009) and references therein. The blue dashed line rectangle marks the inferred location of the studied succession. The Plattenkalk has been added as a transitional unit (due to decreasing dolomitization) between the Hauptdolomit and the Hochalm Mb. of the Kössen Fm. The age of the Hochalm Mb. has been assumed late Norian–early Rhaetian as proposed by Golebiowski (1990) and supported by the observations in this study. The diagram includes also the stratigraphic position of the sedimentary units identified in the study area from Unit A to G. The marker bed represented by the lower Rhaetian coral limestone (Unit C coral boundstone corresponding to Unit 4 of the Hochalm Mb. of the Kössen Fm. according to Golebiowski 1990) separates the Hochalm from the Eiberg members. According to Golebiowski (1990) the shallow-water successions above Unit 4 coral limestone time-equivalent to the Eiberg Basin are labelled as *Oberrhätkalk*/Upper Rhaetian Limestone that corresponds to Unit D in this study. Unit D is capped by subaerial exposure as the Upper Rhaetian Limestone in the Eiberg Basin southern margin in correspondence of the end-Triassic extinction event. Strata belonging to Unit E, F and G are interpreted as post end-Triassic extinction and early Jurassic in age representing a shallow-water setting north of the Eiberg Basin during the early Jurassic. This is a revised interpretation because this succession is reported as Upper Rhaetian Limestone in the published geological maps (Schnabel et al. 2002; Kreuss 2014)

Supplementary Information The online version contains supplementary material available at https://doi.org/10.1007/s10347-023-00662-x.

Acknowledgements The authors warmly thank OMV Exploration and Production GmbH for funding the project. Curzio Malinverno and Matteo Pegoraro (University of Milan) are thanked for thin sections preparation. Michele Azzarone, Mario De Matteis, Andrea Dimartino, Edoardo Chiarelli are thanked for the help provided during field work and sample analyses. The reviewers Hans Jürgen Gawlick and Felix Schlagintweit are thanked for their useful comments as well as Editor Wolfgang Kiessling.

Funding Open access funding provided by Università degli Studi di Milano within the CRUI-CARE Agreement. The Rhaetian Carbonate Project was funded by OMV Exploration and Production GmbH to the Department of Earth Sciences of the University of Milan.

Data availability Data supporting this study are reported in this manuscript and in the Online Supplementary Information. Additional data will be made available upon request to the corresponding author.

Declarations

Conflict of interest There are no conflicts of interest and data are available on request to the corresponding author.

References

Bernecker M (2005) Late Triassic reefs from the Northwest and South Tethys: distribution, setting, and biotic composition. Facies 51:442–453. https://doi.org/10.1007/s10347-005-0067-4

Bernecker M, Weidlich O, Flügel E (1999) Response of Triassic reef coral communities to sea-level fluctuations, storms and sedimentation: evidence from a spectacular outcrop (Adnet, Austria). Facies 40:229–279. https://doi.org/10.1007/BF02537476

Bernoulli D (1964) Zur Geologie des Monte Generoso. Beitr Geol Karte Schweiz 118:1–134

Bernoulli D, Jenkyns HC (1974) Alpine Mediterranean and central Atlantic Mesozoic facies in relation to the early evolution of the Tethys. Special Publication Soc Econ Paleontol Mineral 19:129–160. https://doi.org/10.1007/978-1-4612-3494-4_5

Berra F, Cirilli S (1997) Palaeoenvironmental interpretation of the Late Triassic Fraele Formation (Ortles Nappe, Austroalpine domain, Lombardy). Riv Ital Paleontol Stratigr 103:53–70

Berra F, Jadoul F (1996) Norian serpulid and microbial bioconstructions: Implication for the platform evolution in the Lombardy Basin (Southern Alps, Italy). Facies 35:143–162

Berra F, Jadoul F, Anelli A (2010) Environmental control on the end of the Dolomia Principale/Hauptdolomit depositional system in the central Alps: coupling sea-level and climate changes. Palaeogeogr Palaeoclimatol Palaeoecol 290:138–150. https://doi.org/10.1016/j.palaeo.2009.06.037

Böhm F, Dommergues JL, Meister C (1995) Breccias of the Adnet Formation: indicators of a Mid-Liassic event in the Northern Calcareous Alps (Salzburg/Austria). Geologische Rundschau Berlin Heidelberg 84:272–286

Borsato A, Frisia S, Sartorio D (1994) Late Triassic-Early Liassic stratigraphic and diagenetic evolution of the margin between the Trento platform and the Lombardy Basin in the Brenta Dolomites (Italy). Acta Geol 69:5–35

Bottini C, Jadoul F, Rigo M, Zaffani M, Artoni C, Erba E (2016) Calcareous nannofossils at the Triassic/Jurassic boundary: stratigraphic and paleoceanographic characterization. Riv It Paleontol Strat 122:141–164. https://doi.org/10.13130/2039-4942/7726

Buckovic D, Jelaska V, Tesovic BC (2001) Facies variability in Lower Liassic carbonate successions of the western Dinarides (Croatia). Facies 44:151–162

Caggiati M, Gianolla P, Breda A, Celarc B, Preto N (2018) The start-up of the Dolomia Principale/Hauptdolomit carbonate platform (Upper Triassic) in the eastern Southern Alps. Sedimentology 65:1097–1131

Ciarapica G (2007) Regional and global changes around the Triassic-Jurassic boundary reflected in the late Norian-Hettangian history of the Apennine basins. Palaeogeogr Palaeoclimatol Palaeoecol 244:34–51

Ciarapica G, Passeri L (1990) The Dachstein limestone of the Mt. Canin (Julian Alps) and its paleogeographic meaning. Bollettino Della Società Geologica Italiana 109:239–247

Clémence ME, Gardin S, Bartolini A, Paris G, Beaumont V, Guex J (2010) Bentho-planktonic evidence from the Austrian Alps for a decline in sea-surface carbonate production at the end of the Triassic. Swiss J Geosci 103:293–315. https://doi.org/10.1007/s00015-010-0019-z

Czurda K, Nicklas L (1970) Zur Mikrofazies und Mikrostratigraphie des Hauptdolomites und Plattenkalk-Niveaus der Klostertaler Alpen und des Rhätikon (Nördliche Kalkalpen, Vorarlberg). Univ. Innsbruck, Geolog. Inst.., Innsbruck, pp 165–253

Delecat S, Arp G, Reitner J (2011) Aftermath of the Triassic–Jurassic boundary crisis: spiculite formation on drowned Triassic Steinplatte reef-slope by communities of hexactinellid sponges (northern calcareous Alps, Austria). In: Reitner J. et al. (eds), Advances in Stromatolite Geobiology, Lecture Notes in Earth Sciences 131:355–390. Springer-Verlag, Berlin Heidelberg. https://doi.org/10.1007/978-3-642-10415-2_23

Delecat S, Reitner J (2005) Sponge communities from the Lower Liassic of Adnet (Northern Calcareous Alps, Austria). Facies 51:385–404

Dickson JAD (1966) Carbonate identification and genesis as revealed by staining. J Sediment Res 36:491–505

Eberli GP (1988) The evolution of the southern continental margin of the Jurassic Tethys Ocean as recorded in the Allgäu Formation of the Austroalpine Nappes of Graubünden (Switzerland). Eclogae Geol Helv 81:175–214

Ebli O (1997) Sedimentation und Biofazies an passiven Kontinentalrändern: Lias und Dogger des Mittelabschnittes der Nördlichen Kalkalpen und des frühen Atlantik (DSDP site 547B, offshore Marokko). - Münchner Geowiss. Abh., Reihe A, Geol. Paläont. 32, pp 255, München

Enos P, Samakassou E (1998) Lofer cyclothems revisited (late Triassic, northern Alps, Austria). Facies 38:207–227

Felber R, Weissert HJ, Furrer H, Bontognali TR (2015) The Triassic-Jurassic boundary in the shallow-water marine carbonates from the western Northern Calcareous Alps (Austria). Swiss J Geosci 108:213–224

Fischer AG (1964) The Lofer cyclothems of the Alpine Triassic. In: Merriam, D.F. (ed) Symposium of Cyclic Sedimentation, vol 169. Kansas Geological Survey Bulletin, pp 107–149

Flügel E (1981) Paleoecology and facies of Upper Triassic reefs in the Northern Calcareous Alps. Spec Publ Soc Econ Paleont Miner Tulsa 30:291–359

Flügel E (2002) Triassic reef patterns. In: Kiessling W, Flügel E, Golonka J (eds) Phanerozoic Reef Patterns, SEPM Society for Sedimentary Geology, Special Publication 72, Tulsa, OK, pp 391–463

Flügel E (2004) Microfacies of carbonate rocks. Analysis, interpretation and application. Springer-Verlag, Germany, p 976

Frisch W, Gawlick HJ (2003) The nappe structure of the central Northern Calcareous Alps and its disintegration during Miocene tectonic extrusion—a contribution to understanding the orogenic evolution of the Eastern Alps. Int J Earth Sci 92:712–727. https://doi.org/10.1007/s00531-003-0357-4

Frisch W, Dunkl I, Kuhlemann J (2000) Post-collisional orogen-parallel large-scale extension in the Eastern Alps. Tectonophysics 327:239–265. https://doi.org/10.1016/S0040-1951(00)00204-3

Fruth I, Scherreiks R (1982) Hauptdolomit (Norian)—stratigraphy, paleogeography and diagenesis. Sed Geol 32:195–231

Fruth I, Scherreiks R (1984) Hauptdolomit - Sedimentary and Paleogeographic Models (Norian, Northern Calcareous Alps). Geol Rundsch 73:305–319

Furrer H (1981) Stratigraphie und Facies der trias/Jura-grenzschichten in den oberostalpinen Decken Graubündens. Ph.D. Thesis, Geol. Inst. Univ. Zürich, 111 pp, Zürich

Galli MT, Jadoul F, Bernasconi SM, Weissert H (2005) Anomalies in global carbon cycling and extinction at the Triassic/Jurassic boundary: evidence from a marine C-isotope record. Palaeogeogr Palaeoclimatol Palaeoecol 216:203–214. https://doi.org/10.1016/j.palaeo.2004.11.009

Galli MT, Jadoul F, Bernasconi SM, Cirilli S, Weissert H (2007) Stratigraphy and paleoenvironmental analysis of the Triassic-Jurassic transition in the western Southern Alps (Northern Italy). Palaeogeogr Palaeoclimatol Palaeoecol 244:52–70. https://doi.org/10.1016/j.palaeo.2006.06.023

Gawlick HJ, Böhm F (2000) Sequence and isotope stratigraphy of Late Triassic distal periplatform limestones from the northern Calcareous Alps (Kälberstein Quarry, Berchtesgaden Hallstatt Zone). Int J Earth Sci 89:108–129

Gawlick HJ, Missoni S (2019) Middle-Late Jurassic sedimentary mélange formation related to ophiolite obduction in the Alpine-Carpathian-Dinaridic Mountain Range. Gondwana Res 74:144–172

Gawlick HJ, Frisch W, Vecsei A, Steiger T, Böhm F (1999) The change from rifting to thrusting in the Northern Calcareous Alps as recorded in Jurassic sediments. Geol Rundsch 87:644–657

Gawlick HJ, Frisch W, Hoxha L, Dumitrica P, Krystyn L, Lein R, Missoni S, Schlagintweit F (2008) Mirdita Zone ophiolites and associated sediments in Albania reveal Neotethys Ocean origin. Int J Earth Sci 97:865–881

Gawlick HJ, Missoni S, Schlagintweit F, Suzuki H, Frisch W, Krystyn L, Blau J, Lein R (2009) Jurassic Tectonostratigraphy of the Austroalpine domain. J Alpine Geol 50:1–152

Ge Y, Al-Suwaidi AH, Shi M, Li Q, Morad S, Steuber T (2019) Short-term variation of ooid mineralogy in the Triassic-Jurassic boundary interval and its environmental implications: evidence from the equatorial Ghalilah Formation, United Arab Emirates. Global Planet Change 182:103006

Golebiowski R (1989) Stratigraphie und Biofazies der Kössener Formation (Obertrias, Nördliche Kalkalpen). Ph.D. Thesis (unpubl.) University of Vienna

Golebiowski R (1990) The alpine Kössen Formation, a key for European topmost Triassic correlations. Albertiana 8:25–35

Golebiowski R (1991) Becken und Riffe der alpinen Obertrias: Lithostratigraphie und Biofazies der Kössener Formation. In: Nagel D, Rabeder G (eds) Exkursionen im Jungpaläozoikum und Mesozoikum Österreich. Österreichische Paläontologische Gesellschaft, Vienna, pp 79–119

Guex J, Bartolini A, Atudorei V, Taylor D (2004) High resolution ammonite and carbon isotope stratigraphy across the Triassic-Jurassic boundary at New York Canyon (Nevada). Earth Planet Sci Lett 225:29–41. https://doi.org/10.1016/j.epsl.2004.06.006

Haas J, Kovács S, Krystyn L, Lein R (1995) Significance of Late Permian-Triassic facies zones in terrane reconstructions in the Alpine-North Pannonian domain. Tectonophysics 242:19–40. https://doi.org/10.1016/0040-1951(94)00157-5

Haas J, Budai T, Hips K, Czuppon G, Győri O, Horváth A, Héja G (2022) Dolomitization of Late Norian carbonate deposits of restricted basin facies in the Keszthely Mts., Transdanubian Range, Hungary. Int J Earth Sci 111:245–268

Hallam A (2002) How catastrophic was the end-Triassic mass extinction? Lethaia 35:147–157. https://doi.org/10.1111/j.1502-3931.2002.tb00075.x

Hallam A, Wignall PB (1999) Mass extinctions and sea-level changes. Earth Sci Rev 48(4):217–250. https://doi.org/10.1016/S0012-8252(99)00055-0

Héja G, Kövér S, Csillag G, Németh A, Fodor L (2018) Evidences for pre-orogenic passive-margin extension in a Cretaceous fold-and-thrust belt on the basis of combined seismic and field data (western Transdanubian Range, Hungary). Int J Earth Sci 107:2955–2973

Hesselbo SP, Robinson SA, Surlyk F, Piasecki S (2002) Terrestrial and marine extinction at the Triassic-Jurassic boundary synchronized with major carbon-cycle perturbation:a link to initiation of massive volcanism? Geology 30:251–254. https://doi.org/10.1130/0091-7613(2002)030%3c0251:TAMEAT%3e2.0.CO;2

Hillebrandt AV, Urlichs M (2008) Foraminifera and ostracoda from the Northern Calcareous Alps and the end-Triassic biotic crisis. Berichte Geol. B-A 76:70–72

Hillebrandt AV, Krystyn L, Kürschner WM, Bonis NR, Ruhl M, Richoz S, Shobben MAN, Urlichs M, Bown PR, Kment K, McRoberts CA, Simms M, Tomãsovych A (2013) The global stratotype sections and point (GSSP) for the base of the Jurassic System at Kuhjoch (Karwendel Mountains, Northern Calcareous Alps, Tyrol, Austria). Episodes 36:162–198

Iannace A, Frisia S (1994) Changing dolomitization styles from Norian to Rhaetian in the southern Tethys realm. In Dolomites: A Volume in Honour of Dolomieu, vol. 21. Blackwell Publishing Ltd., Oxford, pp 75–89

Jadoul F, Galli MT (2008) The Hettangian shallow water carbonates after the Triassic/Jurassic biocalcification crisis: the Albenza formation in the western Southern Alps. Riv Ital Paleontol Stratigr 114:453–470. https://doi.org/10.13130/2039-4942/5911

Jadoul F, Galli MT, Calabrese L, Gnaccolini M (2005) Stratigraphy of Rhaetian to Lower Sinemurian carbonate platforms in western Lombardy (Southern Alps, Italy): paleogeographic implications. Riv Ital Paleontol Stratigr 111:285–303

Jadoul F, Masetti D, Cirilli S, Berra F, Claps M, Frisia S (1994) Norian–Rhaetian stratigraphy and paleogeographic evolution of the Lombardy Basin (Bergamasc Alps): Excursion B1, 15th IAS Regional Meeting: 5–38

Jadoul F, Galli MT, Berra F, Cirilli S, Ronchi P, Paganoni A (2004) The Late Triassic-Early Jurassic of the Lombardy Basin: stratigraphy, palaeogeography and palaeontology. International Geological Congress. Field guide book excursion P86

Kaufmann B (2009) The Steinplatte complex (Late Triassic, Northern Calcareous Alps, Austria)—subsidence-controlled development of a carbonate-platform-to-intrashelf basin-transition. Acta Geol Pol 59:341–357

Köppen A, Carter A (2000) Constraints on provenance of the central European Triassic using detrital zircon fission track data. Palaeogeogr Palaeoclimatol Palaeoecol 161:193–204

Kozur H (1991) The evolution of the Meliata - Hallstatt Ocean and its significance for the early evolution of the Eastern Alps and Western Carpathians. Palaeogeogr Palaeoclimatol Palaeoecol 87:109–135. https://doi.org/10.1016/0031-0182(91)90132-B

Kreuss (2014) GEOFAST Zusammenstellung ausgewählter Archivunterlagen der Geologischen Bundesanstalt 1:50.000 - 100 Hieflau: GBA 2014, Ausgabe 2014/09, Wien

Krystyn L, Böhm F, Kürschner W, Delecat S, Pálfy J, Ozsvárt P (2005) The Triassic–Jurassic boundary in the Northern Calcareous Alps. 5th field workshop of IGCP 458:A1–A37

Kuss J (1983) Faziesentwicklung in proximalen Intraplattform-Becken: Sedimentation, Palökologie und Geochemie der Kössener Schichten (Ober-Trias, Nördliche Kalkalpen). Facies 9:61–171

Lakew T (1990) Microfacies and cyclic sedimentation of the Upper Triassic (Rhaetian) Calcare di Zu (southern Alps). Facies 22:187–231. https://doi.org/10.1007/BF02536952

Li F, Yan J, Chen ZQ, Ogg JG, Tian L, Korngreen D, Liu K, Ma Z, Woods AD (2015) Global oolite deposits across the Permian-Triassic boundary: a synthesis and implications for palaeoceanography immediately after the end-Permian biocrisis. Earth Sci Rev 149:163–180

Manatschal G, Bernoulli D (1999) Architecture and tectonic evolution of non-volcanic margins: present-day Galicia and ancient Adria. Tectonics 18:1099–1199. https://doi.org/10.1029/1999TC900041

Mandl GW (1999) Field trip guide – Dachstein Hallstatt – Salzkammergut. Berichte Geol B-A 49:1–113

Mandl GW (2000) The Alpine sector of the Tethyan shelf–examples of Triassic to Jurassic sedimentation and deformation from the Northern Calcareous Alps. Mitteilungen Der Österreichischen Geologischen Gesellschaft 92:61–77

Marzoli A, Bertrand H, Knight KB, Cirilli S, Buratti N, Vérati C, Nomade S, Renne PR, Youbi N, Martini R, Allenbach K, Neuwerth R, Rapaille C, Zaninetti L, Bellieni G (2004) Synchrony of the Central Atlantic magmatic province and the Triassic-Jurassic boundary climatic and biotic crisis. Geology 32:973–976. https://doi.org/10.1130/G20652.1

Masetti D, Stefani M, Burchell M (1989) Asymmetric cycles in the Rhaetic facies of Southern Alps: platform-basin interactions governed by eustatic and climatic oscillations. Riv Ital Paleontol Stratigr 94:401–424

Masetti D, Figus B, Jenkyns HC, Barattolo F, Mattioli E, Posenato R (2017) Carbon-isotope anomalies and demise of carbonate platforms in the Sinemurian (Early Jurassic) of the Tethyan region: evidence from the Southern Alps (Northern Italy). Geol Mag 154:625–650

Matzner C (1986) Die Zlambach-Schichten (Rhät) in den Nördlichen Kalkalpen: Eine Plattform-Hang-Beckenentwicklung mit allochthoner Karbonatsedimentation. Facies 14:1–103

Maurer F, Rettori R, Martini R (2008) Triassic stratigraphy, facies and evolution of the Arabian shelf in the northern United Arab Emirates. Int J Earth Sci 97:765–784

McRoberts CA, Furrer H, Jones DS (1997) Palaeoenvironmental interpretation of a Triassic-Jurassic boundary section from Western

Austria based on palaeoecological and geochemical data. Palaeogeogr Palaeoclimatol Palaeoecol 136:79–95
McRoberts CA, Krystyn L, Hautmann M (2012) Macrofaunal response to the end-Triassic mass extinction in the West-Tethyan Kössen Basin, Austria. Palaios 27:607–616. https://doi.org/10.2110/palo.2012.p12-043r
Mette W, Elsler A, Korte C (2012) Palaeoenvironmental changes in the Late Triassic (Rhaetian) of the Northern Calcareous Alps: clues from stable isotopes and microfossils. Palaeogeogr Palaeoclimatol Palaeoecol 350:62–72. https://doi.org/10.1016/j.palaeo.2012.06.013
Mette W, Thibault N, Krystyn L, Korte C, Clémence MR, Rizzi M, Ullmann CV (2016) Field trip 11 Rhaetian (Late Triassic) biotic and carbon isotope events and intraplatform basin development in the Northern Calcareous Alps, Tyrol, Austria. Geol Alp 13:233–256
Missoni S, Gawlick HJ, Suzuki H, Diersche V (2005) Die paläogeographische Stellung des Watzmann Blockes in den Berchtesgadener Kalkalpen-Neuergebnisse auf der Basis der Analyse der Trias- und Jura-Entwicklung. J Alpine Geol 47:169–209
Muttoni G, Kent DV, Jadoul F, Olsen PE, Rigo M, Galli MT, Nicora A (2010) Rhaetian magneto-biostratigraphy from the Southern Alps (Italy): constraints on Triassic chronology. Palaeogeogr Palaeoclimatol Palaeoecol 285:1–16. https://doi.org/10.1016/j.palaeo.2009.10.014
Pàlfy J, Demény A, Haas J, Hetényi M, Orchard MJ, Veti I (2001) Carbon isotope anomaly and other geochemical changes at the Triassic-Jurassic boundary from a marine section in Hungary. Geology 29:1047–1050
Pálfy J, Zajzon N (2012) Environmental changes across the Triassic-Jurassic boundary and coeval volcanism inferred from elemental geochemistry and mineralogy in the Kendlbachgraben section (Northern Calcareous Alps, Austria). Earth Planet Sci Lett 335:121–134. https://doi.org/10.1016/j.epsl.2012.01.039
Piller WE (1981) The Steinplatte reef complex, part of an Upper Triassic carbonate platform near Salzburg, Austria. In: Toomey DF (ed) European fossil reef models. Geological Society of America SEPM, pp 261–290
Pomar L, Hallock P (2008) Carbonate factories: a conundrum in sedimentary geology. Earth Sci Rev 87:134–169
Preto N, Breda A, Dal Corso J, Franceschi M, Rocca F, Spada C, Roghi G (2017) The Loppio Oolitic Limestone (Early Jurassic, Southern Alps): a prograding oolitic body with high original porosity originated by a carbonate platform crisis and recovery. Mar Pet Geol 79:394–411
Ratschbacher L, Frisch W, Neubauer F, Schmid SM, Neugebauer J (1989) Extension in compressional orogenic belts: the eastern Alps. Geology 17:404–407. https://doi.org/10.1130/0091-7613(1989)017%3c0404:EICOBT%3e2.3.CO;2
Ratschbacher L, Frisch W, Linzer HG, Merle O (1991) Lateral extrusion in the Eastern Alps, part 2: structural analysis. Tectonics 10:257–271. https://doi.org/10.1029/90TC02623
Richoz S, Krystyn L, Hillebrandt AV, Martindale R (2012) End-Triassic crisis events recorded in platform and basin of the Austrian Alps. The Triassic/Jurassic and Norian/Rhaetian GSSPs. J Alpine Geol 54:323–377
Rigo M, Galli MT, Jadoul F (2009) Late Triassic biostratigraphic constraints in the Imagna Valley (western Bergamasc Alps, Italy). Albertiana 37:39–42
Rizzi M, Thibault N, Ullmann CV, Ruhl M, Olsen TK, Moreau J, Clémence ME, Mette W, Korte C (2020) Sedimentology and carbon isotope stratigraphy of the Rhaetian Hochalm section (Late Triassic, Austria). Glob Planet Change 191:103210. https://doi.org/10.1016/j.gloplacha.2020.103210
Ruhl M, Kürschner WM (2011) Multiple phases of carbon cycle disturbance from large igneous province formation at the Triassic-Jurassic transition. Geology 39:431–434. https://doi.org/10.1130/G31680.1
Ruhl M, Kürschner WM, Krystyn L (2009) Triassic-Jurassic organic carbon isotope stratigraphy of key sections in the western Tethys realm (Austria). Earth Planet Sci Lett 281:169–187. https://doi.org/10.1016/j.epsl.2009.02.020
Rychliński T, Uchman A, Gaździcki A (2018) Lower Jurassic Bahamian-type facies in the Choč Nappe (Tatra Mts, West Carpathians, Poland) influenced by paleocirculation in the Western Tethys. Facies 64:1–17
Samankassou E, Enos P (2019) Lateral facies variations in the Triassic Dachstein platform: a challenge for cyclostratigraphy. Deposit Record 5:469–485. https://doi.org/10.1002/dep2.80
Satterley AK (1996a) Cyclic carbonate sedimentation in the Upper Triassic Dachstein Limestone, Austria; the role of patterns of sediment supply and tectonics in a platform-reef-basin system. J Sediment Res 66:307–323
Satterley AK (1996b) The interpretation of cyclic successions of the Middle and Upper Triassic of the Northern and Southern Alps. Earth Sci Rev 40:181–207. https://doi.org/10.1016/0012-8252(95)00063-1
Satterley AK, Brandner R (1995) The genesis of Lofer cycles of the Dachstein Limestone, Northern Calcareous Alps, Austria. Geol Rundsch 84:287–292
Satterley AK, Marshall JD, Fairchild IJ (1994) Diagenesis of an Upper Triassic reef complex, Wilde Kirche, Northern Calcareous Alps, Austria. Sedimentology 41:935–950
Schäfer P (1979) Fazielle Entwicklung und palökologische Zonierung zweier obertriadischer Riff-strukturen in den Nördlichen Kalkalpen ("Oberrhät"-riffkalke, Salzburg). Facies 1:3–245
Schlager W (2003) Benthic carbonate factories of the Phanerozoic. Int J Earth Sci 92:445–464
Schlager W, Schöllnberger W (1974) Das Prinzip stratigraphischer Wenden in der Schichtfolge der Nördlichen Kalkalpen. Mitt Geol Ges Wien 66:165–193
Schmid SM, Fügenschuh B, Kissling E, Schuster R (2004) Tectonic map and overall architecture of the Alpine orogen. Eclogae Geol Helv 97:93–117. https://doi.org/10.1007/s00015-004-1113-x
Schnabel W, Fuchs G, Matura A, Bryda G, Egger J, Krenmayer HG, Scharbert S (2002) Geologische Karte von Niederösterreich 1:200.000 mit Legende und Kurzerläuterung: 3B1, Vienna, Geol.B.A.2 sheets
Schott M (1983) Sedimentation und Diagenese einer absinkenden Karbonatplattform: Rhät und Lias des Brünnstein-Auerbach-Gebietes, Bayerische Kalkalpen. Facies 9:1–59
Schott M (1984) Mikrofaziell-multivariate Analyse einer rhäto-liassischen Karbonatplattform in den Nördlichen Kalkalpen. Facies 11:229–279
Sepkoski JJ (1996) Patterns of Phanerozoic extinction: a perspective from global data bases. In: Walliser OH (ed) Global biological events and event stratigraphy in the Phanerozoic International Interdisciplinary Cooperation in the IGCP-Project 216. Springer, Berlin, pp 35–51
Stanton RJ, Flügel E (1989) Problems with reef models: the late Triassic Steinplatte "reef" (northern Alps, Salzburg/Tyrol, Austria). Facies 20:1–138
Stanton RJ Jr, Flügel E (1995) An accretionary distally steepened ramp at an intrashelf basin margin: an alternative explanation for the Upper Triassic Steinplatte "reef" (Northern Calcareous Alps, Austria). Sed Geol 95:269–286
Steiner P (1965a) Die Eingliederung der Weyerer Bögen und der Gr. Reiflinger Scholle in den Faltenbau des Lunzer-Reichraminger Deckensystems. Mitt. Ges. Geol. Bergbaustudenten, Band, Wien: 14–15
Steiner P (1965b) Zur Geologie der Südwestlichen Lunzer Decke. PhD thesis, University of Vienna: 162 pp

Steiner P (1967) Geologische Studien im Grenzbereich der mittleren und östlichen Kalkalpen (Österreich). Mitt. Ges. Geol. Bergbaustudenten Band, Wien, 18

Strauss P, Granado P, Muñoz JA (2020) Subsidence analysis of salt tectonics-driven carbonate minibasins (Northern Calcareous Alps, Austria). Basin Res 33:968–990. https://doi.org/10.1111/bre.12500

Suess E, Mojsisovics EV (1868) Studien über die Trias- und Juraabildungen in den östlichen Alpen. Die Gebirgsgruppe des Osterhornes. Jahrbuch Des Kaiserlich-Königlichen Geologischen Reichsanstalt 18:168–200

Tollmann A (1965) Geologie der Kalkvoralpen im Ötscherland als Beispiel alpiner Deckentektonik. Mitteilungen Der Geologischen Gesellschaft in Wien 58:103–207

Tollmann A (1976) Analyse des klassischen nordalpinen Mesozoikums. Stratigraphie, Fauna und Fazies der Nördlichen Kalkalpen: pp 1–580, (Deuticke) Wien

Tollmann A (1985) Geologie von Österreich, Band 2: Außerzentralalpiner Anteil: pp 1–710, (Deuticke) Wien

Tomašových A (2004) Microfacies and depositional environment of an Upper Triassic intra-platform carbonate basin: the Fatric Unit of the West Carpathians (Slovakia). Facies 50:77–105. https://doi.org/10.1007/s10347-004-0004-y

Tomašových A (2006) Linking taphonomy to community-level abundance: insights into compositional fidelity of the Upper Triassic shell concentrations (Eastern Alps). Palaeogeogr Palaeoclimatol Palaeoecol 235:355–381

Vlahović I, Tišljar J, Velić I, Matičec D (2005) Evolution of the Adriatic Carbonate Platform: palaeogeography, main events and depositional dynamics. Palaeogeogr Palaeoclimatol Palaeoecol 220:333–360

Vörös A, Galácz A (1998) Jurassic palaeogeography of the Transdanubian Central Range (Hungary). Riv Ital Paleontol Stratigr 104:69–84

Vulpius S, Kiessling W (2018) New constraints on the last aragonite-calcite sea transition from early Jurassic ooids. Facies 64:1–9

Wegerer E, Gawlick H-J (1999) Zur Paläogeographie des gebankten obertriassischen Dachsteinkalkes im Bereich der Staufen-Höllengebirgs-Decke (Nördliche Kalkalpen). Paleogeography of the lagoonal Upper Triassic Dachstein Limestone in the Staufen-Höllengebirgs nappe (Northern Calcareous Alps). Zentralblatt Für Geologie Und Paläontologie, Stuttgart Teil 1:415–434

Wignall PB, Atkinson JW (2020) A two-phase end-Triassic mass extinction. Earth Sci Rev 208:103282

Wright VP, Burgess PM (2005) The carbonate factory continuum, facies mosaics and microfacies: an appraisal of some of the key concepts underpinning carbonate sedimentology. Facies 51:17–23

Zaffani M, Jadoul F, Rigo M (2018) A new Rhaetian $\delta^{13}C_{org}$ record: carbon cycle disturbances, volcanism, End-Triassic mass Extinction (ETE). Earth Sci Rev 178:92–104. https://doi.org/10.1016/j.earscirev.2018.01.004

Zaninetti L, Martini R, Dumont T (1992) Triassic foraminifers from sites 761 and 764, Wombat Plateau, Northwest Australia. In: von Rad U, Haq BU, et al. Proceedings of the Ocean Drilling Program, Scientific Results 122

Online Supplementary Information

Facies character and evolution of a mixed carbonate-siliciclastic shelf: Upper Triassic-Lower Jurassic succession in the eastern Northern Calcareous Alps (Stumpfmauer, Austria)

Giovanna Della Porta[1]*, Alessandro Mancini[1], Fabrizio Berra[1]

*: corresponding author (giovanna.dellaporta@unimi.it)

[1]: Dipartimento di Scienze Della Terra "A. Desio", Università degli Studi di Milano, Via Mangiagalli 34, 20133 Milan, Italy.

Giovanna Della Porta ORCID 0000-0003-3479-0592

Alessandro Mancini ORCID 0000-0002-2303-6538

Fabrizio Berra ORCID 0000-0002-4354-1806

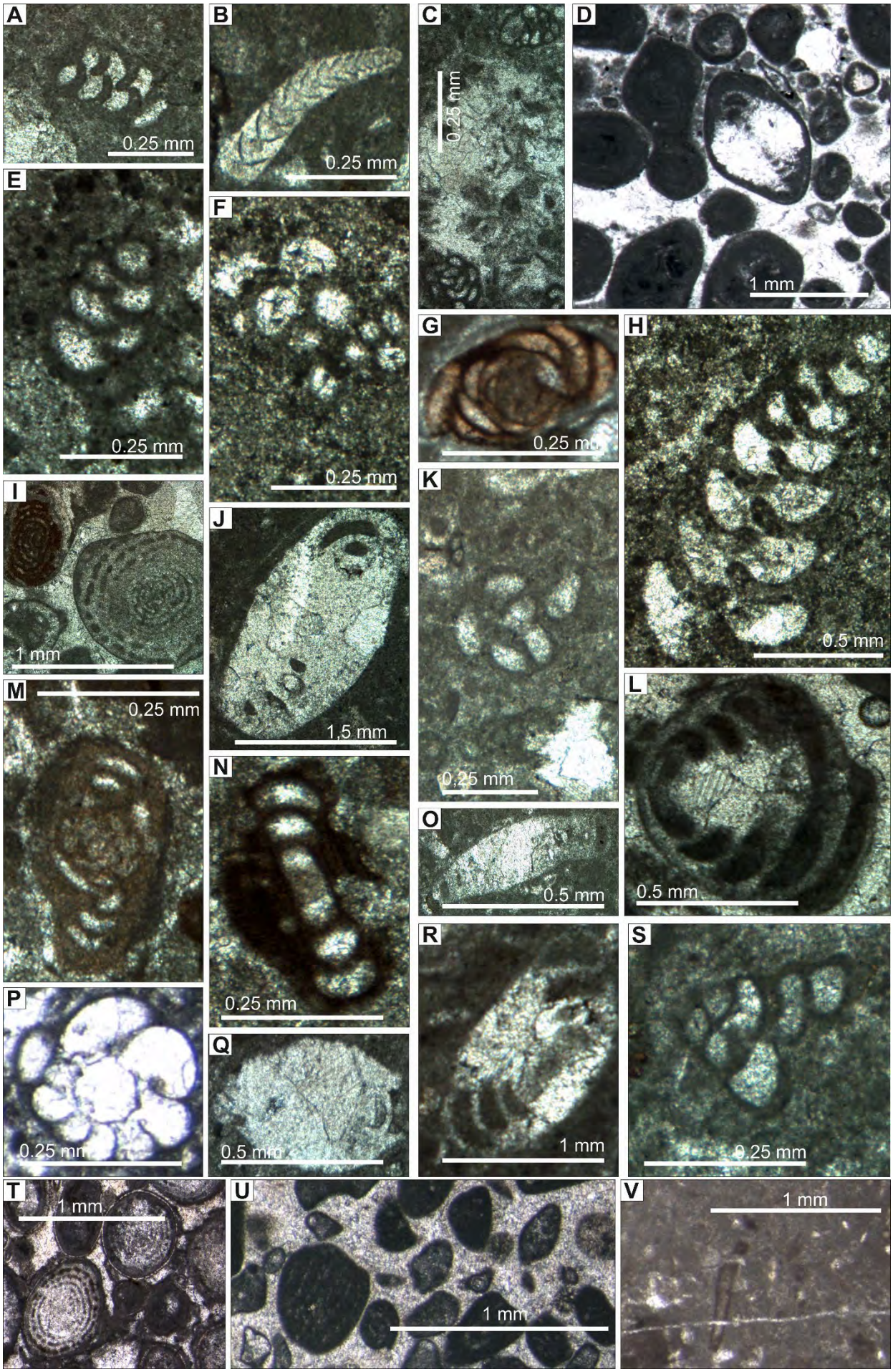
A
0.25 mm
B
0.25 mm
C
0.25 mm
D
1 mm
E
0.25 mm
F
0.25 mm
G
0.25 mm
H
0.5 mm
I
1 mm
J
1,5 mm
K
0,25 mm
L
0.5 mm
M
0.25 mm
N
0.25 mm
O
0.5 mm
P
0.25 mm
Q
0.5 mm
R
1 mm
S
0.25 mm
T
1 mm
U
1 mm
V
1 mm

Figure S1: A) Nodosariids (Sample EA21.4; Log EA, Unit A). B) *Frondicularia* (Sample EA9.9; Log EA, Unit A). C) Textulariids (Sample EC5.8; Log EC, Unit C). D) *Aulotortus sp.* (Sample ED86.5; Log ED, Unit D). E) *Valvulina azzouzi* (Sample EB1; Log EB, Unit B). F) *Mililiopora* (Sample EA2.55; Log EA, Unit A). G) *Gandinella sp.* (Sample EL1.1; Log EL, Unit D). H) *Reophax* (Sample EA2.55; Log EA, Unit A). I) *Triasina hantkeni* (Sample EC20; Log EC, Unit C). J) *Aulotortus gaschei* (Sample ED5.8; Log ED, Unit D). K) *Parvalamella friedi* (Sample EA21.4; Log EA, Unit A). L) *Auloconus sp*. (Sample EL8.10; Log EL, Unit D). M) *Glomospira* (Sample EA6.30; Log EA, Unit A). N) *Glomospirella* (Sample EA6.30; Log EA, Unit A). O) *Aulotortus sinuosus* (Sample ED5.8; Log ED, Unit C). P) Duostomiid (Sample ED58; Log ED, Unit D). Q) *Aulotortus tumidus* (Sample EG35.7; Log EG, Unit A). R) *Trocholina* sp. (Sample ED58.35; Log ED, Unit D). S) *Tetrataxis* sp. (Sample EC4.1; Log EC, Unit B). T) *Triasina hantkeni* (Sample EL4.1; Log EL, Unit D). U) *Parafavreina* (Sample EI40; Log EI, Unit E). V) *Aeolisaccus sp.* (Sample EI103.8; Log EI, Unit G).

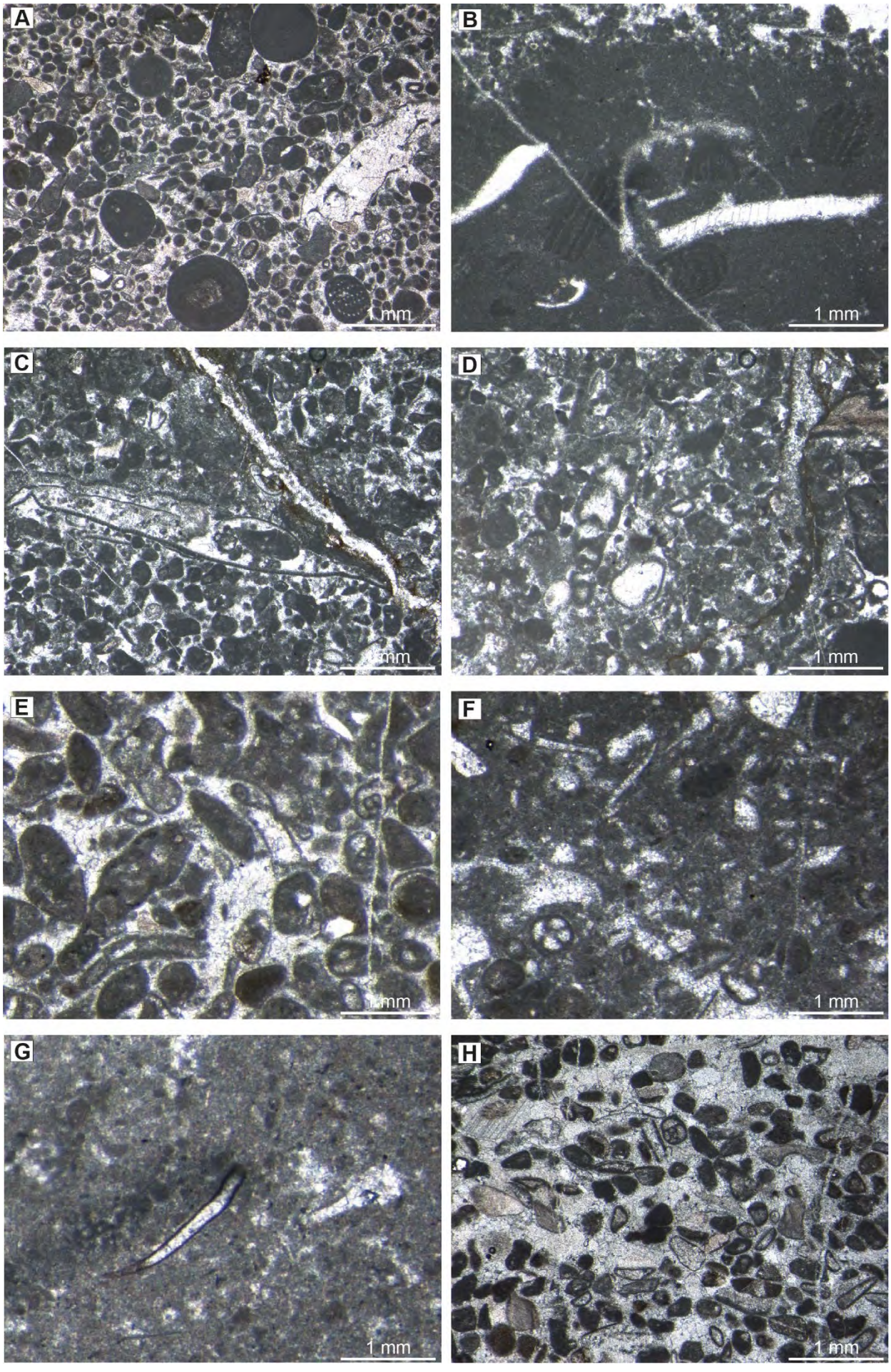
A
1 mm
B
1 mm
C
mm
D
1 mm
E
mm
F
1 mm
G
1 mm
H
1 mm

Figure S2: A) *Parafavreina* in lithofacies F22B coated grain ooidal grainstone (Sample EI52.9; Log EI, Unit E). B) Parafavreina in lithofacies F24 (Sample EI62.9; Log EI, Unit F). C) Thaumatoporella parvovesiculifera F26 (Sample EI71.3; Log EI, Unit F). D) *Evertyciclammina praevirguliana* F26 (Sample EI71.3; Log EI, Unit F). E) *Evertyciclammina praevirguliana* F26 (Sample EI92.7; Log EI, Unit F). F) F31 *Siphovalvulina* (Sample EI91.8; Log EI, Unit F). G) *Aeolisaccus* F31 (Sample EI92.0; Log EI, Unit F). H) F32 foraminifer (Sample EI117; Log EI, Unit G).

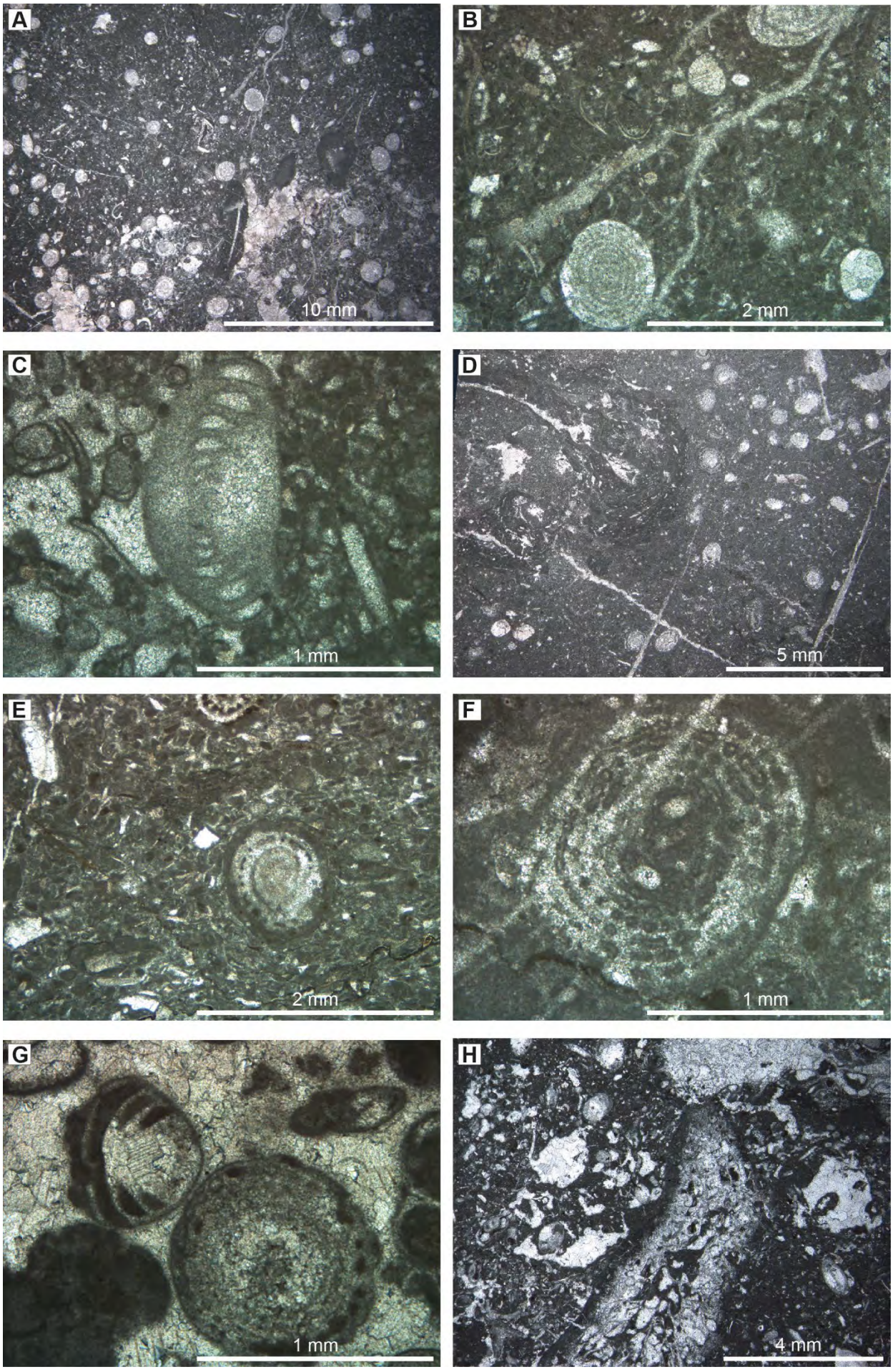
A
10 mm
B
2 mm
C
1 mm
D
5 mm
E
2 mm
F
1 mm
G
1 mm
H
4 mm

Figure S3: First and last occurrences of *Triasina hantkeni* in Unit A and Unit D lithofacies. A) Lithofacies F8B skeletal peloidal packstone/wackestone with foraminifera and dasyclad algae in the lower part of Log EA showing the first occurrences of *Triasina hantkeni* in Unit A (Sample EA21.4; Log EA, Unit A). B) F8B first occurrences of *Triasina hantkeni* in Unit A (Sample EA21.4; Log EA, Unit A). C) F8A skeletal peloidal packstone with *Aulotortus sinuosus* (Sample EA27.0 Log EA, Unit A). D) Lithofacies F14 overlying the F13 coral boundstone of Unit C with oncoidal skeletal packstone with *Triasina hantkeni* (Sample EA132; Log EA, Unit D). E) F14 oncoidal skeletal packstone to floatstone with *Triasina hantkeni* in Unit D (Sample EA133; Log EA, Unit D). F) F2 skeletal wackestone with *Triasina hantkeni* (Sample ED45; Log ED, Unit D). G) F15 coated grain grainstone with last occurrence of *Triasina hantkeni* associated with *Auloconus* (Sample EL8.10; Log EL, Unit D). H) Last occurrence of *Triasina hantkeni* and corals in F12 boundstone to floatstone with phaceloid corals at the top of Unit D showing vugy dissolution due to meteoric diagenesis and subaerial exposure (Sample ED125; Log ED, Unit D).

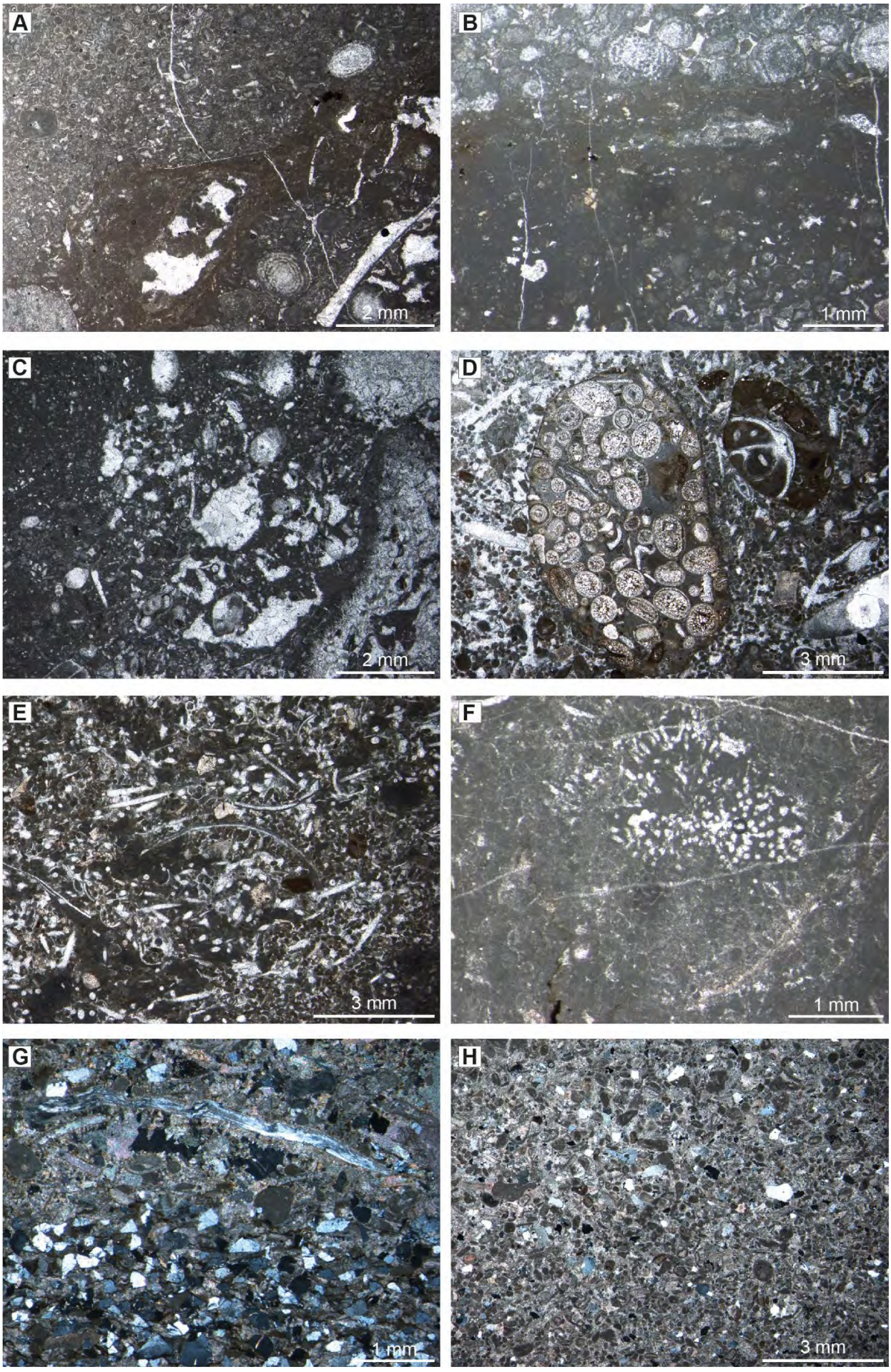
A
2 mm
B
1 mm
C
2 mm
D
3 mm
E
3 mm
F
1 mm
G
1 mm
H
3 mm

Figure S4: A, B, C) Evidence of subaerial exposure at the top of Unit D. A) F15 (Sample EL0.8; Log EL, Unit D). B) F15 (Sample EL0.5; Log EL, Unit D). C) F12 (Sample ED125; Log ED, Unit D). D) F21 (Sample EL13.4; Log EL, Unit E). E) F23 (Sample EL11.1; Log EL, Unit E). F) F27 Cayeuxia (Sample EI79.8; Log EI, Unit F). G) F30 quartz (Sample EI98.2; Log EI, Unit G). H) F30 (Sample EI101.5; Log EI, Unit G).

Log EA sample and thin section list

Sample number	Stratigraphic height from base to top in metres (m)	Sample name	Lithofacies type	Notes
PLATTENKALK (0-2.6 m; 2.6 m thick)				
1	0.02	EA 0.02	F1D	Dolomite
2	0.95	EA 0.95		Dolomite
3	1.10	EA 1.10	F1D	Dolomite
4	1.20	EA 1.20	F2 F2D	Dolomite
5	1.60	EA 1.60	F5 F5D	Dolomite
6	2.10	EA 2.10	F5 F5D	Dolomite
7	2.25	EA 2.25	F5 F5D	Dolomite
8	2.55	EA 2.55	F2 F2D over F5D	Dolomite
UNIT A (2.6-40.20 m; 37.6 m thick)				
9	3.85	EA 3.85	F5 at base/F1 at top	
10	4.30	EA 4.30	F3 F7	
11	5.01	EA 5.01	F7 F5 at top	
12	5.55	EA 5.55	F6	
13	6.30	EA 6.30	F6	
14	6.98	EA 6.98	F2	
15	7.01	EA 7.01	F6 on F1	
16	7.15	EA 7.15	F1 F7	Erosional boundary
17	9.95	EA 9.95	F8A	
18	10.0	EA 10		
19	11.20	EA 11.20	F9	
20	12.20	EA 12.20	F10	*Aulotortus* sp.
21	12.7	EA 12.7	F2	*Aulotortus* sp.
22	13.48	EA 13.48		
23	13.90	EA 13.90	F10	First *Triasina hantkeni*, bivalves oomoulds
24	14.95	EA 14.95	F10	
25	16.96	EA 16.96	F6 F10	
26	17.30	EA 17.30	F10	Marine isopachous fibrous cement, oomoulds
27	18.30	EA 18.30	F10	*Triasina hantkeni, Aulotortus*
28	18.68	EA 18.68	F2 on F1	Erosional unconformity
29	19.90	EA 19.90	F4	Black pebble lithoclasts
30	20.55	EA 20.55	F3	
31	21.40	EA 21.40	F8B	abundant *Triasina hantkeni*, Duostomid *Aulotortus* sp., oncoids
32	21.90	EA 21.90	F2	*Triasina hantkeni*
33	25.41	EA 25.41	F5 F4	
34	27.0	EA 27	F8A	Dasyclads, *Auloconus*
35	27.35	EA 27.35	F6 F20	Lithoclasts, *Triasina hantkeni*
36	28.90	EA 28.90	F5 F4	
37	29.60	EA 29.60	F6 over F4	Burrows, *Auloconus*, megalodontids
38	31.90	EA 31.90	F5	

39	33.15	EA 33.15	F4	
40	35.50	EA 35.50	F6	
41	38.50	EA 38.50	F6 F9	
42	39.30	EA 39.30	F5 F4	
43	39.95	EA 39.95	F6 F20 to F11	
44	40.10	EA 40.10	F5	
UNIT B (40.20-90.20 m; 50 m thick)				
45	65.90	EA 65.90	F11	Oncoids
46	71.3	EA 71.30	F12	Brachiopods, calcispheres
47	76.60	EA 76.40	F12	
48	85.1	EA 115.30	F11	
49	89.6	EA 119.60		
UNIT C (90.20-101 m; 10.8 m thick)				
50	90.5	EA 120.75	F12	Ammonoids, siliceous sponges, foraminifers
51	91.7	EA 121.90	F13	*Lithocodium, Bacinella*
52	93.8	EA 124.50	F13	
53	96.4	EA 126.60	F13	Siliceous sponges
UNIT D (101-103 m; 2 m thick)				
54	101.8	EA 132	F14	Erosional unconformity, oncoids, *Triasina hantkeni*
55	102.8	EA 133	F14	Oncoids, *Triasina hantkeni*

Log EG sample and thin section list

Sample number	Stratigraphic height from base to top in metres (m)	Sample name	Lithofacies type	Notes
PLATTENKALK (0-1.9 m; 1.9 m thick)				
1	1.55	EG 1.55	F1D	Dolomite, erosional surfaces overlain by stromatolites
UNIT A (1.9-56.6 m; 54.7 m thick)				
2	6.10	EG 6.10	F1 F2 F20	F1 with lithoclasts (F20) on F7 overlying erosional surface on stromatolites F5
3	7.20	EG 7.20	F1 F2	
4	7.3	EG 7.3	F10	Lithoclasts, tangential ooids G marine cement
5	9.3	EG 9.3	F10	Recrystallized packstone
6	10.15	EG 10.15	F5 F4	5 cm claystone below F5-F4
7	10.70	EG 10.7	F6 F4	Gastropods
8	14.0	EG 12 (14 m)	F8A	dasyclad lithoclast with meniscus cement, *Aulotortus*
9	15.70	EG 13.5 (15.70 m)	F6	Megalodonts, *Aulotortus*
10	17.20	EG 14.9 (17.2 m)	F10	Ooids, marine cement
11	19.50	EG 17.10 (19.50 m)	F20 F6	Lithoclasts, black pebbles
12	20.80	EG 18.60 (20.80 m)	F20 F2	Lithoclasts, black pebbles
13	27.40	EG 25 (27.40 m)	F8A F20	Dasyclad *Acicularia* F20 above eroded exposed F5 boundary
14	33.50	EG 31.15 (33.50 m)	F8B	*Gandinella*, meniscus cement, calcrete, claystone clasts.
15	35.80	EG 33.40 (35.80 m)	F8A	Dasyclad *Acicularia, Aulotortus Auloconus*, possibly first *Triasina*
16	41.40	EG 38 (41.40)	F9	*Aulotortus*, oomoulds on F6 megalodontid shells, burrows
17	46.60	EG 40.10 (46.60 m)	F2	
18	47.50	EG 40.85 (47.50)	F6 F20	Lithoclasts
19	47.80	EG 41 (47.80 m)	F6 F20	Lithoclasts
20	56.20	EG 46.80 (56.6 m)	F1	

Log EC sample and thin section list

Sample number	Stratigraphic height from base to top in metres (m)	Sample name	Lithofacies type	Notes
UNIT B (0-3.65 m; 3.65 m thick)				
1	0.3	EC 0.3	F12	Corals, serpulids, brachiopods, claystone streaks
2	3.5	EC 3.5	F7	
UNIT C (3.65-10.9 m; 7.25 m thick)				
3	3.8	EC 3.8	F12	Corals encrusted by *Lithocodium Bacinella,* Calcareous sponges pyrite
4	4.10	EC 4.10	F12	Calcareous sponges, faecal pellets
5	4.90	EC 4.90	F11 F20	Lithoclasts reworked, black pebbles
6	5.80	EC 5.80	F13	*Lithocodium Bacinella*
7	6.80	EC 6.80	F13	Corals, *Thaumatoporella,* marine cement in corals
8	8.70	EC 8.70	F13	Corals, oncoids
UNIT D (10.9-31 m; 20.1 m thick)				
9	11.70	EC 11.70	F14	Oncoids overlain by F7 marlstone
10	13.10	EC 13.10	F11 F7	Punctate brachiopods
11	15.45	EC 15.45	F12	Corals, *Triasina hantkeni*
12	19.80	EC 19.80	F11	Brachiopods, bivalves, chert nodules, *Triasina hantkeni*
13	20.10	EC 20.10	F14	Oncoids, *Triasina hantkeni*
14	21.40	EC 21.40	F14	Oncoids, *Triasina hantkeni*
15	25.50	EC 25.50	F14	*Triasina hantkeni*, *Aulotortus*
16	30.0	EC 30	F14	Oncoids, *Triasina hantkeni*
17	30.80	EC 30.80	F7	Marlstone with burrows; cf. with ED 8.5 burrows

Log EL sample and thin section list

Sample number	Stratigraphic height from base to top in metres (m)	Sample name	Lithofacies type	Notes
UNIT D (0-11.4 m; 11.4 m thick)				
1	0.80	EL 0.80	F15	*Triasina hantkeni*
2	1.10	EL 1.10	F20 F17	Subaerial exposures followed by transgressive lag
3	1.20	EL 1.20	F22B	
4	1.25	EL 1.25	F15	*Triasina hantkeni*, alveolar texture
5	1.27	EL 1.27	F15	*Triasina hantkeni*
6	1.28	EL star	F15	*Triasina hantkeni*, subaerial exposure, calcretes
7	4.10	EL 4.10	F15	*Triasina hantkeni*, calcareous and siliceous sponges
8	4.20	EL 4.20	F22A	
9	5.50	EL 5.50	F22B	
10	5.60	EL 5.60	F23	Lithoclasts
11	7.30	EL 7.30	F15	*Triasina hantkeni, Aulotortus*
12	8.10	EL 8.10	F15	*Triasina hantkeni, Aulotortus, Auloconus, Solenopora*, calcareous sponges
13	11.15	EL 11.15	F21 F23	Sponge spicules
UNIT E lower part (11.4-22.75 m; 11.35 m thick)				
14	11.40	EL 11.40	F21 F23	Sponge spicules, quartz, burrows
15	11.70	EL 11.70	F23	sponge spicules burrows
16	13.40	EL 13.40	F21 F23	silicified lithoclasts vadose pisoids
17	15.50	EL 15.50	F23	Chert nodules
18	16.30	EL 16.30	F23	sponge spicules
19	18.45	EL 18.45	F21 F23	lithoclasts spicules
UNIT E upper part (22.75-34.5 m; 11.75 m thick)				
20	20.35	EL 20.35	F22A	Crinoids, silicification
21	20.77	EL 20.77	F23	
22	26.11	EL 26.11	F22B	Radial ooids, marine cement
23	33.31	EL 33.31	F19	Aggregate grains, marine cement

Log ED-EE sample and thin section list

Sample number	Stratigraphic height from base to top in metres (m)	Sample name	Lithofacies type	Notes
UNIT C (0-8.40 m; 8.40 m thick)				
1	4.0	EE 4.0	F13	Corals, serpulids, Lithocodium Bacinella, siliceous sponge spicules, silicification
2	8.50	EE 8.50	F14	Dasyclad *Acicularia*, *Triasina hantkeni*
UNIT D (8.40-117.90 m; 109.50 m thick)				
3	10.0	EE 10.0	F14	With F13 coral fragment
4	12.2	ED 1.20	F14	*Triasina hantkeni, Aulotortus*
5	13.1	ED 2.10	F14	
6	14.0	ED 3.0	F14 F13	*Triasina hantkeni, Auloconus, corals*
7	14.5	ED 3.50	F13 F14	Corals, *Aulotortus*, dasyclad *Griphoporella*
8	15.0	ED 4.0	F13 F14	Dasyclad, *Auloconus*
9	16.0	ED 5.0	F15	Siliceous sponge, *Triasina hantkeni*
10	16.80	ED 5.80	F14	Dasyclad *Griphoporella, Aulotortus*
11	17.30	ED 6.30	F12 F20	Lithoclasts
12	17.50	ED 6.50 x2	F12 F20	Lithoclasts, corals, bivalves
13	18.10	ED 7.10	F13	Corals, *Bacinella Lithocodium*
14	18.60	ED 7.6	F7	Burrows, nodosarids
15	19.5	ED 8.5	F7	Burrows, Zoophycos, calcispheres, bivalves *Rhaetavicola contorta*
16	19.90	ED 8.90	F17	Quartz silt
17	20.80	ED 9.80	F17	Quartz silt
18	21.9	ED 10.90	F2 F8	Dasyclad *Acicularia, Triasina hantkeni*, burrows, erosional surface, lithoclasts
19	25.30	ED 14.30	F7	
20	25.40	ED 14.40	F7	Calcispheres
21	26.6	ED 15.6		
22	30.8	ED 19.80	F2	Dasyclad, exposures above
23	32.50	ED 21.50	F14 F18	Corals, Triasina hantkeni, *Cayeuxia* like calcimicrobes, *Bacinella Lithocodium*
24	32.80	ED 21.80	F16	Aggregate grains, burrows, dasyclad
25	33.0	ED 22.0		
26	34.1	ED 23.10	F2	
27	34.7	ED 23.70	F7	Crinoids
28	35.4	ED 24.40	F16	
29	38.4	ED 27.4	F2 F20	Burrows
30	38	ED 30.70	F11 F20	Lithoclasts, brachiopods
31	38.4	ED 34.35	F7	
32	38.5	ED 45	F20 F2 over F1	Subaerially exposed with gypsum, *Triasina hantkeni*
33	39.14	ED 48.14	F2	Oncoids, *Triasina hantkeni, Aulotortus, Auloconus*
34	43.20	ED 52.20	F18	Siliceous sponge, *Bacinella Lithocodium*

35	47.50	ED 56.50	F2 on F1	Erosional top, burrows, *Aulotortus tumidus*
36	49.35	ED 58.35	F2 F14	Corals, *Triasina hantkeni, Diplotremina,* Duostomids, *Thaumatoporella parvovesiculifera*
37	57.80	ED 66.80	F13 F18	*Aulotortus, Thaumatoporella parvovesiculifera*, oncoids, clotted peloidal micrite
38	50.05	ED 69.05	F2	*Aulotortus tumidus*
39	69.25	ED 78.25	F2 F23	Peloids
40	71	ED 80	F23	Peloidal P/G, aggregate grains
41	77.5	ED 86.50	F19	Aggregate grains, burrows, *Triasina hantkeni, Aulotortus, Auloconus*
42	91.70	ED 100.70	F20 F2	Quartz, lithoclasts, crustacean, *Solenopora*
43	97	ED 106	F23	
44	100.60	ED 109.60	F6 F2	Dasyclad, gastropods, *Aulotortus*
45	106.3	ED 115.3	F2	*Triasina hantkeni*
46	108.4	ED 117.40	F22C	Radial ooids
47	110.10	ED 119.10	F22A	Gastropods, brachiopods
48	112.90	ED 121.90	F22A	Corals, *Triasina hantkeni, Aulotortus,* root traces, alveolar texture
49	116.90	ED 125.90	F12 F18	Last corals, last *Triasina hantkeni, Aulotortus,* alveolar texture, meniscus cement indicative of meteoric vadose diagenesis and subaerial exposure

Log EI sample and thin section list

Sample number	Stratigraphic height from base to top in metres (m)	Sample name	Lithofacies type	Notes
UNIT E lower part (0-13.30 m; 13.30 m thick)				
1	0.1	EI 0.1	F21	Transgressive lag, detrital quartz, lithoclasts, black pebbles
2	1.0	EI 1.0	F21	Transgressive lag, detrital quartz, lithoclasts, black pebbles
3	3.6	EI 3.60	F22A	Detrital quartz
4	5.4	EI 5.40	F23	Detrital quartz, sponge spicules, silicification, burrows
5	7.1	EI 7.10	F23	Burrows, lithoclasts
6	8.2	EI 8.20	F22B F21	Lithoclasts
7	9.2	EI 9.20	F23	Sponge spicules, burrows
8	11.6	EI 11.60	F22A	Detrital quartz, cross bedding
9	13.10	EI 13.10	F22B F21	Detrital quartz, black pebbles, *Lenticulina, Dentalina*
UNIT E upper part (13.30-57.0 m; 43.70 m thick)				
10	14.0	EI 14.00	F22A F21	Lithoclasts
11	14.4	EI 14.40	F22B	Detrital quartz, marine isopachous cement, low angle cross bedding
12	16.4	EI 16.40	F22A	Detrital quartz, cross bedding, crinoids
13	18.0	EI 21.60	F22C	Detrital quartz, siltite extraclasts, radial ooids, marine cement.
14	24.8	Ei 24.80	F22B F21	Pisoids, vadose meniscus cement, lithoclasts affected by meteoric diagenesis, black pebbles
15	26.3	Ei 26.30	F22B	Subaerial exposure and karstic dissolution, *Parafavreina*
16	27.45	Ei 27.45	F22A	Detrital quartz
17	27.60	EI 27.60	F23	Detrital quartz, sponge spicules
18	30.0	Ei 30.00	F22A	
19	33.8	EI 33.80	F22C	
20	37.8	Ei 37.80	F22C	
21	40.2	EI 40.20	F19	*Parafavreina*, marine isopachous cement, lithoclasts
22	44.8	EI 44.80	F19	*Parafavreina,* marine isopachous cement, aggregate grains
23	45.4	Ei 45.40	F19	Marine isopachous cement
24	46.1	Ei 46.10	F22A	Detrital quartz, brachiopods
25	48.0	EI 48.0	F22A	Cross bedding
26	48.2	Ei 48.20	F22A	
27	49.9	Ei 49.90	F22A	Recrystallization probably due to meteoric diagenesis
28	52.9	Ei 52.90	F22A-22B	*Parafavreina*
29	54.9	Ei 54.90	F22A-22B	*Parafavreina*

30	56.5	EI 57.0	F22B	*Parafavreina*, detrital quartz
31	57.0	Ei 57A	F22A	
32	57.0	EI 57B	F22A	Fenestrae/keystone vugs marine cement, shallow to supratidal conditions and exposure.
UNIT F lower part (57.0-63.40 m; 6.40 m thick)				
33	58.5	EI 58.5	F24	Possible angular unconformity. Burrows, bivalves
34	58.8	EI 58.80	F24	Dasyclads, bivalvess
35	58.9	EI 58.8B	F24	Bivalves, burrows
36	59.7	EI 59.7 58.60	F24	Recrystallized, cataclastic
37	60.5	EI 59	F24	Dissolution vugs/fenestrae, subaerial exposure affecting mudstone.
38	61.8	EI 59.2	F24	
39	61.9	EI 59.3	F25	Ostracods, marlstone, burrows
40	62.6	Ei 60.00	F24	Karstic dissolution
41	62.9	Ei 60.30	F24	*Parafavreina*
42	63.1	Ei 60.50	F25	
43	63.2	EI 60.80	F25	
UNIT F upper part (63.40-95.10 m; 31.70 m thick)				
44	71.30	Ei 68.70	F26	*Thaumatoporella parvovesiculifera, Evertyciclammina praevirguliana*
45	72.40	Ei 69.80	F27	
46	73.6	EI 71.0	F27	*Cayeuxia*, fenestrae
47	73.7	Ei 71.10	F26 F27	*Cayeuxia Thaumatoporella parvovesiculifera*, vadose meniscus cement
48	74.8	Ei 72.20	F27 F26	*Thaumatoporella parvovesiculifera*, fenestrae
49	76.3	Ei 73.70	F28	
50	77.3	EI 74.70	F28	*Evertyciclammina praevirguliana*, oncoids
51	77.4	EI 74.80	F28	
52	79.8	EI 76.2	F28 F27	*Cayeuxia*, oncoids
53	83.6	Ei 81.00	F27 F28	Dasyclads, *Cayeuxia, Thaumatoporella parvovesiculifera*
54	85.80	Ei 83.20	F27	Fenestrae with marine cement
55	86.50	Ei 83.90	F27	Microbial boundstone and supratidal fenestrae with red vadose silt, subaerial exposure
56	87.50	Ei 84.90	F26	*Cayeuxia*
57	88.40	EI 85.90	F26	Supratidal facies with with meniscus vadose cement followed by marine cement
58	88.6	Ei 86.00		
59	89.10	Ei 86.50	F26	Supratidal vadose meniscus cement, keystone vugs, silicification
60	89.30	Ei 86.70	F26	Supratidal vadose meniscus cement *Cayeuxia*, Dasyclads.
61	90.0	Ei 87.40		

62	90.1	Ei 87.50	F31	Burrows
63	90.6	EI 87.20	F31	*Cayeuxia*, oncoids
64	90.8	Ei 88.20	F26 F20	Lithoclasts with boring lithodome, reworking subaerial exposure
65	90.95	Ei 88.35		
66	91.0	Ei 88.40	F24 F31	
67	91.8	EI 89.20 (EF 78.4)	F31 F24	*Siphovalvulina*
68	92.0	Ei 89.40	F31 F24	*Thaumatoporella parvovesiculifera, Aeolisaccus*
69	92.7	Ei 90.10	F26	*Evertyciclammina praevirguliana*
70	93.0	EI 90.40	F26	*Aeolisaccus*
71	94.2	EI 91.70	F28	Oncoids, *Thaumatoporella parvovesiculifera*
72	95.0	Ei 92.40	F26	
UNIT G (95.10-129.40 m; 34.30 m thick)				
73	95.2	Ei 92.60	F29	Sponge spicules, detrital quartz silt
74	95.4	Ei 92.80	F29	Sponge spicules, first continuous chert
75	95.7	Ei 93.10	F30	Detrital quartz
76	96.2	EI 93.0	F30	Detrital quartz
77	98.2	Ei 95.60	F30	Detrital quartz, lithoclasts, spicules
78	98.9	Ei 96.30	F30	
79	99.7	Ei 97.10		
80	101.05	Ei 98.45	F30	Detrital quartz, *Siphovalvulina*
81	102.4	Ei 99.80	F31	
82	103	EI 101.5	F31	*Siphovalvulina,* burrows
83	103.8	Ei 101.20	F31	*Aeolisaccus*
	1 metre non exposure			
84	107	Ei 108.40		Quartz, chert
85	108.5	EI 110	F32	Marine isopachous fibrous cement, detritial quartz, silicification, chert, bidirectional cross lamination, crinoids
86	117	EI 117	F32	Detritial quartz, silicification, chert, bidirectional cross lamination, crinoids
87	118.5	EI 119	F32	Detritial quartz, silicification, chert, bidirectional cross lamination, crinoids
88	121.5	Ei 123.00	F32	Glaucony
UNIT H (129.40-181.0 m; 51.60 m thick)	**NOT TOPIC OF THIS STUDY**			
89	129.5	Ei 131.00	F33	Red colour, cinoids, belemnite, *Lenticulina*
90	140.0	EiZ 140	F29	Sponge spicules
91	181.0	EiW 181	F33	Crinoids, bryozoans